

**STRUCTURAL DESIGN OF CONSTRUCTIONS
SUBJECTED TO EXCEPTIONAL OR ACCIDENTAL ACTIONS**

EDITED BY

Ph. BOUILLARD, Y. RAMMER AND J. VANTOMME



**STRUCTURAL DESIGN OF CONSTRUCTIONS
SUBJECTED TO EXCEPTIONAL OR ACCIDENTAL ACTIONS**

STRUCTURAL DESIGN OF CONSTRUCTIONS SUBJECTED TO EXCEPTIONAL OR ACCIDENTAL ACTIONS

Proceedings of the workshop held in Brussels, Belgium
April 9th, 2008

Edited by:

Prof. Ph. Bouillard
Université Libre de Bruxelles
Belgium

Prof. Y. Rammer
Université Libre de Bruxelles
Belgium

Prof. J. Vantomme
Royal Military School
Belgium

Printed by:

Presses universitaires de Bruxelles asbl (P.U.B.)
Av. Paul Héger 42, 1000 Brussels, Belgium
<http://www.ulb.ac.be/ulb/pub>

**STRUCTURAL DESIGN OF CONSTRUCTIONS
SUBJECTED TO EXCEPTIONAL OR ACCIDENTAL ACTIONS**
Ph. Bouillard, Y. Rammer and J. Vantomme (Eds)

Cover photograph: I-40 Bridge Disaster, Oklahoma, USA, May 26, 2002

Credits: Robert Webster [@](#)

'The I-40 Bridge Disaster was a boating accident that occurred in Webbers Falls, Oklahoma on May 26, 2002. Joe Dedmon, captain of the tugboat Robert Y. Love, experienced a blackout and lost control of the ship. This, in turn, caused the barge he was controlling to collide with a bridge support. The result was a 580 foot (180 m) section of the I-40 bridge plunging into Kerr Reservoir on the Arkansas River. Due to the location of the accident, automobiles and tractor trailers fell into the water, killing fourteen people.' [Wikipedia]

First edition: April 2008

Dépôt légal : D/2008/Philippe Bouillard, éditeur

Acknowledgements

The editors and workshop organizers acknowledge the support towards the publication of the book of the contributions to the workshop, to the following organizations:

- Université Libre de Bruxelles, Belgium
- Royal Military School, Belgium,
- Minister Pascal Smet's cabinet



CONTENTS

Foreword

Ph. Bouillard, Y. Rammer, J. Vantomme 9

Chapter 1.

Risk in Civil Engineering and Eurocodes

J.-A. Calgaro 13

Chapter 2.

Wind and Fire

P. E. Spehl 27

Chapter 3.

Effects of explosions on structures

J. Vantomme, J. M. Ndambi, B. Reymen 53

Chapter 4.

Numerical, analytical and experimental investigations on the response of steel and composite buildings further to the loss of a column

J.-P. Jaspart, J.-F. Demonceau, H.N.N. Luu 69

Chapter 5.

Progressive collapse simulation techniques for RC structures

Ph. Bouillard, K. Menchel, B. Santafé, T. J. Massart 91

Chapter 6.

The Millau viaduct: an outstanding structure. The safety during the deck launching

V. de Ville de Goyet, J.-M. Crémér, J.-Y. Del Forno 115

Chapter 7.

Gare TGV de Liège-Guillemins : comportement sous les effets du vent

V. de Ville de Goyet, Y. Duchêne, Cl. Counasse 129

Chapter 8.

Introduction to risk assessment strategies for accidental design situations in civil engineering

Y. Rammer 141

FOREWORD

For many years structural safety has been one of the main issues addressed by all the actors involved in structural design: engineers, architects, public or private clients, contractors, etc. As a result of the development of the Eurocodes, the structural safety has been deeply improved and redefined. It is now clear that the structural safety is nothing but an issue of risk assessment and risk management. After having developed the idea of *reliability* (EN 1990) covering the aspects of safety, serviceability and durability, Eurocodes now impose the important concept of *robustness*.

The robustness of a structure is defined as the '*ability of a structure to withstand events like fire, explosions, impact or the consequences of human error, without being damaged to an extent disproportionate to the original cause.*' [NBN EN 1991-1-7]

The philosophy of the Eurocode is presented in Chapter 1 ('*Risk in Civil Engineering and Eurocodes*') by Prof. J.-A. Calgaro and was also presented during the workshop by Prof. G. Sedlacek ('*Eucodes and accidental actions*'). Eurocode also provides a description of principles and application rules for the design of load bearing structures subjected to accidental actions. Prof. Y. Rammer, in Chapter 8 ('*Risk assessment strategies for accidental design situations in civil engineering*'), illustrates the basic concepts behind risk analysis, and proposes a unified framework for the assessment of accidental project situations.

The definition of the robustness also requires an in-depth understanding of all the accidental actions, i.e. fire, explosions, impact, together with a proper way to model them in a design situation. According to Eurocodes, '*the accidental actions that should be taken into account depend upon: the measures taken for preventing or reducing the severity of an accidental action; the probability of occurrence of the identified accidental action; the consequences of failure due to the identified accidental action; public perception; the level of acceptable risk.*' These actions are presented and analysed in Chapter 2 ('*Wind and Fire*') by Prof. P. Spehl and Chapter 3 ('*Effects of explosions on structures*') by Prof. J. Vantomme *et al.*

These first contributions show that the general concepts of robustness, risk management, and accidental actions are more and more developed. However, we think that there still exists a gap between these concepts and their implementation in real-life applications.

To help bridging this gap, the research community has been very active in the last years. This is here illustrated by two original contributions dedicated to specific material behaviours (steel and reinforced concrete) together with recent advances in numerical simulations: Chapter 4 (*'Numerical, analytical and experimental investigations of the response of steel and composite buildings further to the loss of a column'*) by Prof. J.-P. Jaspart *et al.*, and Chapter 5 (*'Progressive collapse simulation techniques for RC structures'*) by Prof. Ph. Bouillard *et al.*

Last but not least, this book presents two related recent applications developed by Greish and presented by Prof. V. de Ville *et al.*: Chapter 6 (*'The Millau viaduct: an outstanding structure. The safety during the deck launching'*) and Chapter 7 (*'Gare TGV de Liège-Guillemins : comportement sous les effets du vent'*) – in French.

The editors would like to acknowledge all the authors for their contribution. We hope that this book will be useful to help for practitioners and researcher to build a common understanding of robustness, risk management and accidental actions.

Ph. Bouillard, Y. Rammer and J. Vantomme
April 9th, 2008.

RISK IN CIVIL ENGINEERING AND EUROCODES

J.-A. Calgaro

Chairman of CEN/TC250 "Structural Eurocodes"
Conseil Général des Ponts et Chaussées
Tour Pascal B – F-92055 La Défense Cedex
e-mail: Jean-Armand.Calgaro@equipement.gouv.fr

Keywords: Risk, Reliability, Structural Design, Accidental Actions, Eurocodes, Proceedings.

Abstract. *This paper examines how the Eurocodes tackle with risk assessment and risk management in civil engineering. The questions of responsibility of the designer and/or the architect are underlying, but are not treated in detail. On one hand, the public aversion to failure and the societal desire of protection are increasing ; on the other hand, the social organization of the construction industry (research of profits, lower cost of construction processes, position of engineering companies, exaggerate increasing of subcontracting) is a serious source of risks. What can be done in the codes of practice to invite engineers to exert better their professional skill? The current format of verification of construction works is the semi-probabilistic format, called limit state design, and based on the partial factor method. Of course, it is possible to alter the codified reliability levels by adjusting the numerical values of the partial factors, but, in reality, this way is very limited : changes of political nature are needed to reduce risks in civil engineering.*

1 INTRODUCTION

Code of Hammurabi, Babylon, 1760 BC

If a builder builds a house for some one, and does not construct it properly, and the house which he built fall in and kill its owner, then that builder shall be put to death.

The concepts of risk and hazard scenario are defined and mainly commented in two Eurocodes: EN 1990 “Basis of structural design” and EN 1991-1-7 “Eurocode 1 - Actions on structures – Part 1-7 : General actions - Accidental actions”. The seismic risk is dealt with in EN 1998 “Eurocode 8 – Design of Structures for Earthquake Resistance” which gives the general performance requirements, the definition of the seismic action, analysis procedures, and general concepts and rules applicable to civil engineering structures.

From a general point of view, risk and uncertainty are key features of most business and government problems and need to be understood for rational decisions to be made. A risk is an issue, item, event which may occur or not, and which may have a negative impact.

Of course, in the Eurocodes, which are codes for the design of buildings and civil engineering structures, the concept of risk is limited to structural risk: possible consequences of an accidental situation on the environment are out of their scope except in the case of fire and earthquakes, but the main objective remains the structural resistance to ensure safety of people.

This paper is a tentative description of the approach of risk in civil engineering in the Eurocodes.

2 DEFINITIONS

The developments of the present paper use the following definitions, derived from the definitions given in the Eurocodes.

Accidental design situation (EN 1990, 1.5.2.5): *design situation involving exceptional conditions of the structure or its exposure, including fire, explosion, impact or local failure.*

Hazard (EN 1990, 1.5.2.9): *for the purpose of EN 1990 to EN 1999, an unusual and severe event, e.g. an abnormal action or environmental influence, insufficient strength or resistance, or excessive deviation from intended dimensions.*

Hazard scenario (EN 1991-1-7, B.2.2): *a critical situation at a particular time consisting of a leading hazard together with one or more accompanying conditions which leads to an unwanted event (e.g. complete collapse of the structure).*

Risk (EN 1991-1-7, 1.5.13): *a measure of the combination (usually the product) of the probability or frequency of occurrence of a defined hazard and the magnitude of the consequences of the occurrence.*

Risk analysis (EN 1991-1-7, B.2.5): *a systematic approach for describing and/or calculating risk. Risk analysis involves the identification of undesired events, and the causes, likelihoods and consequences of these events.*

Risk management (EN 1991-1-7, B.2.7): *systematic measures undertaken by an organisation in order to attain and maintain a level of safety that complies with defined objectives.*

(Good risk management will not prevent bad things from happening. But when bad things happen, good risk management will have anticipated them and will reduce their negative effects).

Risk acceptance criteria (EN 1991-1-7, B.2.4): *acceptable limits to probabilities of certain consequences of an undesired event and are expressed in terms of annual frequencies. These*

criteria are normally determined by the authorities to reflect the level of risk considered to be acceptable by people and society.

Consequence (EN 1991-1-7, B.2.1): a possible result of an (in risk analysis usually unwanted) event. Consequences may verbally or numerically be expressed in terms of loss of life, injury, economic loss, environmental damage, disruption to users and the public, etc. Both immediate consequences and those that arise after a certain time has elapsed are to be included.

Robustness (EN 1991-1-7, 1.5.14): the ability of a structure to withstand events like fire, explosions, impact or the consequences of human error, without being damaged to an extent disproportionate to the original cause.

Localised failure (EN 1991-1-7, 1.5.12): that part of a structure that is assumed to have collapsed, or been severely disabled, by an accidental event.

As it can be seen, the concept of risk is introduced in the Eurocodes. And in EN 1991-1-7, information is given about risk assessment and risk analysis, limited to the concepts and the general procedures. From a general point of view, risk assessment refers to the quantifying, either qualitatively or quantitatively, of the probability and the potential impact of some risk. Risk Analysis refers to the whole process from risk identification, through qualitative and quantitative assessment of a risk, to the resultant management decisions and communication to the various stakeholders of the assessment of that risk and the decision that has been or is to be made.

3 GENERAL REQUIREMENTS FOR CONSTRUCTION WORKS

Section 2 of EN 1990 gives the general requirements for a structure. Of course, a structure shall be designed to have adequate structural resistance, serviceability, and durability (EN 1990, 2.1(2)P), and in the case of fire, the structural resistance shall be adequate for the required period of time (EN 1990, 2.1(3)P). But, moreover, a structure shall be designed and executed in such a way that it will not be damaged by events such as explosion, impact, and the consequences of human errors, to an extent disproportionate to the original cause (EN 1990, 2.1(4)P).

This last requirement is at the origin of the definition of structural robustness. It derives from Essential Requirement Nr. 1 of Council Directive 89/106/EEC of 21 December 1988 (CPD) on the approximation of laws, regulations and administrative provisions of the Member States relating to construction products (Annex I)¹ and its interpretation is not fully obvious, in particular the “consequences of human errors”.

In addition, potential damage shall be avoided or limited by appropriate choice of one or more of the following:

- avoiding, eliminating or reducing the hazards to which the structure can be subjected;
- selecting a structural form which has low sensitivity to the hazards considered ;
- selecting a structural form and design that can survive adequately the accidental removal of an individual member or a limited part of the structure, or the occurrence of acceptable localised damage ;
- avoiding as far as possible structural systems that can collapse without warning ;
- tying the structural members together (EN 1990, 2.1(5)P).

Specific requirements are taken into account in case of fire: the load bearing capacity is adequate for the required period of time, the generation and spread of fire and smoke are limited,

¹ In principle, this requirement will be kept in the future “Regulation of the European Parliament and of the Council” which should replace the CPD.

the spread of fire to neighbouring construction is limited, the occupants can leave the works or be rescued, the safety of rescue teams is taken into account.

In short, the first step of risk management is a good design to limit potential damage in case of undesired events. These events, idealised by accidental design situations, shall be sufficiently severe and varied so as to encompass all conditions that can reasonably be foreseen to occur during the execution and use of the structure (EN 1990, 3.2(3)P).

In EN 1991-1-7, the global strategy concerning accidental actions distinguishes “identifiable” accidental actions (impact, explosions) and actions “resulting from an unspecified cause” (in clear, unidentified actions). Of course, the selected design situations shall be sufficiently severe and varied so as to encompass all conditions that can reasonably be foreseen to occur during the execution and use of the structure (EN 1990, 3.2(3)P). Finally, it is the responsibility of the designer to define, for the client, possible reliability levels associated with risk levels (financial, economical, loss of human life, etc.).

4 APPROACH OF STRUCTURAL RELIABILITY IN THE EUROCODES

4.1 Reliability and reliability levels

Reliability is defined in EN 1990 (1.5.2.17) as the ability of a structure or a structural member to fulfil the specified requirements, including the design working life, for which it has been designed. Reliability is usually expressed in probabilistic terms. Structural reliability covers in fact three aspects: safety, serviceability and durability of a structure. A fourth concept was added in EN 1991-1-7, the concept of robustness.

Different levels of reliability may be adopted for structural resistance and for serviceability: they are selected by the designer who takes into account the possible cause and /or mode of attaining a limit state (i.e. an undesired phenomenon), the possible consequences of failure in terms of risk to life, injury, potential economical losses, public aversion to failure, the expense and procedures necessary to reduce the risk of failure.

4.2 How structural safety may be ensured?

The levels of reliability relating to structural resistance and serviceability can be achieved by various methods, or a combination of various methods, listed in EN 1990:

- a) preventative and protective measures ;
- b) measures relating to design calculations : representative values of actions, choice of partial factors ;
- c) measures relating to quality management ;
- d) measures aimed to reduce errors in design and execution of the structure, and gross human errors ;
- e) other measures relating to the following other design matters : the basic requirements ; the degree of robustness (structural integrity) ; durability, including the choice of the design working life ; the extent and quality of preliminary investigations of soils and possible environmental influences ; the accuracy of the mechanical models used ; the detailing ;
- f) efficient execution, *e.g.* in accordance with execution standards referred to in EN 1991 to EN 1999 ;
- g) adequate inspection and maintenance according to procedures specified in the project documentation.

Concerning design calculations, the first difficulty is that they are a method of representation of a highly complex reality, following rules which are sufficiently simple to be used by

designers. The simplifications do not have absolutely general validity, and any rule must have an assigned sphere of validity, and application of the Codes often necessitates a properly based appraisal (engineering judgment). Another difficulty arises from the fact that no universal measure of safety exists; *even a probability of failure is not invariant at the level of practical applications*, since it varies considerably depending on the information data and assumptions according to which it is calculated. For dealing with problems of structural safety there are three possible approaches: pragmatic (related to the past), dogmatic (related to the future), and progressive (related to the present).

4.2.1 - Definition, choice and classification of phenomena to be avoided; limit-states.

It is usually considered that the fundamental phenomena to be avoided are limit-states, generally highly idealized and hence conventional. However the concept of performance criteria is more general (it can directly include the past history of the structure).

For some limit-states (exceeding the bearing capacity), the first occurrence should be avoided; for other limit states (crack opening), only numerous repetitions cause damage; but many limit-states are of an intermediate nature (for example upheaval from a support).

Exceeding some limit-states involves immediate collapse (brittle fracture, loss of equilibrium) while other cases involve slow or progressive failure (ductile fracture, cracking). And there are intermediate cases.

Exceeding limit-states involves consequences which may be more or less serious. The most important of these consequences is the probability-greater or smaller - of the loss of human lives in greater or smaller numbers; it is seldom possible, where failure occurs, to assert that the risk of this is zero. In most cases the risks for the persons are indirectly taken into account by considering the risks for the structure itself.

Taking account of the above distinctions, the limit-states are grouped in categories corresponding to probabilities of the same order of magnitude. One category comprises the ultimate limit-states, another comprises the serviceability limit-states. Each category should then be sub-divided, e.g. according to whether the limit-state can be reached by the occurrence, on one or more occasions, of certain values of the variable actions, in order to determine the probabilities or permissible frequencies of reaching the corresponding action-effects.

Only certain limit-states can, more or less exactly, be studied by comparing the action-effects applied to a cross-section with resistances. To enlarge the field of application of a numerical value by artificial modification of another factor (compensation) can lead to confusion.

4.2.2 - Nature of the choices of acceptable probabilities of occurrence of phenomena to be avoided.

The choices of degrees of structural safety are not simple technical operations but, between certain limits, the result of arbitrary options of a political nature. It may however be supposed that dimensions close to the lower envelope of those resulting from different national codes should give satisfaction to the competent authorities.

As a consequence of the relative nature of the probability of occurrence of a limit state, the acceptance of a certain value (whether or not stated explicitly) of this probability is linked with the knowledge available at the time of this acceptance; the probability often has to be re-evaluated later on, and the consequences drawn from its acceptance then have to be reconsidered.

4.2.3 - The criteria which may be called into consideration when choosing the probabilities of phenomena to be avoided.

a) **Economic criteria**, when used for a simple optimization, have often led, for ultimate limit-states, to safety factors which are too low to be accepted. This is explained by the fact that aversion to the risk increases more than proportionally to the magnitude of the risk and

the corresponding probability. These criteria do however permit useful analyses and lead, for example, to introduction of the concept of economic barrier (important for ultimate states) and the concept of lifetime of a structure (design working life, important for some serviceability states and for fatigue).

b) **Analogic criteria** are based on knowledge of the risks supported or accepted in circumstances of human life unconnected with the safety of structures. Their relevance is indicative only. In particular, the death rate due to traffic accidents is very much higher than the rate that could be accepted as a result of accidents connected with structural failure.

c) **Psychological criteria** intervene in appraisals by individuals or groups of persons. Appraisals by the widest and the most permanent group constitute the public opinion. This one is subjective, deterministic, variable, emotional, and thus far from rational. For example, it pays more attention to the number of victims in a particular accident than to the total number of victims. Broadly, its demands result from recorded accidents and hence depend on the number of existing structures of different types.

d) **Legal criteria**, at the present time, have remained essentially deterministic, and hence cannot be used for making the choice. Attention is drawn to the fact that the need for clarification of the legal aspects of safety is keenly felt in many countries. Moreover, certain legal practices which automatically link accidents with mistakes and faults, as far as penalties are involved, without drawing certain distinctions, should be reformed.

e) **Ethical criteria** make it possible to take account of the value of human life by determining it indirectly by reference to analogic criteria. But they require in addition that account should be taken of the evolution of probabilities in the course of time in each particular case.

f) **Risks acceptable during execution** should be subjected to a special analysis which should examine certain specific concepts (consequences for the completed construction, nature of the accident at work, safety concerning the contractors execution measures, possibility of influencing the risk, temporary nature of the risk).

4.2.4 - Modification of acceptable probabilities depending on different criteria.

Modifications of this kind (reliability differentiation) should not be confused with modifications of factors intended to maintain the probabilities constant.

Several proposals of numerical values have been put forward during the last 30 years. Although they are of interest, they must be regarded as debatable and at all events not sufficiently defined to be able to be accepted at present as codified values.

In EN 1990 (Annex B), the question of relating different levels of control (or, better, of quality) to different design rules was introduced for the first time in an international design code.

4.2.5 - Conditional phenomena

The taking into account of conditional phenomena involves special technical methods and may necessitate certain specific options, depending for example on whether the conditional phenomena relate to structures considered in isolation or to a large number of structures simultaneously.

5 THE SEMI-PROBABILISTIC FORMAT (PARTIAL FACTOR DESIGN)

The basic principles of the semi-probabilistic format for the verification of construction works may be expressed as follows. The verification rules introduce safety:

- by selecting appropriate representative values of the various random variables (actions and resistances),

- through the application of a set of calibrated partial factors,

- through safety margins, more or less apparent, in the various models (models of actions, of effects of actions and of resistances).

In the most common cases, the verification of the safety of construction works is based on the verification of an equation of the following type:

$$E_d \leq R_d$$

where :

E_d is the design value of the effect of actions such as internal force, moment or a vector representing several internal forces or moments;

R_d is the design value of the corresponding resistance.

The general expressions for E_d and R_d are $E_d = E \gamma_{F,i} F_{rep,i}; a_d \}$ and

$$R_d = R \left\{ \eta_i \frac{X_{k,i}}{\gamma_{M,i}}; a_d \right\}$$

$F_{rep,i}$ is the relevant representative value of the action Nr. i (characteristic or other value);

a_d is the design values of the geometrical data

$X_{k,i}$ is the characteristic value of the material or product property Nr. i

η is the mean value of the conversion factor taking into account volume and scale effects, effects of moisture and temperature, and any other relevant parameters

$\gamma_{F,i}$ and $\gamma_{M,i}$ are the global partial factors for action effects and resistances. In fact, they may be considered as deriving from the following expressions: $\gamma_{F,i} = \gamma_{Sd} \times \gamma_{f,i}$

and $\gamma_{M,i} = \gamma_{Rd} \times \gamma_{m,i}$

where :

γ_{Sd} is a partial factor for the action which takes account of the possibility of unfavorable deviations of the action values from the representative values

$\gamma_{f,i}$ is a partial factor taking account of uncertainties in modelling the effects of actions, in some cases, in modelling the actions.

$\gamma_{m,i}$ is the partial factor for the material or product property to take account of:

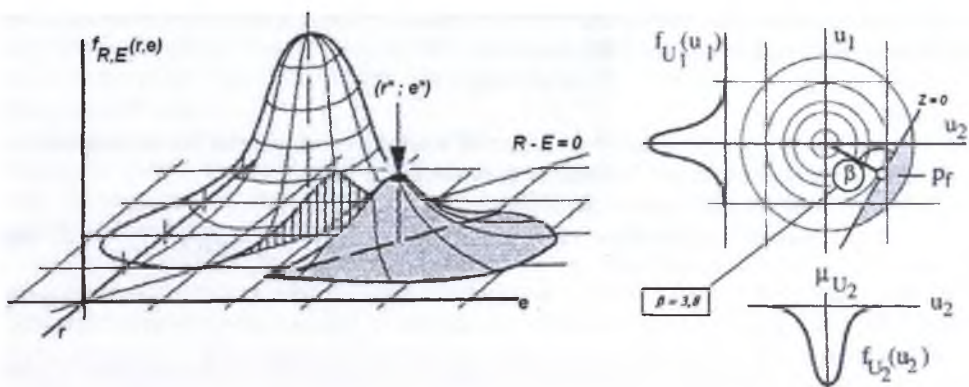
- the possibility of an unfavourable deviation of a material or product property from its characteristic value ;

- the random part of the conversion factor η .

γ_{Rd} is a partial factor covering uncertainty in the resistance model, plus geometric deviations if these are not modelled explicitly.

Thus, it may be observed that in the semi-probabilistic format of verification of construction works, the partial factors are not intended to cover gross errors.

Their numerical values, which have been partially calibrated by using the structural reliability methods, are, in principle, based on a target value of the reliability index β equal to 3,8, which means a probability of failure of $7,2 \cdot 10^{-5}$ in 50 years. The principles of the reliability theory (limited to the basic case of two random variables: E , effect of actions, and R , resistance) are summarized in figure 1.



Physical representation of the failure probability and coordinates of the design point Reliability index in the normalised space

Figure 1 – Principles of the reliability theory

Nevertheless, it is obvious that the partial factors cover “small errors”. But where is the boundary between “small” and “gross” errors? Is it possible to compare a human error during execution and the misuse of a sophisticated software?

6 RISKS IN CIVIL ENGINEERING

Structural failures may happen during execution, immediately after execution or during normal use of construction works. In the following, a few recent cases are mentioned with some comments.

6.1 Accidents during execution, due to the design and execution process

Accidents are very frequent during execution. For example, there is probably one failure or collapse per week during construction of bridges in the World. In general, if the number of fatalities is low, information of the public is limited. The causes may be varied:

- human error (the most frequent) associated to a lack of supervision of execution,
- errors or underestimations in the design (inappropriate mechanical models, underestimation of actions –direction and magnitude – hazard scenarios not taken into account, construction processes, etc.);
- underestimation of problems due to an insufficient appraisal of scaling effects;
- excessively ambitious projects (architects, engineers, etc.).

Examples

- Seven Indian workers were killed and 24 injured when a bridge under construction collapsed in Dubai Marina in the new part of the city, November 2007, in the evening. An ‘error’ by a crane driver as well as poor site-supervision could have caused the accident. Apparently, the crane driver had tried to lift a 1,5 tonne load of steel onto the bridge. The load, however, hit against the bridge columns causing it to collapse. The fault is two-fold: the driver’s miscalculation of the height of the steel columns, and lack of site supervision. But other eye witnesses described an excessive amount of steel placed on a bridge segment during a crane movement.

- Hyderabad flyover collapsed during execution (September 2007). The causes are probably wilful negligence and faulty design.

- Bridge near Fenghuang (China, August 2007) – 64 fatalities, 22 injured.

Apparently, planners had opted for a traditional stone design so that it would be “in harmony with the local natural environment.” The bridge had been capped by four large stone

arches. It was immediately recognised that the design was poor and that the reinforcement of concrete parts was underestimated.

6.2 Accidents immediately after execution

Accidents arriving “immediately” after execution, i.e. after a few months or one or two years after the construction works are in use, are often difficult to explain. They may be due to an unforeseen short term behavior of the ground supporting the foundations.

Examples

- The failure may be due to an exceptional event but with effects not recognised or highly underestimated : the first Tay Bridge fell down in 1879 under wind loading ; the Tacoma Narrows bridge failure in 1940 highlighted how much there was to learn about wind aerodynamics and since that time several structures have suffered from oscillation in wind.

- Roissy Airport Terminal 2E in May 2004. 4 fatalities. The phenomenon which originated the collapse is not perfectly clear: punching of vault? Excessive deformation due to creep of concrete connecting precast members, underestimation of thermal effects? In fact, the structural design process was weak in the early phases, the structural section was not intrinsically robust, the time effects were underestimated, and the quality control process of the design was poor. And, overall, nobody took care of the progressive cracking of concrete members, cracking which started immediately after construction.

- Karachi, September 2007. The bridge was opened only two months ago. The cause of the accident was not immediately clear. Witnesses said a portion of the bridge known as Northern Bypass fell with a huge bang while traffic was on it.

In short, some structures have a “global safety factor” just higher than 1, and the little safety margin evaporates very quickly.

6.3 Accidents during normal use of construction works

Accidents during normal use of construction works may have many origins : scour effects due to exceptional flood, impacts and explosions, errors in dynamics (footbridges, football stands under crowd loading), errors in stability (in particular in case of structural modification of a building), lack of maintenance, etc.

Concerning gas explosions, the recent accident in the French city Lyon (28 February 2008 – 1 death, 40 injured) shows that external explosions should be taken into account, where relevant, as possible hazard scenarios.



Figure 2 – Gas explosion in the city Lyon

In this case, a few floors of neighboring buildings were destroyed because they had not been designed to resist the overpressure due to such an event. Gas explosions due to works in urban streets are rather frequent ...

The following non exhaustive list gives some hazards which may be encountered for construction works in use, or between uses and after use.

a) in use

to people in building

- stairs, floor finishes, glazing

to structure and people

- inadequate maintenance
- change of use

b) in maintenance

to people doing maintenance

- access, confined spaces
- hot materials, toxic materials
- falls from height, fragile roofs

c) in extension refurbishment and repair

- misunderstanding the original structure
- faults in the original structure
- earlier inappropriate modifications

d) in assessment

- incorrect assumptions (materials, structural form, loads)
- inadequate inspection

e) in demolition

- misunderstanding structure
- defects in structure
- inappropriate approach
- premature collapse, flying debris
- high risk elements; cantilevers, flat slabs, prestressed structures, retaining structures.

Of course, at any time, you may encounter risks like abnormal settlement, chemical attack in the ground, overload, misuse, terrorism, explosion, impact, instability, lack of redundancy or other robustness, novel materials and design concepts, corrosion and ageing, progressive/disproportionate collapse, risks to, or from, adjacent buildings, structures and other facilities.

6.4 Accidents and Codes of practice

Codes of Practice provide guidance to designers. Many contain the stipulation that they must be used by qualified and experienced engineers like in the general assumptions of the Eurocodes. In effect, the judgements which are common to most designs have been taken by the authors of the code, and the results set down in a manner which can be applied in design. By using a code of practice, the engineer implicitly accepts those judgements, in many cases without fully understanding the basis for them, or the limits on their application.

In particular, codes assume that the structures they are applied to are 'normal' structures, and designers are not always able to recognise complexity. Complexity in the field of bridges may be more easily identified than complexity in the field of buildings. Outstanding structures are sometimes design by Architects who consider themselves as artists, and the problems of safety are to be dealt with by engineers, with poor fees !...



Figure 3 – Future Concert Hall in Paris-La Villette (design Jean Nouvel – A finite element model was established to check the stability immediately after the first sketch).

Should innovation be limited to avoid risks due to complexity? Of course, no. But for that reason the Eurocodes have introduced the principle, and some rules, of robustness.

Robustness is the ability of a system to resist damage but maintain its important functions. It is not limited to structures or even to physical systems; robustness principles can be applied to management systems. Robustness is somewhat different to other risk management systems in that it does not necessarily eliminate or reduce known risks, although it may do. Its primary value is in reducing the effect of unknown risks.

Strength and robustness are different. A single cantilever beam as a part of the main stability system should not be considered robust, however strong it might be, since its failure would lead to failure of the whole system. Although none of the design load cases could cause it to fail, it might be vulnerable to terrorist attack or a previously undiscovered form of brittle fracture.

For the first time, in an international code, EN 1990 proposes a classification of construction works, for the purpose of reliability differentiation, based on “consequences classes” (CC), i.e. by considering the consequences of failure or malfunction of the structure. This classification is described in the following Table (EN 1990, Table B1).

Consequences Class	Description	Examples of buildings and civil engineering works
CC3	High consequence for loss of human life, <i>or</i> economic, social or environmental consequences very great	Grandstands, public buildings where consequences of failure are high (e.g. a concert hall)
CC2	Medium consequence for loss of human life, economic, social or environmental consequences considerable	Residential and office buildings, public buildings where consequences of failure are medium (e.g. an office building)
CC1	Low consequence for loss of human life, <i>and</i> economic, social or environmental consequences small or negligible	Agricultural buildings where people do not normally enter (e.g. storage buildings), greenhouses

Table 1: Definition of consequences classes

The criterion for classification of consequences is the importance, in terms of consequences of failure, of the structure or structural member concerned. Reliability classes are associated to these consequence classes.

This classification is refined for buildings in EN 1991-1-7 as shown in the following table (EN 1991-1-7, Table A.1).

Consequence class	Example of categorisation of building type and occupancy
1	Single occupancy houses not exceeding 4 storeys. Agricultural buildings. Buildings into which people rarely go, provided no part of the building is closer to another building, or area where people do go, than a distance of $1\frac{1}{2}$ times the building height.
2a Lower Risk Group	5 storey single occupancy houses. Hotels not exceeding 4 storeys. Flats, apartments and other residential buildings not exceeding 4 storeys. Offices not exceeding 4 storeys. Industrial buildings not exceeding 3 storeys. Retailing premises not exceeding 3 storeys of less than $1\,000\text{ m}^2$ floor area in each storey. Single storey educational buildings All buildings not exceeding two storeys to which the public are admitted and which contain floor areas not exceeding 2000 m^2 at each storey.
2b Upper Risk Group	Hotels, flats, apartments and other residential buildings greater than 4 storeys but not exceeding 15 storeys. Educational buildings greater than single storey but not exceeding 15 storeys. Retailing premises greater than 3 storeys but not exceeding 15 storeys. Hospitals not exceeding 3 storeys. Offices greater than 4 storeys but not exceeding 15 storeys. All buildings to which the public are admitted and which contain floor areas exceeding 2000 m^2 but not exceeding 5000 m^2 at each storey. Car parking not exceeding 6 storeys.
3	All buildings defined above as Class 2 Lower and Upper Consequences Class that exceed the limits on area and number of storeys. All buildings to which members of the public are admitted in significant numbers. Stadia accommodating more than 5 000 spectators Buildings containing hazardous substances and /or processes

Table 2 : Categorisation of consequences classes

Strategies are recommended for each class. For example, for buildings in Consequences Class 2b (Upper Group), their design should provide horizontal ties for framed and load-bearing wall construction, together with vertical ties, in all supporting columns and walls, or alternatively, the building should be checked to ensure that upon the notional removal of each supporting column and each beam supporting a column, or any nominal section of load-bearing wall (one at a time in each storey of the building) the building remains stable and that any local damage does not exceed a certain limit.

For buildings in Consequences Class 3, a systematic risk assessment of the building should be undertaken taking into account both foreseeable and unforeseeable hazards.

The proposed rules are only recommended rules to ensure some structural robustness.

7 CONCLUSIONS

Should design codes, and Eurocodes in particular, go beyond what is currently proposed? It is clear that the principles are good, but after, it is a matter of quality in the design, construction and maintenance processes. Lessons from accidents inspire the following additional list of design principles:

- Even if all individual parts of a structure are correctly designed, check the stability of the structure as a whole and ensure a minimum robustness.
 - Avoid structures the stability of which is ensured by ties anchored in the ground and not protected against corrosion, exceptional or malicious actions.
 - Avoid structures which are not damage-tolerant with regard to fatigue.
 - Avoid structures with brittle members or sections: in case of rupture there is no pre-warning (the structure should be fault tolerant up to a certain degree).
 - Avoid a too slender structure if a refined and pertinent dynamic analysis cannot be performed.
 - Take into account structural effects of climatic changes.
- Concerning the design process, risks are increasing for the following reasons:
- The societal needs are increasing.
 - The cost of the structural part of construction works is decreasing (competition, global economy).
 - As a consequence of the previous observation, engineering services are not correctly remunerated, time for design and construction is more and more shortened, the design is ensured by very small (and cheap) design offices without real technical competence, personnel on construction sites are not experienced, the control of quality by specialised companies is underpaid. All that is represented in Figure 4.

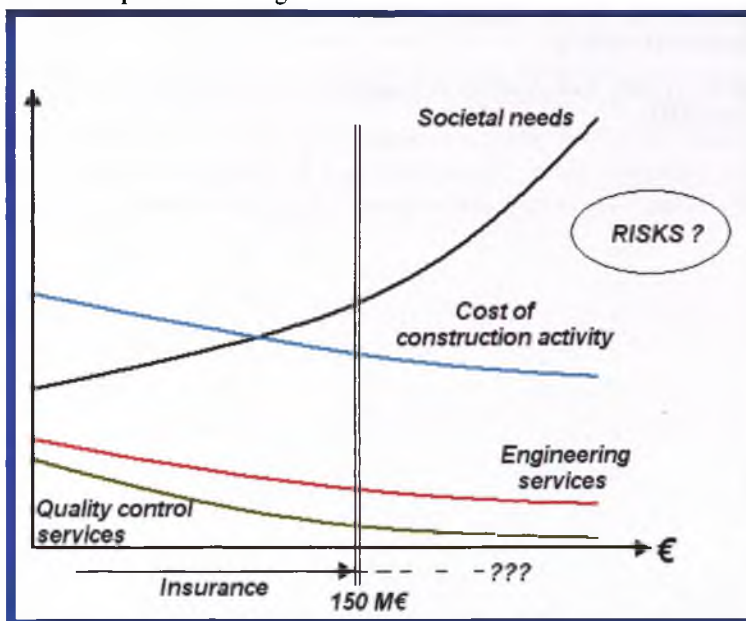


Figure 4 – Risks and engineering activity: a dilemma

Finally, a system where all the calculations produced in a small design office are checked by the same person is not robust. Due to time constraints, the models may be inappropriate, the designer may have misunderstood the code, an important principle or a rule, or may fail to

spot an error due to a particular combination of personal circumstances. Hopefully, for big projects, there is often a panel of experts following seriously the design process and give their opinion in reviews of the proposed approach. In some cases, sensitivity studies may be one way to judge the severity of a risk.

Finally, it is difficult to envisage an extension of the design codes to improve the situation concerning the management of risks in civil engineering: it is not a matter of partial factors or of probabilistic approach; it is more a matter of education, in particular in engineering schools and universities and of organisation of the construction industry.

BIBLIOGRAPHY

- [1] J. Schneider, Introduction to Safety and Reliability of Structures. Structural Engineering Documents Nr.5, IABSE, 1997.
- [2] La Sécurité des Grands Ouvrages, coordonné par P. Delage, P. Habib, V. De Gennaro. Presses des ponts et Chaussées, 2000
- [3] J.-A. Calgaro, H. Gulvanessian “ Management of reliability and risk in the Eurocode system”. IABSE International Conference “Safety, Risk and Reliability – Trends in Engineering”, Malta 21-23 mars 2001
- [4] J.-A. Calgaro, Maîtrise des Risques et Codes Européens de Conception et de Calcul. Colloque international « Risque, vulnérabilité et fiabilité dans la construction » - Alger, 11 et 12 octobre 2003.
- [5] ISO/CD 13824 N180. General Principles on Risk Assessment of Systems Involving Structures.TC98/SC2
- [6] Bilal M. Ayyub, Risk Analysis in Engineering and Analysis. Chapman Hall/CRC, Boca Raton (2003).

WIND AND FIRE

Prof. Pierre E. Spehl

Bureau de contrôle SECO
Rue d'Arlon 53,B-1040 Brussels, Belgium
p.spehl@seco.be
Maître de conférences à l'ULB et à l'ENPC
Head of the Belgian delegation to CEN TC 250 « Structural Eurocodes »

Keywords: Wind, Fire, Regulation, Calculation, Standard, Eurocode.

Abstract. *This paper describes how to evaluate exceptional actions due to wind and accidental actions on structures exposed to fire. It refers to the structural Eurocodes, the most advanced set of standards, which have been completed in 2007. The paper reviews the possible wind actions and their dynamic effects on structures and presents alternative evaluation methods for each phenomenon. It explains the influence of legislation on the design procedures and presents different approaches available to evaluate the heating of structures by fires, and its effects.*

1 INTRODUCTION

Wind and fire engineering have been developed in the last 50 years.

During the First International Conference on Wind engineering at TEDDINGTON (UK) in 1963, the first calculation models of wind dynamics were presented by C. SCRUTON and A. G. DAVENPORT for buildings. Since then, every 4 years, the next international conferences have been the key events to record the progresses made in wind engineering. National standards have been published to provide simple calculation methods of wind pressures and forces on buildings and civil engineering works. In 2010, these standards will have to be replaced in the member States of the European Union by Eurocode 1, Part 1.4 "Wind actions".

The starting point of the development of fire engineering has been the publication of the International standard ISO 834 in 1968, which defines a nominal fire heating curve over time. This ISO curve remains the only curve on which most of the national fire regulations are based. From fire tests of resistance to fire of structural elements, calculation methods have been developed for structures made of concrete, steel, timber and masonry. They have been standardized directly as European standards, i.e. Parts 1.2 of Eurocodes 2 to 6. Heating models alternative to the ISO curve are intended to represent more accurately the "natural fires" i.e. the heating produced by the real burning materials and their quantities present in the buildings. They are presented in informative annexes to the Part 1.2 of Eurocode 1 and may be useful when these materials and quantities are known and are not likely to change too much over time.

2 WIND

2.1 Natural wind

Wind is a random variable action. Storms may have devastating effects, as shown in figure 1.

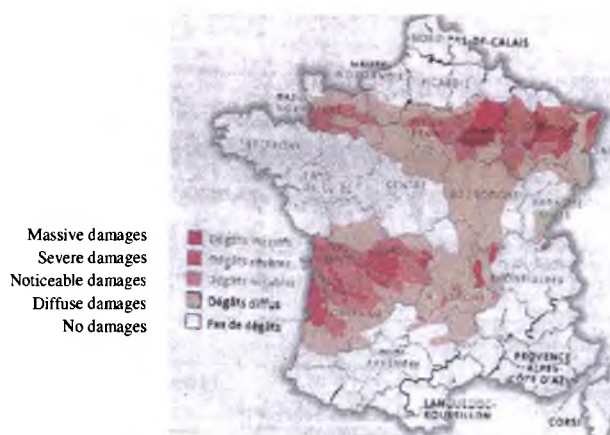


Figure 1: Damages to the forests of France from two wind storms in December 1999.

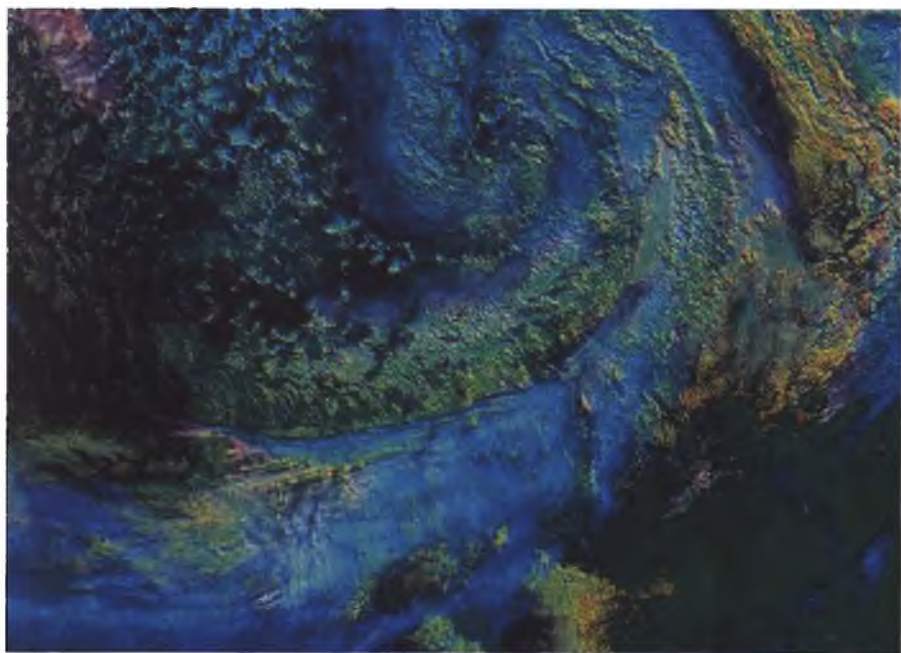


Figure 2: The wind storm of 25 January 1990 over Central Europe.

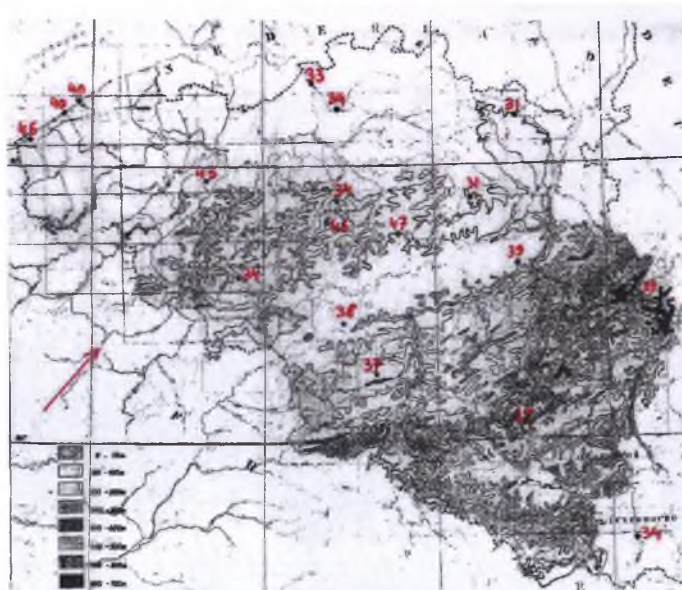


Figure 3: Maximum peak wind velocities (m/s) measured on 25 January 1990 in Belgium (WMO standard).

The satellite picture of figure 2 shows the exceptional cyclonic storm of 25 January 1990 moving from West to East over Central Europe. The wind velocity in a cyclone is greatest when the low pressure is lowest. The maximum wind velocities measured at 18 Belgian meteorological stations (figure 3) denote variations due to the non-simultaneity of the greatest mean velocity and an extreme gust.

Figures 4 and 5 give the wind velocity during that storm recorded at two of these met stations, one in open country (BEAUVECHAIN), where the turbulent fluctuations are low, and one in a suburb of BRUSSELS (UCCLE), where they are high. During 15 minutes around 14h15, a general increase of the velocities is to be noticed, due to a jet stream approaching the ground.

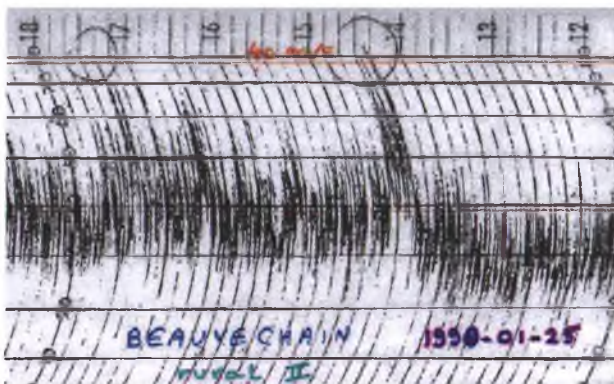


Figure 4: Wind velocity recorded (in knots) on 25 January 1990 in BEAUVECHAIN airport.

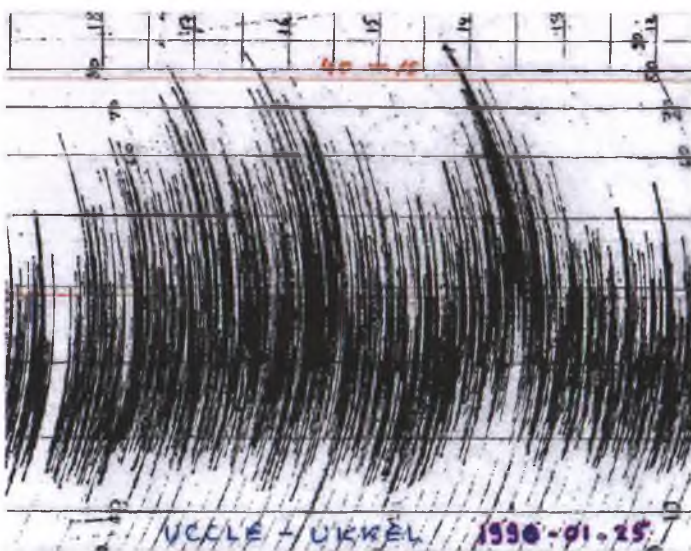
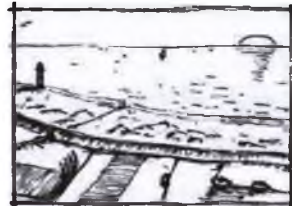


Figure 5: Wind velocity recorded (in knots) on 25 January 1990 in UCCLÉ (Brussels).

The friction of the wind flow on the ground creates a turbulent boundary layer which extends in height and in intensity as a function of the roughness of the terrain. The European standard EN 1991-1-4:2002 (Eurocode 1, Part 1-4) defines 5 standard terrain categories (figure 6).

Terrain category 0

Sea, coastal area exposed to the open sea



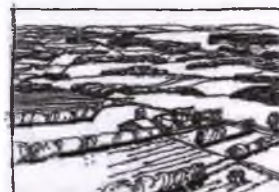
Terrain category I

Lakes or area with negligible vegetation and without obstacles



Terrain category II

Area with low vegetation such as grass and isolated obstacles (trees, buildings) with separations of at least 20 obstacle heights



Terrain category III

Area with regular cover of vegetation or buildings or with isolated obstacles with separations of maximum 20 obstacle heights (such as villages, suburban terrain, permanent forest)



Terrain category IV

Area in which at least 15 % of the surface is covered with buildings and their average height exceeds 15 m

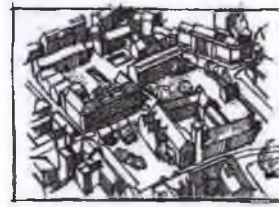


Figure 6: Illustration of the upper roughness of the standard terrain categories (EN 1991-1-4:2002).

The peak velocity pressure $q_p(z)$ at height z above the terrain, which includes mean and short-term velocity fluctuations is given by equation (4.8)

$$q_p(z) = [1 + 7 \cdot I_v(z)] \cdot \frac{1}{2} \cdot \rho \cdot v_m^2(z) = c_e(z) \cdot q_b \quad (4.8)$$

where:

$v_m(z)$ is the mean wind velocity, depending on the terrain roughness and orography

$I_v(z)$ is the turbulence intensity, defined as the standard deviation of the turbulence divided by $v_m(z)$

ρ is the air density, which depends on the altitude, temperature and barometric pressure to be expected in the region during wind storms

$c_e(z)$ is the exposure factor given in Expression (4.9)

$$c_e(z) = \frac{q_p(z)}{q_b} \quad (4.9)$$

q_b is the basic velocity pressure given in Expression (4.10)

$$q_b = \frac{1}{2} \cdot \rho \cdot v_b^2 \quad (4.10)$$

v_b is the basic wind velocity (characteristic 10 minutes mean wind velocity, irrespective of wind direction and time of year, at 10 m above flat ground of terrain category II, having an annual probability of exceedence of 0,02 (which is equivalent to a mean return period of 50 years)

Figure 7: Peak velocity pressure $q_p(z)$ at height z above the terrain (EN 1991-1-4:2002).

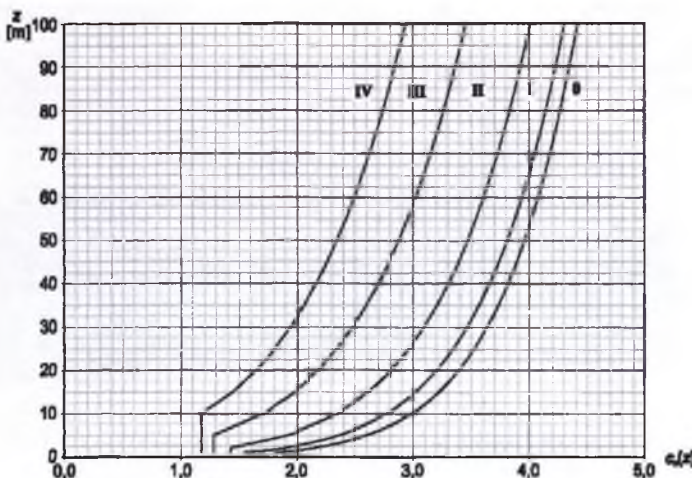


Figure 8: Exposure factor $c_e(z)$ on flat terrain (EN 1991-1-4 :2002).

The statistical distribution of the maximal value of the peak velocity pressure in central Belgium is illustrated by figure 9 : the maximal value each year may remain for several years around the 500 Pa and suddenly become more than 2 times that value the next year.

Figure 10 gives an illustration of the variation of the basic wind velocity in Europe (ECCS – European Convention for Constructional Steelwork – Report 52, 1988) and the wind map of Belgium given in the new National Annex (NBN EN 1991-1-4-NA:2008).

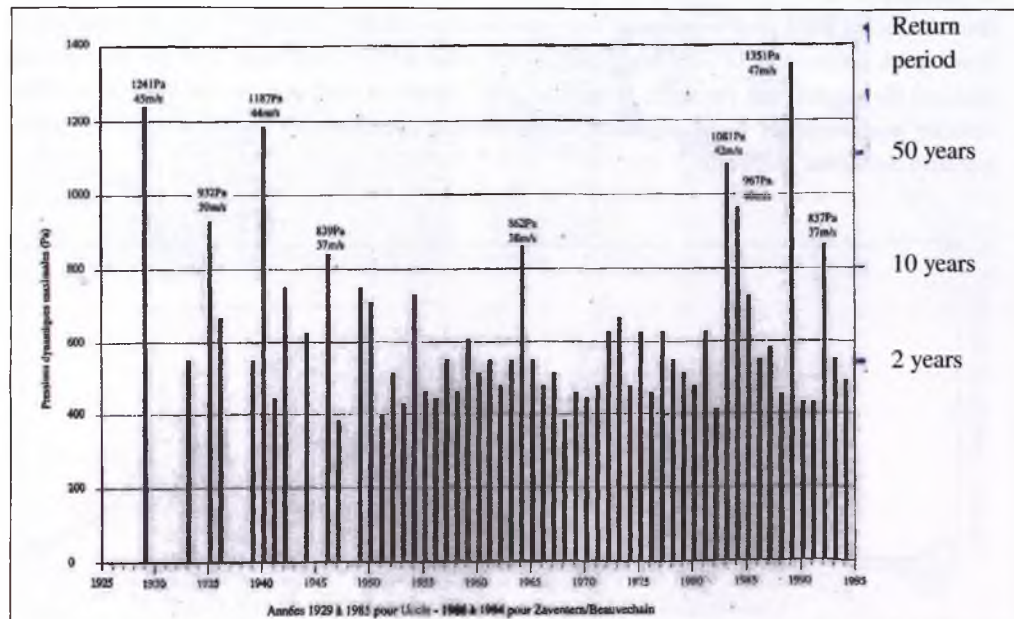


Figure 9: Annual maximal value of the peak velocity pressure in central Belgium (WMO standard).

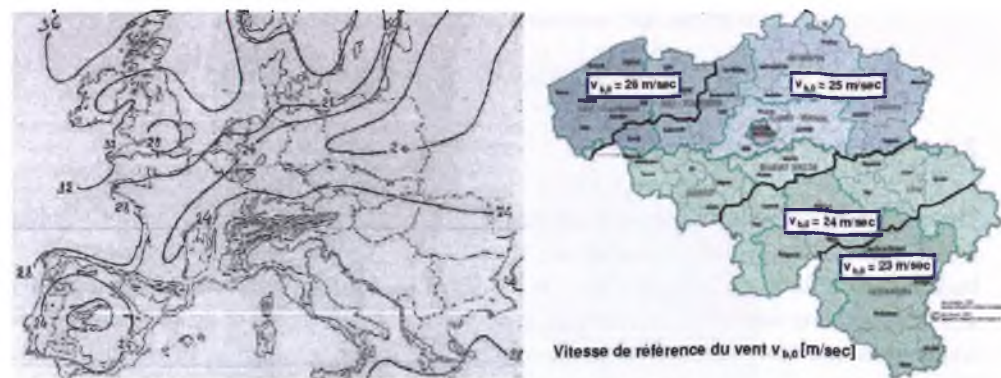


Figure 10: Basic wind velocity in Europe (ECCS:1988) and in Belgium (NBN EN 1991-1-4-NA:2008).

The turbulence intensity may be analyzed statistically in the frequency domain : by a FOURRIER transformation of the velocity measured over time, a spectral density function may be calculated. Figure 11 illustrates one of the first wind spectrum established over the full frequency domain by VAN DER HOVEN from wind measurements at BROOKHAVEN (NEW YORK). From right to left, a first peak centered at a wind fluctuation periodicity of 1 minute represents the wind turbulence, a second peak centered on 4 days represents the periodicity of the cyclones displacements from West to East (with a secondary peak at $\frac{1}{2}$ day for the nights and days fluctuations), a third peak centered at one year (winter-summer variations), and an hypothetical fourth peak centered at 11 year depending on the solar activity variations. The gap between the first and the second peak (between 10 minutes and 2 hours) is used as period of integration of the velocity measurements when calculating the statistical parameters of the wind velocity (mean, standard deviation, spectrum).

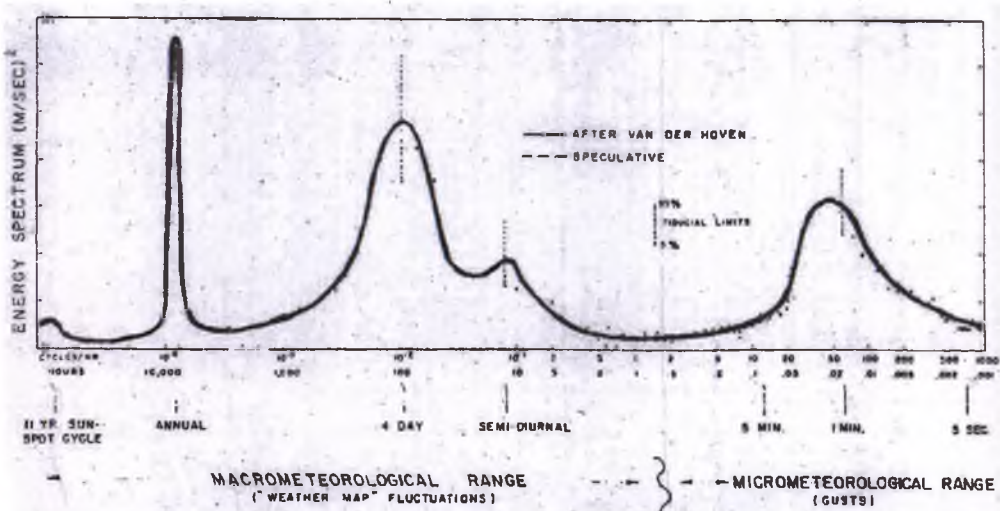


Figure 11: Wind velocity spectrum in BROOKHAVEN (NEW YORK) after VAN DER HOVEN.

2.2 Wind pressure on surfaces

The on-coming wind flow is deviated by the building creating an overpressure on the windward façade (figure 12). At the corners of the front façade, the deviated flow separates from the building and a turbulent boundary layer is generated by the friction between itself and the air along the building sides and vertical vortices are formed alternately along the two building sides, which grow and move leeward. In addition, the deviated flow recirculates behind the building. These air circulations generate wind suction (depressurization) on the lateral and rear façades, and on the roof.

The wind pressure acting on the external surfaces of a building is given by equation (5.1) of figure 13. The external pressure coefficients values given in standards for a large variety of buildings and civil engineering works are derived from pressure coefficient distributions obtained from wind tunnel tests or sometimes from full scale measurements (figure 14).

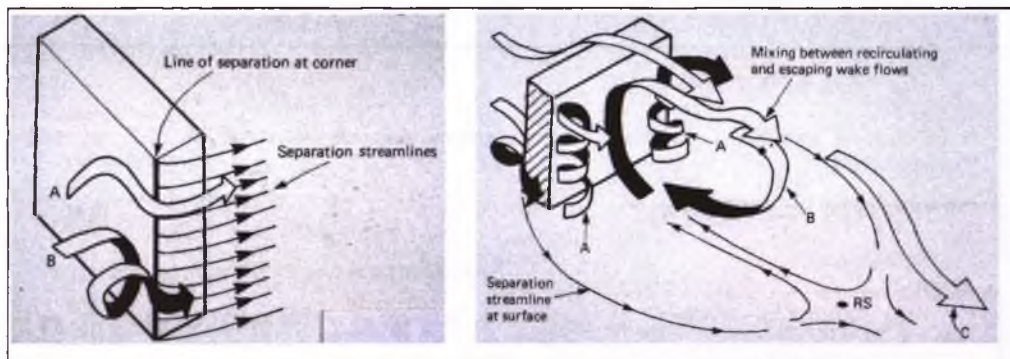


Figure 12: Flow deviations around a building.

$$w_e = q_p(z_e) \cdot c_{pe} \quad (5.1)$$

where:

$q_p(z_e)$ is the peak velocity pressure

z_e is the reference height for the external pressure given in Section 7

c_{pe} is the pressure coefficient for the external pressure, see Section 7.

Figure 13: Wind pressure w_e acting on an external surface (EN 1991-1-4 :2002).

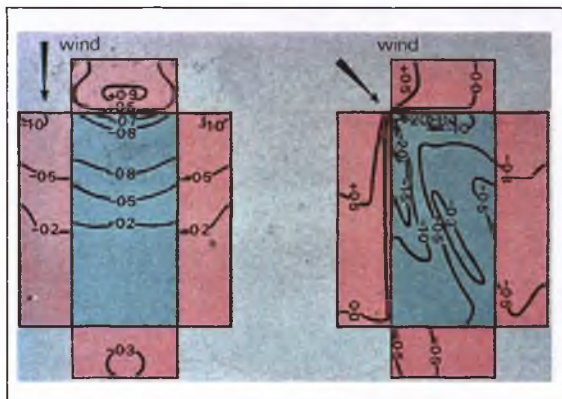


Figure 14: Example of external pressure coefficient distribution from wind tunnel tests.

2.3 Wind forces

The wind force acting on a structure or a structural component should be determined :

- by calculating forces F_w using force coefficients c_f (see figures 15 and 16),
- or by calculating forces F_w from surface pressures (see figure 17).

$$F_w = c_s c_d \cdot c_f \cdot q_p(z_e) \cdot A_{ref} \quad (5.3)$$

or by vectorial summation over the individual structural elements (as shown in 7.2.2) by using Expression (5.4)

$$F_w = c_s c_d \cdot \sum_{elements} c_f \cdot q_p(z_e) \cdot A_{ref} \quad (5.4)$$

where:

$c_s c_d$ is the structural factor as defined in Section 6

c_f is the force coefficient for the structure or structural element, given in Section 7 or Section 8

$q_p(z_e)$ is the peak velocity pressure (defined in 4.5) at reference height z_e (defined in Section 7 or Section 8)

A_{ref} is the reference area of the structure or structural element, given in Section 7 or Section 8

Figure 15: Wind force F_w calculated using force coefficients c_f (EN 1991-1-4 :2002).

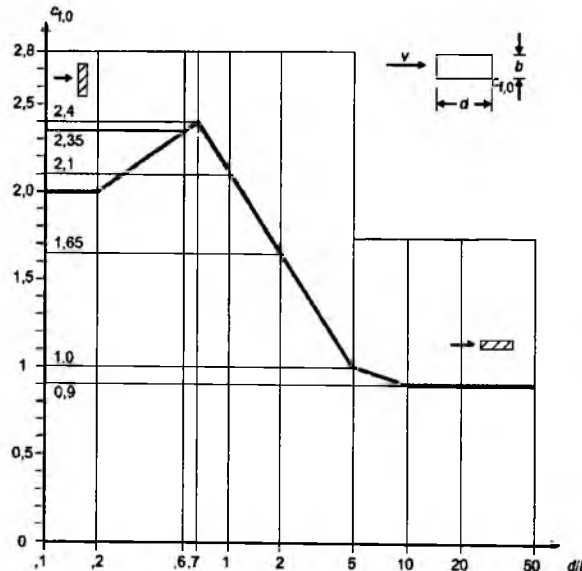


Figure 16: Example of force coefficients for a prismatic tall building (EN 1991-1-4 :2002).

external forces.

$$F_{w,e} = c_s c_d \cdot \sum_{\text{surfaces}} w_e \cdot A_{\text{ref}} \quad (5.5)$$

internal forces:

$$F_{w,i} = \sum_{\text{surfaces}} w_i \cdot A_{\text{ref}} \quad (5.6)$$

friction forces:

$$F_{fr} = c_{fr} \cdot q_p(z_e) \cdot A_{fr} \quad (5.7)$$

where:

- $c_s c_d$ is the structural factor as defined in Section 6
- w_e is the external pressure on the individual surface at height z_e , given in Expression (5.1)
- w_i is the internal pressure on the individual surface at height z_i , given in Expression (5.2)
- A_{ref} is the reference area of the individual surface
- c_{fr} is the friction coefficient derived from 7.5
- A_{fr} is the area of external surface parallel to the wind, given in 7.5.

Figure 17: Wind forces F_w calculated from surface pressures (EN 1991-1-4 :2002).



Figure 18: Wind tunnel model of ANTWERP Central Station

Data from standards are mostly used for design of new structures where a simple and safe approach is sufficient. When a more precise evaluation of wind pressures is needed to derive wind forces, for example when preparing rehabilitation works in existing structures, more accurate data from wind tunnel tests are usually preferred. For example (figure 18), the arched steel structure supporting the main hall of Antwerp Central Station, a wind tunnel test has authorized a reduction of the wind loads of about 50 % of the wind loads from standards.

2.4 Structural factor for along wind dynamic effects

The structural factor $c_s c_d$, defined in Eurocode 1 Part 1-4, takes into account

- the effect on wind actions from the non-simultaneous occurrence of peak wind pressures on the surface (size factor c_s)
- together with the effect of the vibrations of the structure due to resonance between turbulence and structural vibration modes (dynamic factor c_d).

The parameters defining the natural wind are determined at the height z_s defined in figure 19. The calculation procedure of the structural factor is described in figure 20.

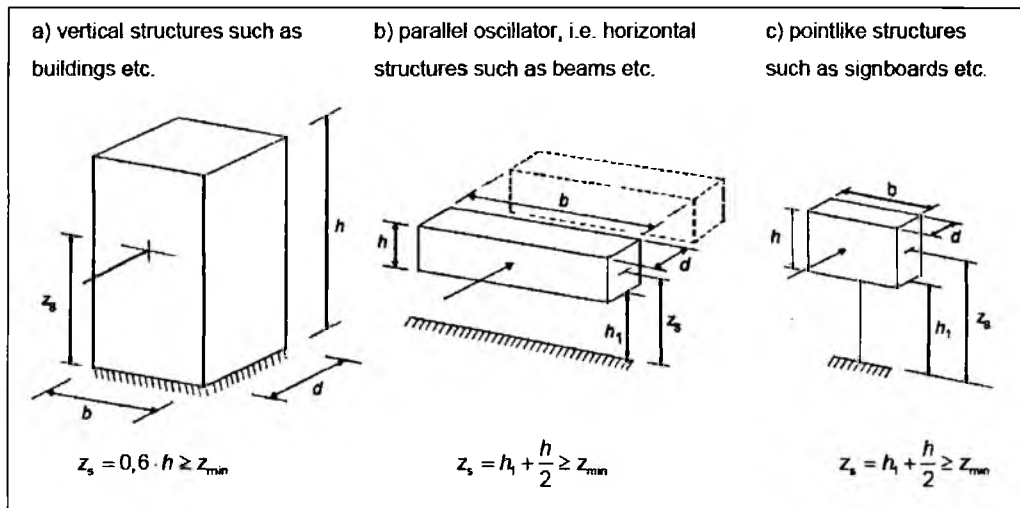


Figure 19: Structural dimensions and reference height z_s (EN 1991-1-4 :2002).

$$c_s c_d = \frac{1+2 \cdot k_p \cdot I_v(z_s) \cdot \sqrt{B^2 + R^2}}{1+7 \cdot I_v(z_s)} \quad (6.1)$$

where:

z_s is the reference height for determining the structural factor, see Figure 6.1. For structures where Figure 6.1 does not apply z_s may be set equal to h , the height of the structure.

k_p is the peak factor defined as the ratio of the maximum value of the fluctuating part of the response to its standard deviation

I_v is the turbulence intensity defined in 4.4

B^2 is the background factor, allowing for the lack of full correlation of the pressure on the structure surface

R^2 is the resonance response factor, allowing for turbulence in resonance with the vibration mode

$$B^2 = \frac{1}{1 + 0,9 \cdot \left(\frac{b+h}{L(z_s)} \right)^{0,63}} \quad (B.3)$$

where:

b, h is the width and height of the structure, see Figure 6.1.

$L(z_s)$ is the turbulent length scale given in B. 1 (1) at reference height z_s defined in Figure 6.1. It is on the safe side to use $B^2 = 1$.

$$L(z) = L_t \cdot \left(\frac{z}{z_t} \right)^\alpha \quad \text{for } z \geq z_{\min}$$

$$L(z) = L(z_{\min}) \quad \text{for } z < z_{\min} \quad (B.1)$$

with a reference height of $z_t = 200$ m, a reference length scale of $L_t = 300$ m, and with $\alpha = 0,67 + 0,05 \ln(z_0)$, where the roughness length z_0 is in m. The minimum height z_{\min} is given in Table 4.1.

$$R^2 = \frac{\pi^2}{2 \cdot \delta} \cdot S_L(z_s, n_{1,x}) \cdot R_h(\eta_h) \cdot R_b(\eta_b) \quad (B.6)$$

where:

δ is the total logarithmic decrement of damping given in F.5 (see figure 21)

S_L is the non-dimensional power spectral density function given in B.1 (2) (see figure 22)

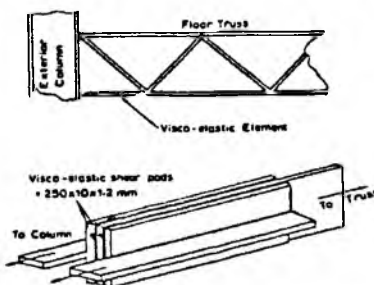
R_h, R_b are the aerodynamic admittance functions given in (6) (see figure 22)

Figure 20: Calculation procedure of the structural factor $c_s c_d$ (EN 1991-1-4 :2002).

$$\delta = \delta_s + \delta_a + \delta_d \quad (\text{F.15})$$

where:

- δ_s is the logarithmic decrement of structural damping
- δ_a is the logarithmic decrement of aerodynamic damping for the fundamental mode
- δ_d is the logarithmic decrement of damping due to special devices (tuned mass dampers, sloshing tanks etc.)



Example of special devices : 10.000 visco-elastic elements used in the New York twin towers.

Figure 21: Logarithmic decrement of damping δ (EN 1991-1-4 :2002).

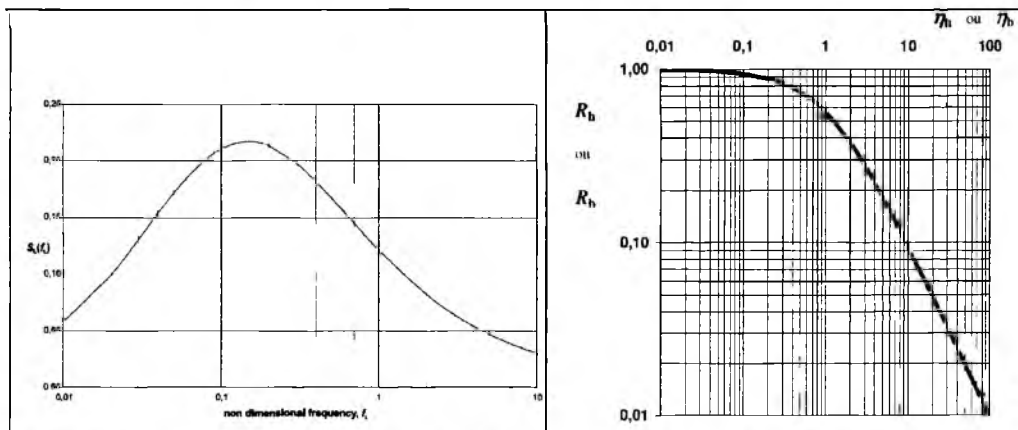


Figure 22: Power spectral density function S_L and aerodynamic admittance functions R_h and R_b (EN 1991-1-4 :2002).

When a more accurate evaluation is needed, wind tunnel tests may be performed to determine the simultaneous variation over time of the external pressure measured on a large amount of points and to use the results as external forces on a fully dynamic equations system representing the structure. Figure 23 shows the model of the new LIEGE Station (200 measurement points).



Figure 23: Wind tunnel model of the new TGV Station of LIEGE GUILLEMIN.

2.4 Across-wind dynamic effects

Vortices are shedding alternately from opposite sides of a structure and give rise to fluctuating load perpendicular to the wind direction. Structural vibrations may be amplified by resonance effect if the frequency of vortex-shedding is the same as a natural frequency n of the structure. This condition is obtained when the wind velocity is equal to a critical wind velocity V_{crit} (figure 24). Typically, the critical wind velocity is a frequent wind velocity indicating that fatigue, and thereby the number of load cycles, may become relevant. The vibrations may be reduced by reducing the fluctuating load (e.g. by increasing of the surface roughness of cylinders, see figure 25) or by increasing the damping by special devices such as tuned mass dampers.

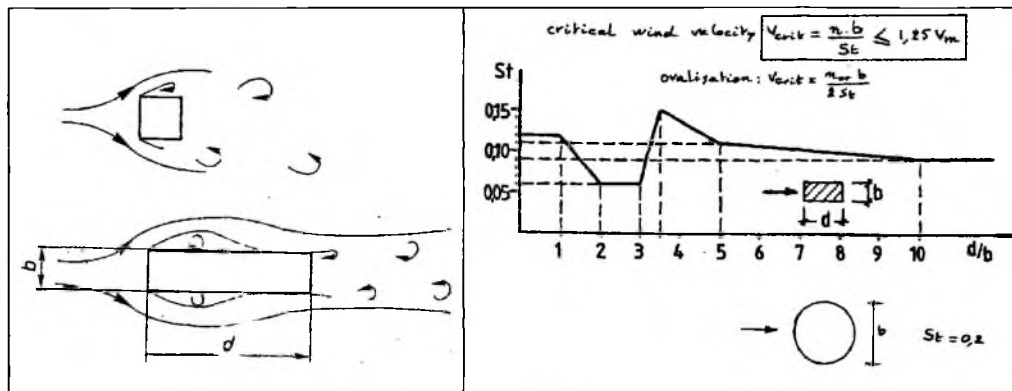


Figure 24: Vortex-shedding and critical wind velocity (EN 1991-1-4 :2002).

In addition, very flexible structure may be susceptible to aerodynamic instabilities. These may occur when the across-wind vibrations increase progressively the energy of the vortices :

- Galloping is a self-induced vibration in cross bending mode. Non circular cross sections including L-, I-, U- and T-sections are prone to galloping. Ice may cause a stable cross section to become unstable.
- Divergence and flutter are instabilities that occur for flexible plate-like structures, such as signboards or suspension-bridge decks, above a certain wind velocity. The instability is caused by the deflection of the structure modifying the aerodynamics to alter the loading. Divergence and flutter should be avoided. Figure 25 shows the torsional flutter oscillation of the TACOMA bridge near SEATTLE (USA) which caused collapse in 1940.

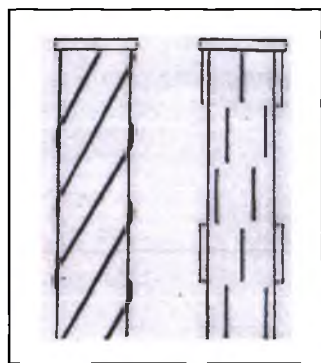


Figure 24: Means to reduce the fluctuating load on a cylinder.

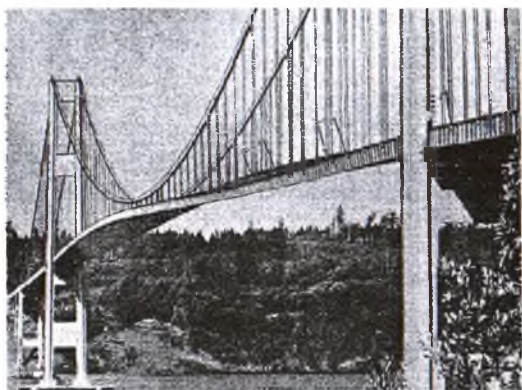


Figure 25: Torsional flutter oscillation of TACOMA bridge.

2.5 Tornadoes

Tornadoes are rising vortices which may have very local but devastating effects (on about 1 km²) every 2 or 3 years in central Europe (figures 26 and 27). Their risk to occur on a structure is approximately 10⁻⁵/year. Tornadoes are therefore not considered for design ordinary structures.



Figure 26: Tornado of 4 May 1961 at EVREUX and physical principle.



Figure 27: Erosion of a tornado in freshly ploughed ground.

However structures in Europe classified as “major risk” (reliability class RC3 according to NBN EN 1990, Annex B) have to be designed against tornadoes. In this case, a peak velocity pressure $q_p = 6000 \text{ N/m}^2$ should be considered independently of height and terrain category. Red areas and arrows on the world map of figure 28 show where tropical cyclones occur (hurricanes, typhoons).

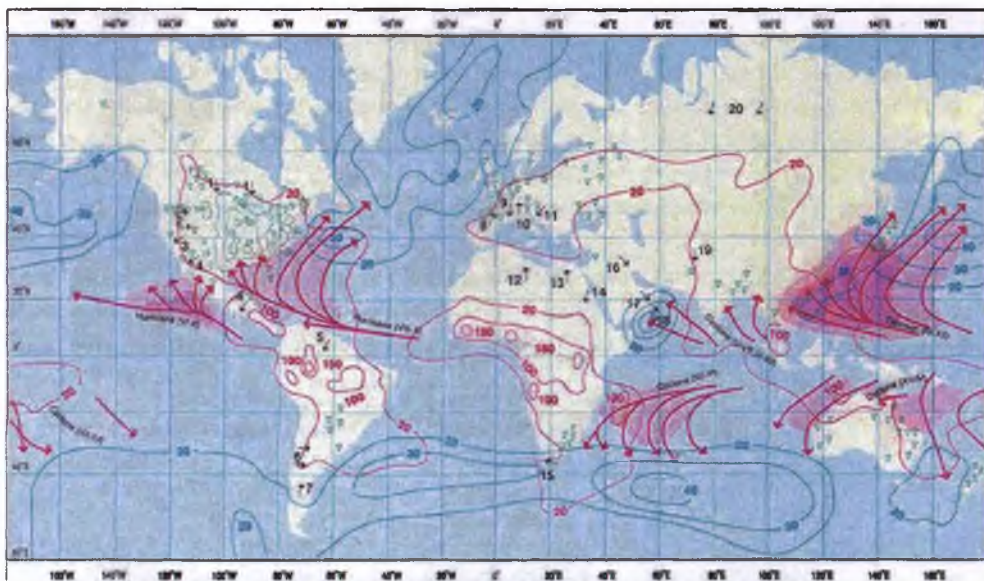


Figure 28: World map of tropical cyclones (Münchener Rückversicherungs-Gesellschaft).

3. FIRE

3.1 Legislation on safety of constructions

The legislation on safety of constructions, in Belgium like in other Latin countries, is derived from the principles defined more than two centuries ago, at the time of the French revolution.

The stability and mechanical resistance of constructions is regulated since 1804 by article 1792 of the Civil Code of NAPOLEON :

"If the edifice, built at a set price, perish in whole or in part by defect in its construction, even by defect in the foundation, the architect and the contractor are responsible therefore for ten years."

This principle is one of the first performance requirement and probably the most important one. In Belgium, there is no other building regulation, except for fire safety and electrical installations. The responsibilities of the architects and the contractors are evaluated a posteriori (i.e. after a damage) by the Courts of Justice. In their judgments, they refer to the rules of good practice (standards, codes, published and accepted technical information documents, ...) available at the time of the construction, and the jurisprudence of the Courts has a quasi-regulatory character.

The experience of big fires in buildings has shown that the same principle of responsibility doesn't provide a similar level of safety, mainly because of the low probability of big fires. Fire safety rules should be a priori imposed by the public authorities. In 1790, a decree of the French National Assembly has stated "*The commune has the mission to prevent and let cease the fires*". It is still applied today through the advices of the Fire Brigades requested and imposed by the communes. More recently, innovative and industrialized construction methods have created new needs for technical requirements imposed uniformly throughout the country, leading the Public Authorities to introduce fire regulations. It is the case since 1952 for the work places (General Regulation for the Protection of the Work), and since the law of 30 July 1979 for any building (Royal Decree of 7 July 1994 imposing basic standards for fire safety in new buildings).

Under the Civil Code, standards like Eurocodes are the referenced good practice but they are not compulsory ("if you know better, you may do it"). On the contrary, a law and its regulations, like fire regulations, apply a priori, and standards imposed by regulations are compulsory (figure 29).

Source	CIVIL CODE	LAW
Technical requirements	JURISPRUDENCE of the COURTS	REGULATIONS
Application	a posteriori	a priori
Standards (e.g. Eurocodes)	Referenced good practice but not compulsory	Compulsory only if imposed by regulation

Figure 29: Applicability of standards on safety of constructions

In addition, the Construction Products Directive 89/106/EEC is introducing an obligation to declare the characteristics of construction products on the European market (CE marking) according to harmonized European standards or Technical assessments (figure 30), whereas the competences of the Member States remains entire for constructions (buildings and civil engineering works).

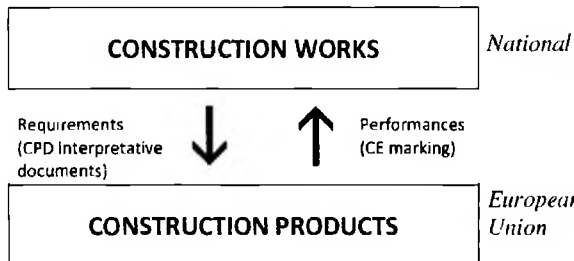


Figure 30: Competences of the European Union and of the Member States

3.2 Regulatory fire : the ISO curve

Fires are random accidental events. They depend from the architecture of the building spaces, the building materials, the fire load (furniture, goods,...), the circumstances of the fire ignition, the ventilation, etc. As shown on figure 31 for 3 real fires (in black), the evolution of the temperature over time in a compartment, from the beginning of the flash over, may be very different.

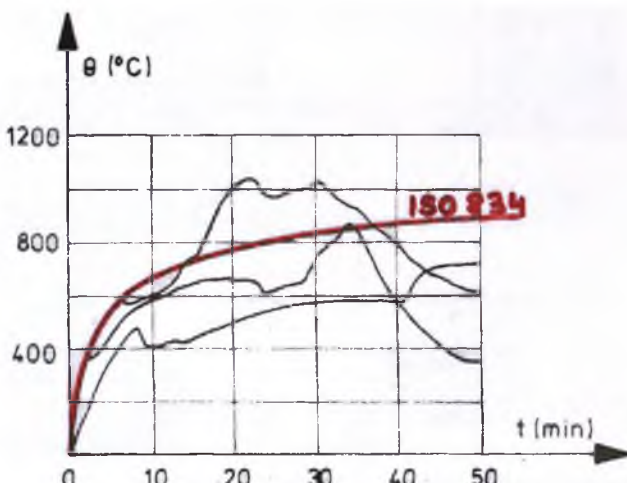


Figure 31: Standard temperature-time curve (ISO 834 / EN 1991-1-2:2002)

The need to standardize a temperature-time curve has been expressed at about the same time in the years sixties all over the world, and it is one of the few examples of a standard which has been established directly world wide, by ISO, the International Standardization Organization.

The ISO curve represent a conventional fire enveloping about 95 % of the real fires. This curve is used to evaluate the resistance to fire of building elements by testing. Figure 32 shows a standardized furnace used to test fire resisting walls, partitions, doors, etc in laboratory. The resistance to fire is defined as the duration of an ISO fire during which specific criteria (mechanical resistance, stability, integrity, surface temperature on the protected side of a compartment wall, etc). It is to be noted on figure 31 that the ISO curve is always limited for each test to a certain duration (target duration of the test), after which the heating of the furnace is cut off and the temperature decreases. More than 30 European standards defining testing methods for different building elements have been developed by CEN TC 127 "Fire safety in buildings".

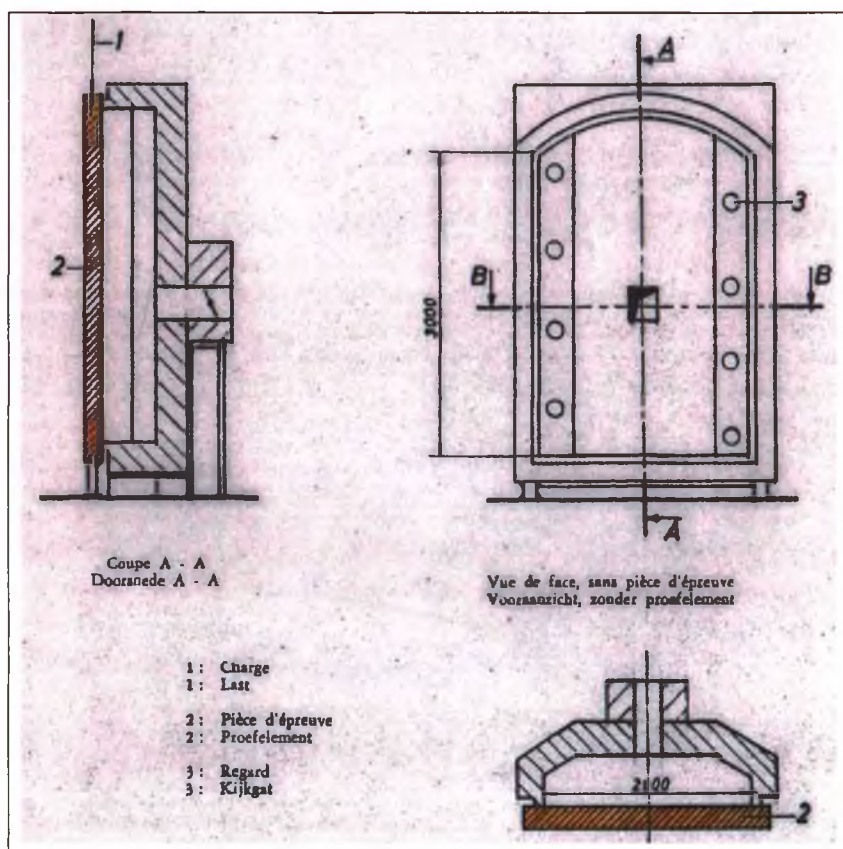


Figure 32: Test furnace for fire resisting walls (NBN 713-020:1968)

From the large amount of available tests results accumulated over years, it has been possible to derive methods of evaluation of the resistance to fire of many types of building elements, and to propose tabulated values of properties corresponding to specific durations of the resistance to fire, or calculation methods. These methods, alternative to testing (figure 33), have been defined by CEN TC 250 "Structural Eurocodes" and are now published in Part 1.2 of Eurocodes 1, 2, 3, 4, 5, 6 and 9.

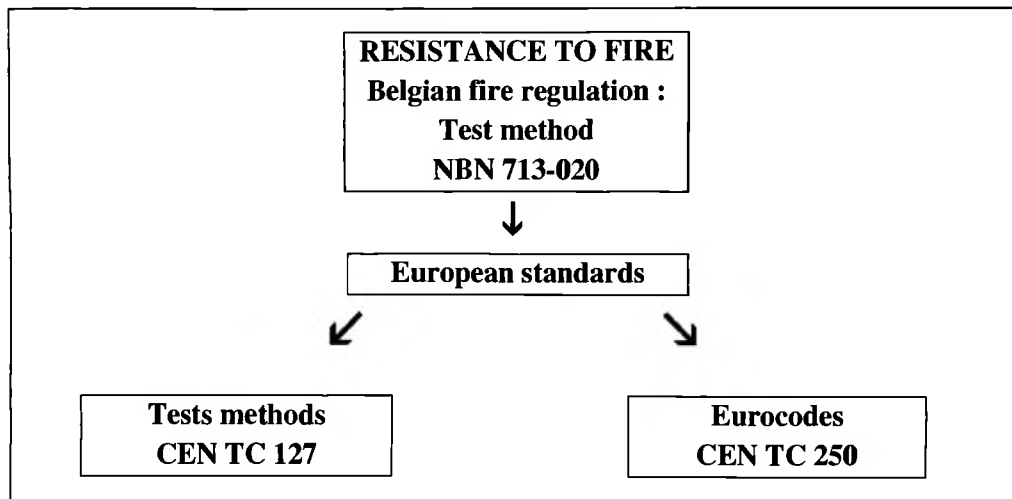


Figure 33: Determination of the resistance to fire

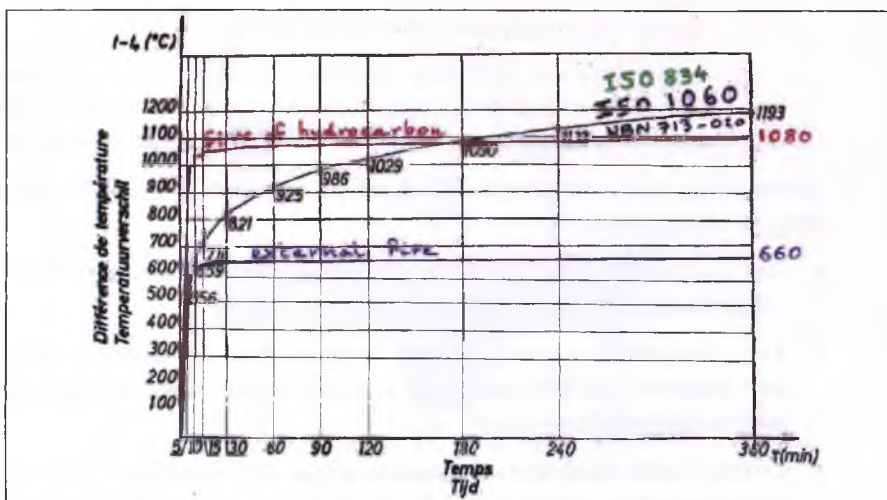


Figure 34: Nominal temperature-time curves (EN 1991-1-2:2002)

3.3 Natural fires

The Part 1.2 of Eurocode 1 (EN 1991-1-2:2002 “Actions on structures exposed to fire”) is defines

1. Standard temperature-time curves (the use of other curves than the ISO curve is subjected to the agreement of the public authority in charge of the fire regulation to be applied) :
 - The ISO standard temperature-time curve (in black on figure 34)
 - External fire curve (in blue on figure 34), which is used to evaluate the resistance to fire of building elements outside the building envelope ;
 - Hydrocarbon curve (in red on figure 34), which is mainly used to evaluate the resistance to fire of petroleum industry plants ;
2. Natural fire models :
 - Parametric temperature-time curve calculated for a defined compartment fire (an example is shown in figure 35) ;
 - Heating action on external members exposed to fire through openings in a façade calculated as the sum of the contributions of the fire compartment and of the flames emerging from the openings as shown on figure 36 ;
 - Thermal actions of localized fires where flash over is unlikely to occur (figure 37) :
 - compartment where flammable materials are not covering more than 10 % of the surface,
 - compartment under a roof automatically opening on 50 % of its surface to open air when the air temperature reaches 200°C,
 - compartment with permanent openings to open air in two opposite façades (open sections in each façade exceeding 1/6 of the total surface of the vertical walls (external and internal) along the whole perimeter of the compartment).
3. Advanced fire models taking into account the gas properties, the mass exchange and the energy exchange (figure 38) :
 - One-zone models assuming a uniform, time dependent temperature distribution in the compartment ;
 - Two-zones models assuming an upper layer with time dependent thickness and with time dependent uniform temperature, as well as a lower layer with a time dependent uniform and lower temperature ;
 - Computational Fluid Dynamic models giving the temperature evolution in the compartment in a completely time dependent and space dependent manner.

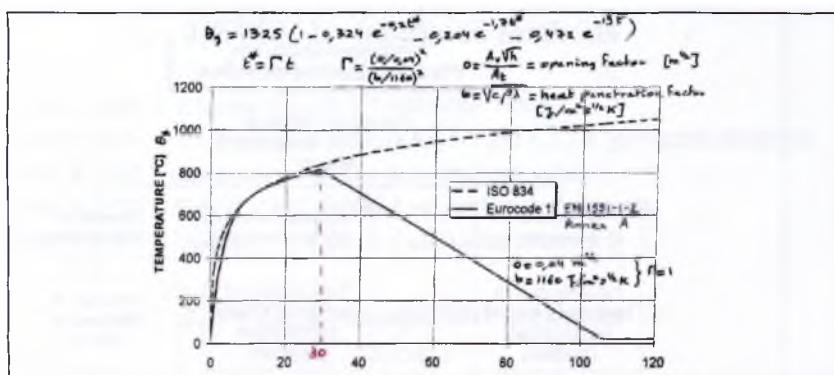


Figure 35: Parametric temperature-time curve (EN 1991-1-2:2002, Annex A)

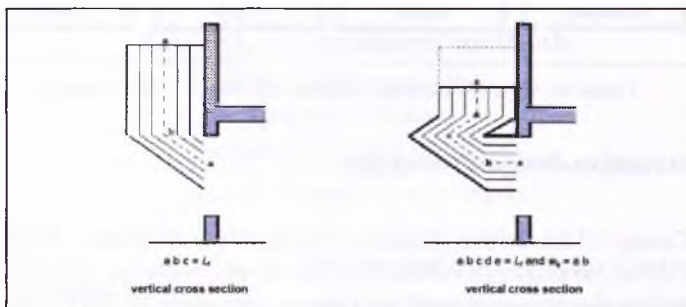


Figure 36: Heating actions on external members (EN 1991-1-2:2002, Annex B)

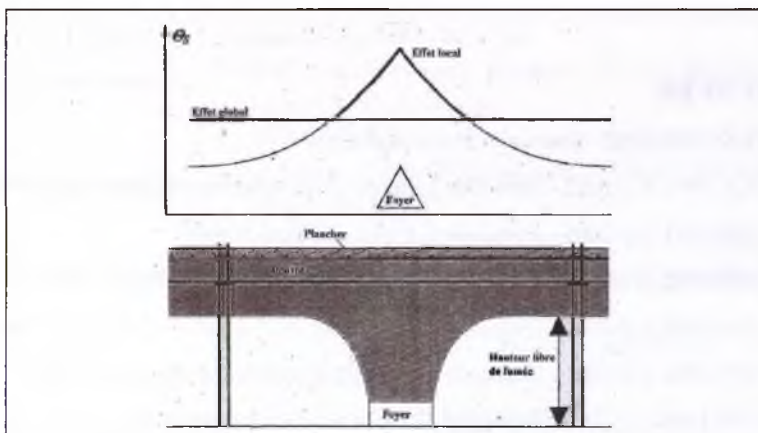


Figure 37: Localised fires (EN 1991-1-2:2002, Annex C)

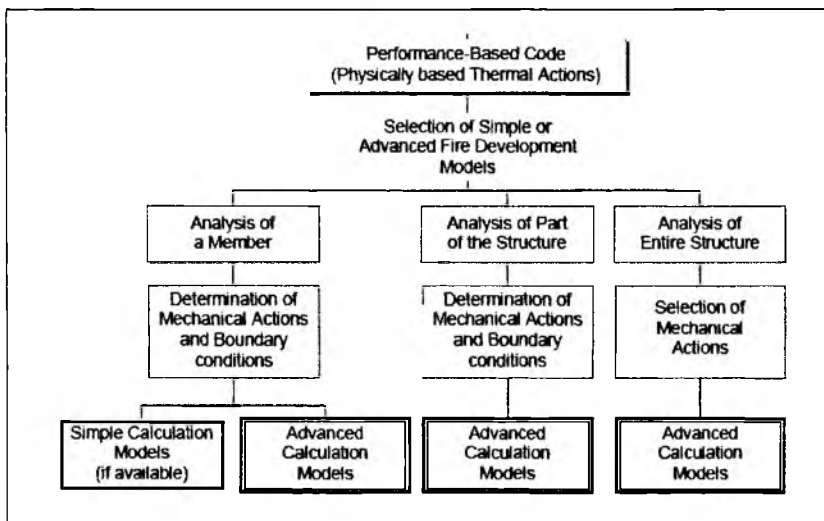


Figure 38: Advanced calculation models (EN 1991-1-2:2002: Annex D)

3.4 Alternative design procedures

The Superior Council of the Belgian Ministry of the Interior is preparing a Royal decree defining the alternative design procedures available for 3 levels of complexity of the evaluations (figure 39) and establishing procedures to assist the controls performed for the Communes by the Fire Brigades (figure 40) : for level 2 methods, a conformity assessment will be required, and the use of level 3 methods will only be possible via a derogation to the fire regulation.

REFERENCES

- [1] NBN EN 1990:2002 - Eurocode "Basis of design"
- [2] NBN EN 1991-1-2:2002 - Eurocode 1, Part 1-2 "Actions on structures exposed to fire"
- [3] NBN EN 1991-1-4:2005 - Eurocode 1, Part 1-4 "Wind actions"
- [4] NBN EN 1992-1-2:2004 - Eurocode 2 "Design of concrete structures", Part 1-2 "fire"
- [5] NBN EN 1993-1-2:2005 - Eurocode 3 "Design of steel structures", Part 1-2 "fire"
- [6] NBN EN 1994-1-2:2005 - Eurocode 4 "Design of composite structures", Part 1-2 "fire"
- [7] NBN EN 1995-1-2:2005 - Eurocode 5 "Design of timber structures", Part 1-2 "fire"
- [8] NBN EN 1996-1-2:2005 - Eurocode 6 "Design of masonry structures", Part 1-2 "fire"
- [9] NBN EN 1999-1-2:2007 - Eurocode 9 "Design of aluminium structures", Part 1-2 "fire"

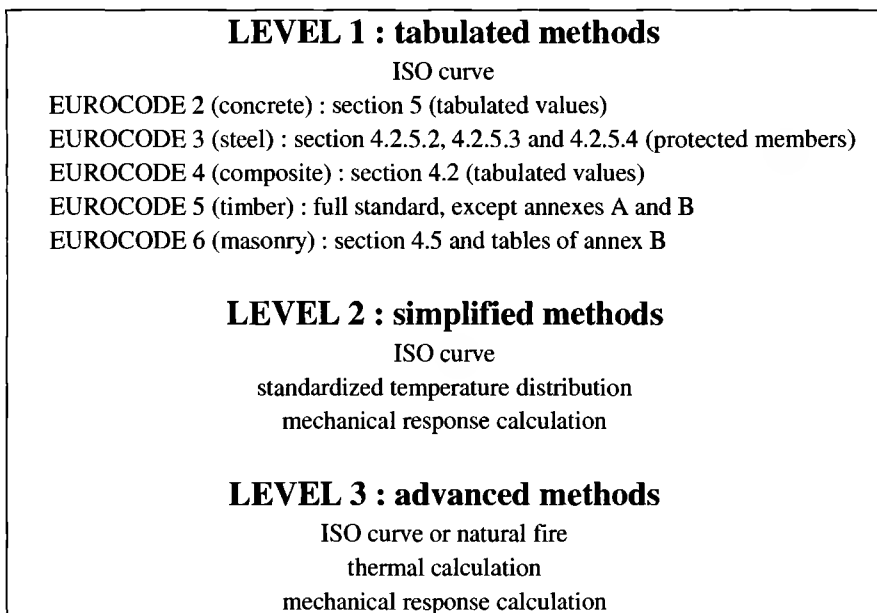


Figure 39: Alternative design procedures

Calculation methods	Proposal of the Superior Council of the Ministry of the Interior
CONTROL LEVEL 1 (tabulated methods)	Responsibility of the consultant Eventual control by the Commune, advised by the Fire Brigade
CONTROL LEVEL 2 (simplified methods)	Responsibility of the consultant Control by the Commune, advised by the Fire Brigade, based on a conformity assessment : <ul style="list-style-type: none"> • the consultant is certified by a certification body accredited by BELAC (EN 45013) and attests himself the conformity of the calculation • or (if the consultant is not certified), the conformity of the calculation is attested by a control body accredited by BELAC (EN 45004) An advisory council groups the public authorities, the trainers and the accredited bodies (certification and control bodies)
CONTROL LEVEL 3 (advanced methods)	Only possible via the derogation procedure

Figure 40: Control procedures proposed in Belgium

EFFECTS OF EXPLOSIONS ON STRUCTURES

J. Vantomme, J.M. Ndambi, B. Reymen

Royal Military School, Civil and Materials Engineering Dept
Avenue de la Renaissance 30, B-1000 Brussels
e-mail: John.Vantomme@rma.ac.be

Keywords: Explosions, Blast loads, Impulse loading, Structural dynamics.

Abstract. *The loss of life and damage to infrastructure are factors that have to be minimized by means of improved protection of buildings against explosions and adapted site organization. This paper first focuses on some essential definitions regarding the explosion phenomenology, the used terminology and classification of different types of explosions. Next, attention is paid to the determination of blast wave parameters and the analysis of the interaction with structures. Finally, some fundamental aspects of structural analysis for blast loads are introduced. Attention is first paid to analytical models and the simplification of the real problem. It is observed that numerical simulation may offer advantages for parametric analysis. However, the paper pleads for a close combination of theoretical modeling with experimental validation.*

1 INTRODUCTION

The analysis of the effects of explosions has always been related to industrial accidents, but has gained in public attention due to the regrettable reality of terrorism worldwide. Risks to people and assets due to high explosive attacks can result from

- projectiles such as glass, cladding and doors ;
- blast overpressures, which can cause injuries to human organs for example ;
- local and total collapse of structures (buildings, vehicles, etc.).

The loss of life and damage to infrastructure are factors that have to be minimized by means of improved protection of buildings against explosions and adapted site organization. This paper first focuses on some essential definitions regarding the explosion phenomenology, the used terminology and classification of different types of explosions. Next, attention is paid to the determination of blast wave parameters and the analysis of the interaction with structures. Finally, some fundamental aspects of structural analysis for blast loads are introduced

2 EFFECTS OF EXPLOSIONS: FOCUS ON BLAST WAVES

2.1 Introduction

An explosion can be described in very general terms as a fast transformation of a material system with important gas production [1]. The gas is more or less compressed depending on the open or confined nature of the volume where the gas is produced and the speed of production. The expansion of the gas can give rise to the creation of a shock wave, mechanical effects and in particular to an intensive sound wave.

An explosion is most of the times considered as a destructive phenomenon or even as a calamity. However, one should not forget that explosive energy is also used for positive purposes such as in rocket motors. And even the destructive power is often used in useful applications such as the exploitation of quarries, oil prospect, demolition of structures, etc.

2.2 Classification

Explosions can be classified according to various criteria [2,3]. One of the most important ones is the physical-chemical point of view. Physical explosions are characterized by the fact that the energy is released by a physical process, such as for example:

- a pneumatic explosion such as the bursting of a pressure vessel;
- an electrical explosion which takes place in the case of a short circuit, the lightning, the sublimation of a metal wire subjected to an intense electrical current;
- the sudden mixing of two liquids at highly different temperatures causes the rapid conversion to vapour of the cooler fluid at a rate that does not permit venting, resulting in a shock wave generation.

Chemical explosions are due to chemical decomposition of an explosive or to the rapid oxidation of fuel elements (carbon and hydrogen atoms) contained within the explosive mixture; the oxygen which is needed for the reaction is contained in the mixture. A chemical explosion is characterized by the production of heat and of gas; the rapid expansion of gas results in

- the generation of shock pressures in solid materials with which the explosive is in contact;
- blast waves in air.

Most of the practical explosives are condensed: they are solids or liquids. However, explosions in the gas-phase are also possible, when an optimum gas-oxygen balance has been

reached (case of fuel-air explosions). Dispersion of fine (combustible) particles in air can lead to a so called dust explosion.

2.3 Explosion process terminology

Explosions in condensed phase are further classified according to the speed of the chemical reaction.

A thermal explosion or combustion occurs when a chemically unstable material has been kept at too high temperature for too long time (the case of some peroxides and mixes with nitrates). This process is also denoted as burning.

Deflagration (explosive combustion) occurs when the reaction zone in the explosive propagates with subsonic speed (cm/s to m/s). The propagation mechanism is based on the heat transfer of the reaction zone towards the intact explosive (the case of some fertilizers and propulsive powders for ballistic projectiles and rockets).

Detonation occurs when the reaction zone in the explosive propagates with supersonic speed (1 to 9 km/s). This type of reaction produces a high intensity shock wave and is characteristic for so called high explosives (the case of some fertilizers and most civil and military explosives). High explosives are subdivided into two classes:

- primary explosives, which are very sensitive to heat, friction or pressure changes; a small stimulus is sufficient for the initiation of the decomposition process;
- secondary explosives are less sensitive and need to be initiated by the detonation energy liberated by small quantities of primary explosives.

2.4 Comparison of explosives : TNT equivalence

The performance of different high explosive materials is generally compared on the basis of their TNT equivalence (TNT = trinitrotoluene). Normally, the comparison is made of the quantity of energy liberated by the explosion, starting from the mass specific energy of TNT equal to 4520 kJ/kg [3]: it should be noted that this value changes slightly from one reference to another. The specific energy of explosives can be determined in laboratories via the measurement of the explosion heat. However, the TNT equivalence can also be defined for other explosion effects such as the fragmentation capacity (brisance) or the mechanical energy (expansion capacity). Some values are reported in Table 1.

Secondary high explosive	Explosion energy		Brisance	Expansion capacity
	kJ/kg	TNT equivalent	TNT equivalent	TNT equivalent
TNT	4520	1	1	1
PETN (pentriet)	5800	1,3	1,3 to 1,4	1,6 to 1,8
RDX (hexogen)	5360	1,2	1,4	1,7

Table 1 : TNT equivalence for some secondary high explosives [2]

2.5 Blast waves in free air

The initiation of a high explosive leads to a sequence of events. First, the explosion reaction generates hot gas (pressures up to 30 GPa and temperature up to 4000°C). A violent expansion of this gas occurs and the surrounding air is forced out of the volume it occupies. A layer of compressed air (the blast wave) forms in front of the gas, containing most of the energy released by the explosion. The discontinuous character (instantaneous shock load) of the blast wave is accentuated by the fact that the gas molecules at high pressure and temperature are accelerated and catch up the progressing wave front (which is thus steepened). Figure 1

shows in a schematic way the evolution of pressure with time in a measurement position during the passage of the blast wave. As the gas expands, its pressure falls to atmospheric pressure as the blast wave moves outwards from the source: the shock wave transforms into a sound wave at large distance. As the gas continues to expand, it cools down and the pressure falls below atmospheric pressure; this over-expansion is related to the momentum of the gas molecules. The over-expansion results in a reversal of flow towards the source; this is called the negative phase. The whole process is summarized in figure 1 which also permits to identify the "blast wave parameters", which are:

- p_s the peak side-on overpressure (with respect to ambient pressure p_0);
- T_s the duration of the positive overpressure phase;
- i_s the side-on impulse associated with the positive overpressure phase (this is the integral of pressure with time)
- t_a the arrival time of the blast front

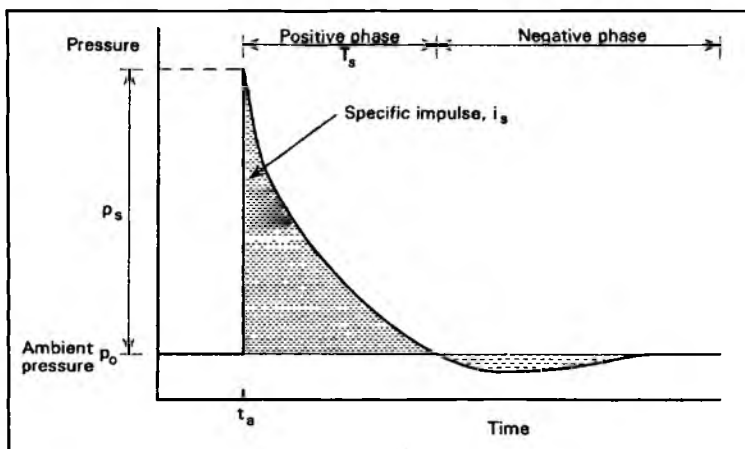


Figure 1 : Blast wave in free air : evolution of overpressure with time [4]

The theoretical analysis of the blast wave parameters has been developed for the normal shock in ideal gases, based essentially on conservation equations (mass, energy and momentum) leading to the Rankine-Hugoniot relations [5]. However, the ideal conditions of the Rankine-Hugoniot theory often do not match with real conditions. Today, wavefront parameters can be determined most readily from empirical relationships obtained from experiments; these relationships are presented in numerous publications [1,3,6]. The parameters are traditionally presented graphically (see figure 2) as a function of the scaled distance parameter Z , which is defined as $Z = R/W^{1/3}$, with R the distance (in m) of the measurement point from the centre of a spherical charge of TNT and W the weight of the charge in kg. The empirical curves [1] are frequently used (in software format), but it should be noted that the curves are only valid for the following assumptions which are not easy to be fulfilled:

- free air detonation (in practice, there are often reflecting surfaces or some confinement!);
- spherical charge in TNT (in general, the charge has a non-spherical shape and the effect of the packing should be taken into account; problem of use of TNT-equivalence factors);
- standard atmospheric conditions and homogeneous atmosphere.

An important practical conclusion from the curves is that shock wave peak overpressures decrease drastically with distance from the explosion point. It should also be noted that for large explosions, a blast induced wind, which consists of air, gases and combustion products, is generated after the shock front has passed. This wind causes additional dynamic pressures.

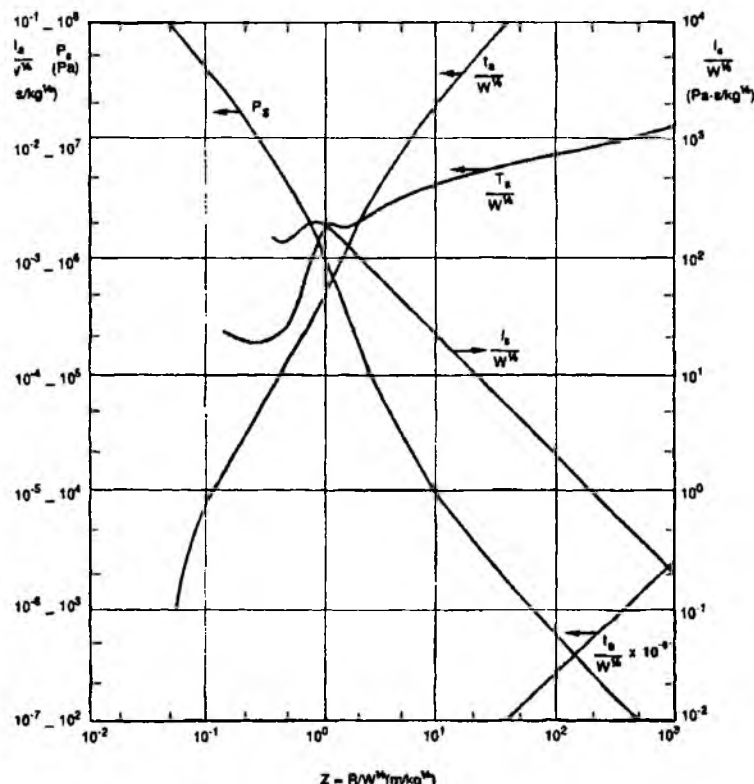


Figure 2 : Side-on blast wave parameters for spherical charges of TNT in free air [1]. Side-on means that the measurement equipment does not affect the progression of the shock wave (no reflection)

3 BLAST EFFECTS ON STRUCTURES: EVALUATION OF ACTIONS

3.1 Reflection of blast waves

A blast wave will be reflected by the ground surface (see figure 3) and by the surface of a building. These reflections create complex loading conditions and lead to an increase of pressures. Again, the Rankine-Hugoniot model can be used for the theoretical evaluation of blast wave parameters for regular (surface perpendicular to blast wave progression) and oblique reflection on surfaces [5]. Empirical charts can also be found in literature for regular reflection [1,6]. A particular aspect is the Mach stem effect, which is a result of the reflected wave catching up with the incident wave. Mach reflection causes a substantial increase in reflected overpressures, which depends on the initial incident peak overpressure magnitude.

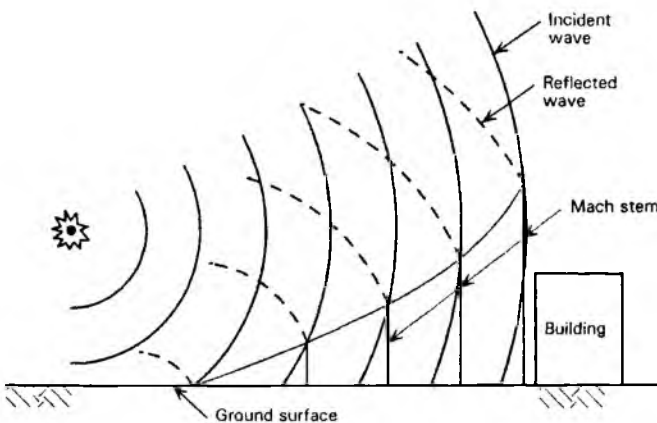


Figure 3 : Blast wave progression due to air burst with ground reflections [4]

3.2 Surface explosions

For a surface burst, the blast wave front is not spherical but hemispherical due to the immediate reflection by the ground surface. The blast wave characteristics can be determined from free air characteristics by assuming that the mass of the explosive W is modified by an enhancement factor. If the ground surface were a perfect reflector, the enhancement factor would be 2, but as the explosion energy is partially absorbed by the ground (crater effect), the enhancement factor is commonly taken equal to 1,8.

3.3 Blast loads on buildings due to explosions outside the building

Based on experiments and computational fluid dynamics calculations, the US Technical Manual TM5-1300, which is used worldwide in this domain [6] presents a simplified approach for the evaluation of overpressures and impulses on rather simple (geometrically speaking) buildings of finite size with a roof, sides, and a rear face. Because of its finite size and solid shape, a building will experience a time-varying system of pressures that are more complex than the simple side-on and reflected overpressures presented in the previous paragraph. The simplified approach considers each face of the building in separate phases. The location of the building is assumed to be outside the region of regular reflection and in the region of Mach reflection.

The front face of the building experiences enhanced peak overpressures due to reflection of the incident blast wave. Once the initial blast wave has passed the front face of the building, the peak (reflected) overpressure on the front face decays to zero at a rate dependent on the duration of the blast wave, which is very much determined by the stand-off distance of the building to the explosion (see figure 4). However, as the sides and top faces of the building receive side-on overpressures (which are lower than the reflected overpressures on the front face), a relieving effect of blast overpressure is observed on the front face, which can lead to a faster decay rate of the overpressure on the front face. This relieving phenomenon clearly highly depends on the dimensions of the building. Other particular aspects are the diffraction phenomena at the corners of the building and the dynamic pressures (blast wind) which also act on the front face after the passage of the blast wave, but these effects are of limited importance for buildings.

The sides and top faces of the building are exposed to side-on overpressure. As the shock wave travels along the sides and top faces away from the explosion point, the overpressure decreases and the duration of the positive phase increases (see figure 5). The load on the sides and top faces thus increases at a rate which is not Dirac-like, gets a maximum value (corresponding to the position of the blast wave in point D in figure 5) and then smoothly decreases. The most dangerous position of the blast wave corresponds to the most important internal forces in the structural elements of the sides and top faces. It should also be noted that if the side walls and roofs are oriented parallel to the direction of the blast wave, the effects of drag loads caused by the blast wind are negligible.

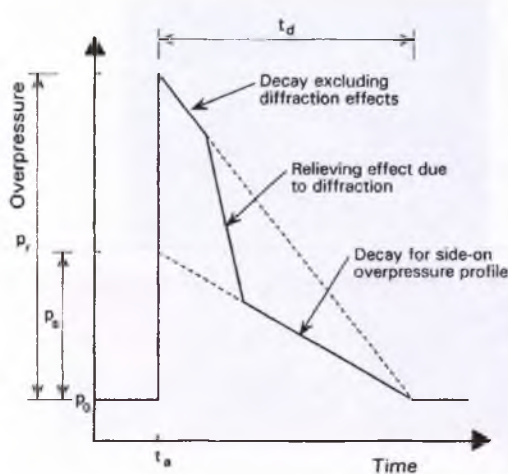


Figure 4 : Schematic representation of the blast overpressure with time, acting on the front face of a building [4]

The rear of the structure experiences no overpressure until the blast wave has traveled the length of the structure and a compression wave has begun to move inwards, towards the bottom of the rear face. This means that the pressure build up is not instantaneous. One sees the similarity with the sides and top faces; the function that gives the overpressure with time for the rear of the structure is similar to the one depicted in figure 5.

As the building has a finite depth, there will be a time lag in the development of pressures and loads on the front and back faces. This time lag causes translational forces to act on the building in the direction of the impinging blast wave. The translational forces depend on the dimensions of the building. For thin structures, such as truss systems, loads on front and rear side take place almost instantaneously and the residual action will be the drag force due to the blast wind; this type of structures are called to be of the "drag type". For long structures, the action on the rear takes place after the elimination of the action on the front face; this type of structure is called to be of the "diffraction type".

When a relatively small charge is detonated near a substantially-sized building, blast loading is considered to act locally on the front face of the building only, hence the front face can be assumed to be infinite. In this case, individual elements of the building can be analyzed separately because the components are likely to be loaded sequentially.

The TM5-1300 approach is characteristic for the calculation of hardened structures, but is adopted in all bibliographic references worldwide. However, one should be careful in the interpretation of the results from the hardened buildings approach, when modern non-hardened

buildings with complex architectural shapes have to be examined. The loading on exposed faces of buildings is a function of the size, shape, and orientation of the walls of the building, the presence of large windows, awnings, canopy roofs, the location and orientation of other objects nearby, etc.

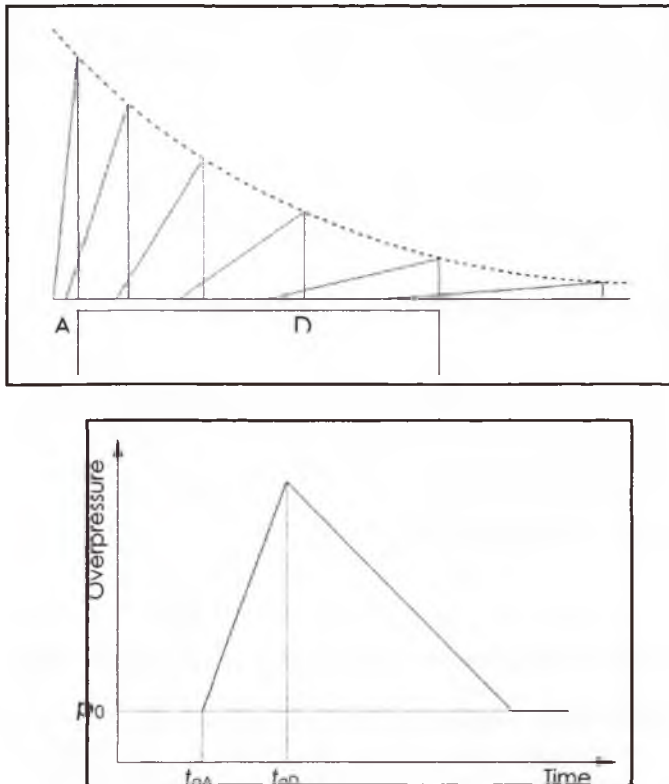


Figure 5 : Schematic representation of the blast overpressure with time, acting on the sides and top faces of a building

3.4 Evaluation of blast loads : numerical prediction and experimental verification

Software tools for extended computational fluid dynamics calculations are now available permitting a better understanding of the actions on structures due to explosions. These software's are explicit numerical codes that are used for the modelling of the nonlinear dynamics of solids, fluids, gas and their interactions. The problems to be analysed with these software's can be characterized as highly time dependent with both geometric and material nonlinearity's. The user has to choose the appropriate solver for each part of the numerical model (structure or fluid) and to manage their interactions; the main solvers used for blast analysis are the following: Euler (for large deformations and for fluids and gas), Lagrange (for solids and structures) and mixed versions for interface regions. Figure 6 is the result of a numerical simulation showing the progression of a blast wave along the façade of a building. The explosion takes place on the ground surface, under the canopy. One observes the reflexion of the shock wave by the canopy, giving rise to high upward loads on the canopy and high transver-

sal loads on the ground level wall. The shock wave turns around the canopy, which leads to the attenuation of the loads on the windows in the upper part of the façade (which is the effect that is searched for by using the canopy).

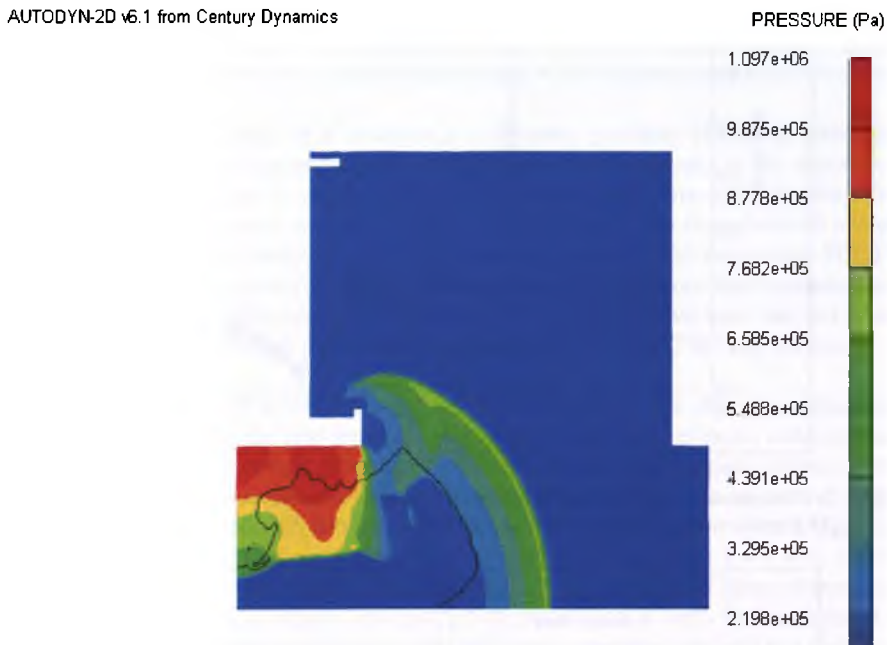


Figure 6 : Simulation of the progression of a blast wave along the façade of a building, obtained with the software AUTODYN (Century Dynamics)

A general characteristic for numerical methods is that the results depend on the nature and accuracy of the parameters that are used to define the problem. Therefore, experimental validation is necessary. Throughout the last 50 years, several large scale tests have been realized by individual nations or by international research teams, in order to get experimental data about shock wave progression, the Mach stem phenomenon, etc. Another source of information is undoubtedly the interpretation of industrial accidents and terrorist attacks. Experimental simulation on scaled structures is also an interesting approach, but the application of scale laws to the structure itself is not straightforward (for example the adaptation of the dimensions of the structure, its stiffness characteristics, etc).

A nice example of the usefulness of real scale measurements has been collected during a recent RMA study in the port of Antwerp regarding the effects of underwater explosions on an existing quay wall (see figure 7). An underwater explosion produces two pressure pulses: a shock wave followed by a bubble pulse associated with the expansion of the products of the detonation. For the shock wave, analysis proceeds such as for air blasts although there are quantitative differences (transmission medium is water!). Although the underwater explosion seems to be at first sight a complex case, with multiple reflection effects on the water surface and on the bottom, the experimentally measured overpressure on a quay wall can easily be explained as the superposition of different waves (see figure 7b).

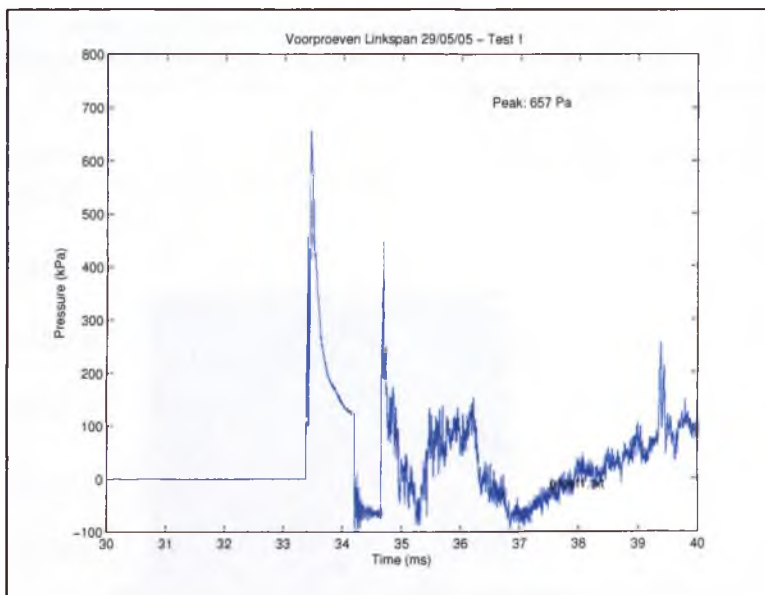


Figure 7a : Overpressure with time signal, measured on a quay wall after an underwater explosion of 0,5 Kg TNT with a stand-off distance of 29m; depth of the charge is 15m, on the bottom of the dock

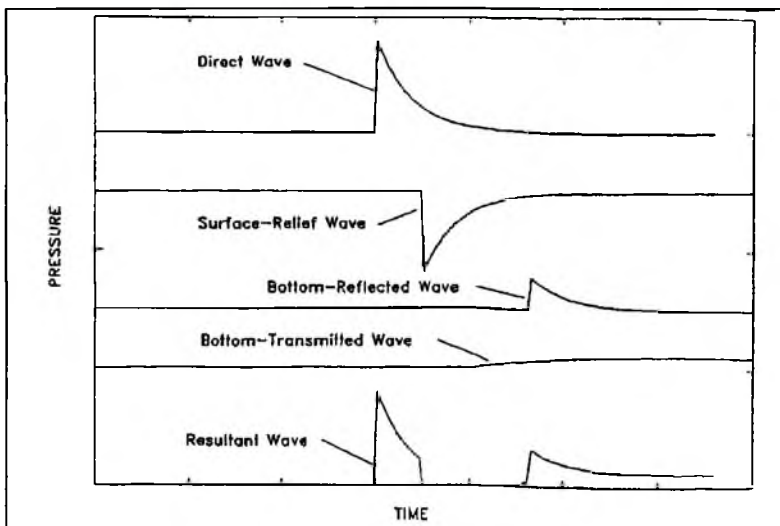


Figure 7b : The measured signal in figure 7a is the superposition of the different shock waves resulting from that explosion

4 BLAST EFFECTS ON STRUCTURES: STRUCTURAL BEHAVIOUR

4.1 Calculation of the dynamic response of structures for shock loads

Analytical methods for the determination of the dynamic response of a structure or a structural element that is loaded by a blast load are presented in TM5-1300 which is the main

reference for many other reference books on this topic; the methods are based on theory presented by BIGGS [7]. The methods in TM5-1300 focus on the determination of the maximum deflection of the structure because this is directly related to the failure of the structure (which is the main problem to examine). Indeed, in assessing the behaviour of a blast loaded structure, it is often the case that the calculation of the final state is the principal requirement for a designer; he needs to know what is the maximum displacement of a structure given a specified form of blast loading, rather than a detailed knowledge of the displacement-time history of the structure.

The action of a blast load on a structure is a dynamic problem. However, although the blast wave gives a sudden load and excites the different vibration modes of the structure, it is observed that the deflection is mainly related to the first mode. That explains why the response of real distributed mass structures and structural elements is often idealized using single-degree-of-freedom and multiple-degree-of-freedom methods. The equivalent SDOF and MDOF systems are determined by means of the conservation equations (deformation energy, kinetic energy and potential energy) and based on the assumption that both the real structure and the equivalent system adopt the same deformation (that is indeed the key parameter to be calculated).

For the solution of the SDOF equation, BIGGS introduced the energy method, which equals the energy put into the real structure and in the model. However, in order to use the right portions of energy, it is first necessary to identify the response regime: indeed, how the structure responds to blast loading is linked closely to the ratio between its natural period T (calculated via the SDOF model) and the duration t_d of the blast. Three response regimes can be produced, which are defined as impulsive for $t_d < 0,4 T$; dynamic for $0,4 T < t_d < 2 T$ and finally quasi-static for $t_d > 2 T$. These criteria may be slightly different in other references.

In an impulsive response regime, duration of the blast load is very short compared with the natural period of the structural element. The duration is such that the load has finished acting before the element has had time to respond. Due to inertial resistance of the structure, most of the deformation occurs after the blast load has passed. When an impulse is delivered to a structure, it produces an instantaneous velocity change, where momentum is acquired and the structure gains kinetic energy. In the energy method, the impulse of the blast is used to evaluate the kinetic energy, which can be put equal to the deformation energy. Impulse is an important aspect of damage-causing ability of this type of blast, and may become a controlling factor in design in situations where the blast wave is of a relatively short duration (often for short stand-off distances).

When the duration of the blast load is much longer than the natural period of the structural element, the loading is termed quasi-static. In this case, the blast loading magnitude may be considered constant while the element reaches its maximum deformation. The response tends to that for an equivalent static force. For quasi-static loading, the blast will cause the structure to deform while the loading is still being applied. The loading therefore does work on the structure, causing it to deform and acquire strain energy.

In between the impulsive and quasi-static regimes, there is a more complicated, time-dependent regime, commonly called the dynamic regime. In this regime, the load duration is similar to the natural period of vibration of the structural element, and the duration of the load is similar to the time taken for the element to respond significantly. There is amplification of response above that which would result from static application of blast load. For dynamic load response, the complete energy relationship is applied where the work done by the blast load is equal to the kinetic energy and strain energy imparted to the structure.

The deformation energy for a structural element is calculated on the basis of its “resistance function” which is a graph of the load (force or uniform pressure) versus displacement

of the structure; this function expresses the resistance that the structural element offers against deformation. Figure 8 presents the typical aspect of a resistance function for a steel beam with clamped edges and loaded by a uniform blast pressure. The curve is composed of three parts: an elastic, elastic-plastic and plastic domain. The transition between these domains is determined by the occurrence of plastic hinges. Each structure has its own resistance function which is determined by the dynamic (high strain rate) behaviour of the material, the geometry and the boundary conditions.

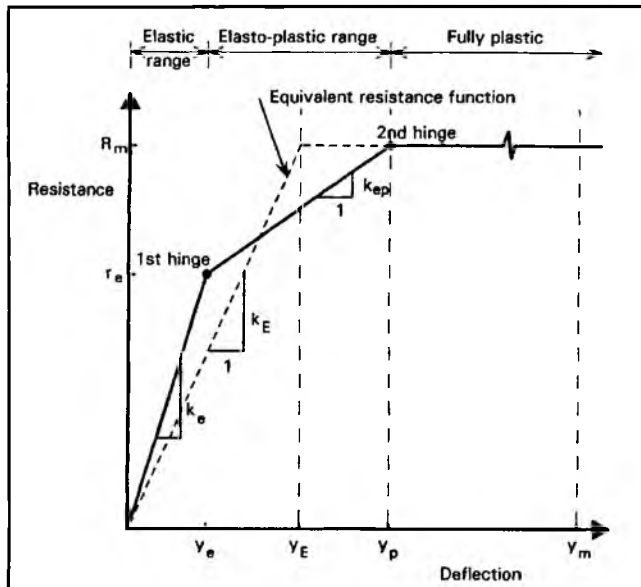


Figure 8 : General aspect of a resistance function for a steel beam with clamped edges [4].

4.2 Pressure-impulse diagrams

For some structures, pressure-impulse diagrams are available. These diagrams are obtained by considering and representing the behaviour of a system over the whole range of possible response regimes. This may be achieved by calculations, but has to be validated by experiments. Figure 9 shows a well known example of a pressure-impulse diagram, which has been obtained by the analysis of damage patterns to masonry buildings due to bomb blasts in World War 2 [3]. The curves show pressure-impulse combinations that lead to a particular degree of damage. Other traditional pressure-impulse diagrams focus on the behaviour of the human body for blast loads. Today, one can find this type of (experimentally determined) pressure-impulse diagrams for modern blast-resistant glazing systems, for retrofit systems in existing buildings, etc. One important observation can be made from the general aspect of a pressure-impulse diagram: a particular type of damage can be obtained by large pressures with small impulse (short duration, short distance to the explosion) but also by large impulses for a particular pressure (long duration, large distance to the explosion).

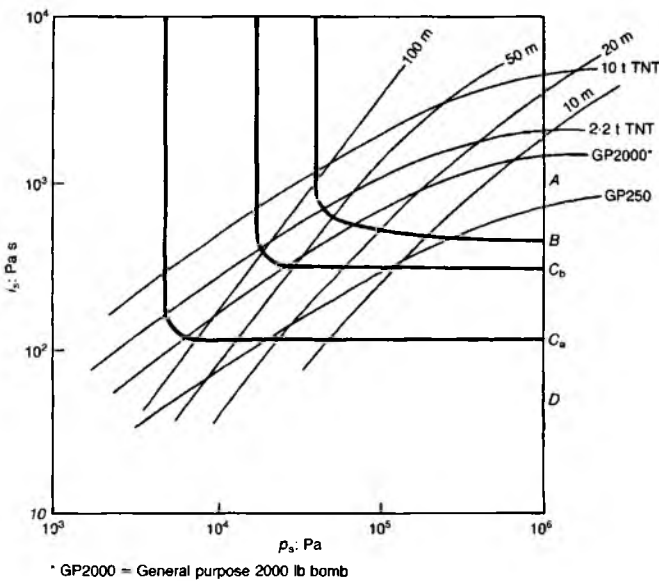


Figure 8 : Pressure-impulse diagram for masonry as a result of the analysis of the effects of World War 2 bombing on brick buildings in UK ; curve Ca corresponds to minor damage, curve Cb corresponds to major damage, curve B corresponds to destruction [3].

4.3 Parameters that influence the structural response for blast loads

The two most important parameters are the material behaviour and the structural robustness.

Steel and reinforced concrete are excellent materials for taking up shock wave energy because of the ductile character: the blast resistance is based on the capacity to form plastic hinges in the structure. This is the case in figure 9, where a steel column presents a plastic hinge after the impact of a blast wave. The plastic deformation capacity is also shown in figure 10, where the deformation of the flanges of a steel column is observed, due to the impact of a very close explosion [8]; this type of damage may lead to the loss of the load-bearing capacity of the column.

Masonry and traditional glass are not adapted for blast loads because of their brittleness. The resistance function for analytical models of masonry walls is totally different from the one for steel: instead of plastic hinges, one observes tensile and shear failure of the mortar joints between the masonry blocs. The weak links between the blocs may lead to damage patterns such as the one illustrated in figure 11: the blast load is so important causing all joints to fail simultaneously; the wall acts as a membrane. This numerical prediction is confirmed experimentally; however, other experimental results show different damage patterns: figure 12 shows that the global attack by the blast wave has been complemented by a local transmission of stress waves into the masonry blocs, causing a local scabbing effect (the disruption of a part of the wall at the tensile side). Today, novel systems are developed to increase the ductility of the materials and thus the blast resistant capacity of modern structures: ductile concrete, introduction of fibres in concrete, application of special plastic layers on masonry walls, etc.



Figure 9 : Metal column with plastic hinge after impact of blast wave

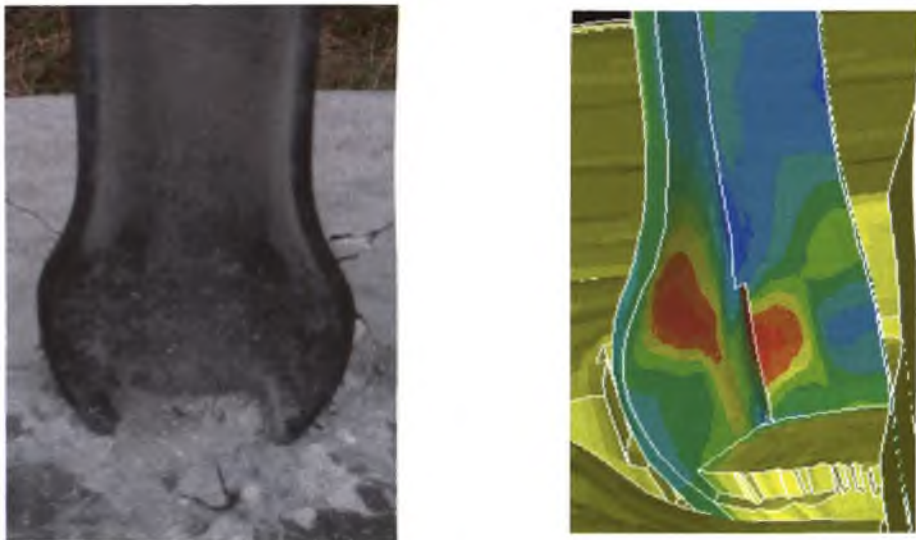


Figure 10 : Metal column subjected to a short distance explosion: plastic deformation of the flanges [8]

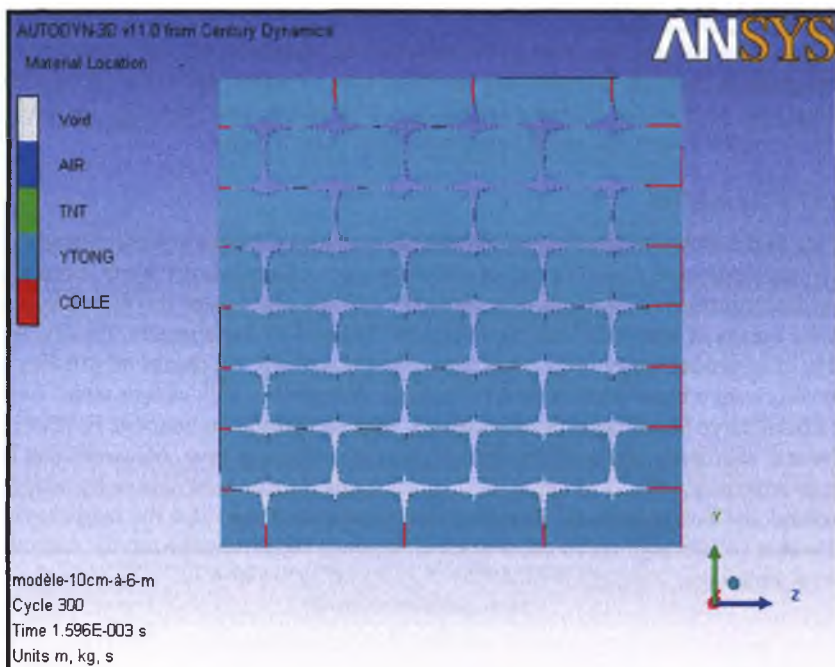


Figure 11 : Numerical simulation of masonry wall loaded by a blast wave: the first damage pattern is related to the failure in tension and shear of the mortar layer between the masonry blocs



Figure 12 : Back side of a masonry wall subjected to blast load: scabbing effect in complement to the membrane effect

Today, much attention is also paid to the design of buildings to avoid the progressive collapse phenomenon, which is defined as the process where a relatively small damage pattern (the collapse of a column due to a contact explosion) leads to an unreasonable large damage

of the building (the collapse of one third of the building for example). The problem of avoiding progressive collapse has lead to the thorough development of new material models to be implemented in numerical codes, but has also lead to additional technical measures on the building site, such as for example in the case of prefabricated buildings the prescription of chains of reinforcement that should keep structural parts together.

5 CONCLUSIONS

This paper introduced essential definitions regarding the explosion phenomenology, the used terminology and classification of different types of explosions. Next, attention was paid to the determination of blast wave parameters and the analysis of the interaction with structures, by means of analytical and numerical models and by experiments. Finally, fundamental aspects of structural analysis for blast loads were discussed. By means of some examples, the paper pleads for a close combination of theoretical modeling with experimental validation.

Lessons have been learnt from accidents, terrorist attacks, numerical simulations and experimental validations on scale models or on real scale structures. Measures can be taken in order to reduce the effects of explosions by choosing ductile materials or by adaptation of architectural and design aspects. However, one should not forget that the increase of the stand-off distance (if this is possible off course) is the most effective measure for reduction of blast loads on structures.

REFERENCES

- [1] W.E. Baker, W.E. Cox, P.S Westine, J.J. Kulesz, R.A. Strehlow, *Explosion hazards and evaluation*, Elsevier Amsterdam, 1983.
- [2] R. Bourgois, *Constructies onderworpen aan explosiebelastingen*, Course notes RMA, 1999.
- [3] P.D. Smith, J.G. Hetherington, *Blast and ballistic loading of structures*, Butterworth Heinemann, 1999.
- [4] SCI 244, *Protection of buildings against explosions*, SCI publication 244, The Steel and Concrete Institute, UK, 1999
- [5] G.F. Kinney, K.J. Graham, *Explosive shocks in air*, 2nd Ed., Springer-Verlag Inc., New York, 1985.
- [6] US Army TM5-1300, *Structures to resist the effects of accidental explosions*, US Department of Commerce, National Technical Information Service, Washington DC, 1990.
- [7] J.M. Biggs, *Introduction to structural dynamics*, McGraw-Hill, New York, 1964.
- [8] F. Halleux, J. Art, J.M. Ndambi, J. Vantomme, *Resistance Analysis of Steel and Mixed Steel-Concrete Columns subjected to close-contact Explosions*, Proceedings 16th DYMAT Technical meeting, Brussels, October 27-28 2005.

NUMERICAL, ANALYTICAL AND EXPERIMENTAL INVESTIGATIONS ON THE RESPONSE OF STEEL AND COMPOSITE BUILDINGS FURTHER TO THE LOSS OF A COLUMN

J.P. Jaspart¹, J.F. Demonceau² & H.N.N. Luu²

¹ ArGENCo Department, Liège University
1, Chemin des Chevreuilis, B-4000 LIEGE, Belgium
Jean-Pierre.Jaspart @ulg.ac.be

² ArGENCo Department, University of Liège, Liège Belgium
1, Chemin des Chevreuilis, B-4000 LIEGE, Belgium
jfdemonceau@ulg.ac.be

Keywords: Robustness, Structural Integrity, Catenary Action, Membrane Forces, Composite Structures, Joint Ductility, Exceptional Actions and Experimental Testing.

Abstract. *Recent events such as natural catastrophes or terrorism attacks have highlighted the necessity to ensure the structural integrity of buildings under exceptional events. According to Eurocodes and some different other national design codes, the structural integrity of civil engineering constructions should be ensured through appropriate measures but, in most of the cases, no precise practical guidelines on how to achieve this goal are provided. A European RFCS project entitled "Robust structures by joint ductility" has been set up in 2004, for three years, with the aim to provide requirements and practical guidelines ensuring the structural integrity of steel and composite structures under exceptional events through an appropriate robustness. In particular, one substructure test simulating the loss of a column in a composite building has been performed at Liège University. Present paper describes analytical, numerical and experimental investigations carried out at Liège University as part of this European project.*

1 INTRODUCTION

A structure should be designed to behave properly under service loads (at SLS) and to resist design factored loads (at ULS). The type and the intensity of the loads to be considered in the design process may depend on different factors such as:

- the intended use of the structure: type of variable loads...
- the location (region, altitude, ...): wind action, snow, level of seismic risk...
- and even the risk of accidental loading: explosion, impact, flood...

In practice, these individual loads are combined so as to finally derive the relevant load combination cases.

In this process, the risk of an exceptional (and therefore totally unexpected) event leading to other accidental loads than those already taken into consideration in the design process in itself is not at all covered. This is a quite critical situation in which the structural integrity should be ensured, i.e. the global structure should remain globally stable even if one part of it is destroyed by the exceptional event (explosion, impact, fire as a consequence of an earthquake ...).

In conclusion, the structural integrity will be required when the structure is subjected to exceptional loads not explicitly considered in the definition of the design loads and load combination cases.

According to Eurocodes (prEN 1991-1-7, 2004, ENV 1991-2-7, 1998) and some different other national design codes (BS 5950-1:2000, 2001, UFC 4-023-03, 2005), the structural integrity of civil engineering structures should be ensured through appropriate measures but, in most of the cases, no precise practical guidelines on how to achieve this goal are provided. Even basic requirements to fulfil are generally not clearly expressed. Different strategies may therefore be contemplated:

- Integrate all possible exceptional loads in the design process in itself; for sure this will lead to non-economic structures and, by definition, the probability to predict all the possible exceptional events, the intensity of the resulting actions and the part of the structure which would be affected is seen to be "exceptionally" low.
- Derive requirements that a structure should fulfil in addition to those directly resulting from the normal design process and which would provide robustness to the structure, i.e. an ability to resist locally the exceptional loads and ensure a structural integrity to the structure, at least for the time needed to save lives and protect the direct environment. Obviously the objective could never be to resist to any exceptional event, whatever the intensity of the resultant actions and the importance of the structural part directly affected.

In the spirit of the second strategy, a European RFCS project entitled "Robust structures by joint ductility – RFS-CR-04046" has been set up in 2004, for three years, with the aim to provide requirements and practical guidelines ensuring the structural integrity of steel and composite structures under exceptional events through an appropriate robustness.

The robustness is required from the structural system not directly affected by the exceptional event (to avoid the local destruction of the structural element where the event occurs being often not possible). In this process, the ability to redistribute plastically extra forces resulting from the exceptional event is of high importance. This requires from all the structural elements and from the constitutive joints a high degree of plastic deformability under combined bending, shear and/or axial forces.

The partners involved in this previously mentioned project are:

- Stuttgart University, Germany;
- Liège University, Belgium;

- ArcelorMittal Long Carbon Europe R&D, Luxembourg;
- Feldmann + Weynand Ingenieure, Germany and;
- Trento University, Italy.

The present article which summarizes works performed at Liège University is organized as follows:

- Section 2 presents the different exceptional events covered within the project and the adopted strategy;
- then, first numerical and analytical developments are described in Section 3 and;
- finally, in Section 4, the substructure test is presented together with the main results.

2 EXCEPTIONAL EVENTS COVERED AND STRATEGY ADOPTED

As a general procedure to derive robustness requirements, different structural systems subjected to exceptional events are analytically and numerically investigated within the previously mentioned project in order to see how steel and composite structures work when part of the structure is destroyed as well as how and how far redistribution takes place.

Exceptional events have been selected; many could be contemplated, but few preliminary ones have been considered as reference cases to be studied first:

1. loss of a column in an office or residential building frame;
2. loss of a beam in an office or residential building frame;
3. loss of a column in an industrial portal frame;
4. loss of a bracing in an industrial portal frame;
5. loss of a bracing in a car park;
6. unexpected earthquake;
7. unexpected fire.

For the five first cases, finite element (FEM) numerical simulations are carried out so as to understand how the structure and its constitutive elements behave and how the redistribution of forces takes place in the unaffected part of the frame. In this process, a special attention is devoted to the study of the loading sequence inside the joints. As a result of these FEM numerical simulations and associated parametrical studies, simplified behavioural models should be developed and validated; these ones should progressively lead to analytical models, from which requirements to be satisfied by the structural system and by the joints could be derived.

Progressively, other exceptional situations should be investigated in the same way and related design requirements should be derived.

Possibly similarities between different exceptional events and their corresponding failure modes could be identified and more general requirements are so expected to be formulated.

For the six and seventh here-above listed events, the work consists in expressing requirements that structures which have not been explicitly designed for fire and/or seismic actions should fulfil so as to possess a certain amount of robustness against such unexpected extreme situations. In different countries, “good practice” detailing recommendations and conceptual design guidelines exist (for instance for so-called “non-engineered structures”) and the work should therefore consist in gathering and analysing this available material and present it into an adequate format.

Within the previously mentioned European project, the analytical and numerical investigations have been shared among the partners:

- Trento University is in charge of “event 6” (earthquake);
- Long Carbon R&D covers “event 7” (fire);

- Stuttgart University studies “event 5” (loss of a bracing in a car park);
- Liège University focuses on “events 1 and 3” (loss of a column in office or residential composite building frames and in industrial steel structures);
- F+W contributes to the knowledge on “events 1 and 3” by studying 3-D aspects as well as the loss of more than one column.

Liège University is in charge of coordinating the whole activity.

Also, one of these exceptional events, the loss of a column in a composite structure, is intended to be tested experimentally at Liège University, as part of the project; one of the objectives is to validate the numerical FEM tool.

Finally, through parametrical studies carried out numerically for the selected events, robustness requirements are aimed to be derived.

In Figure 1, the strategy adopted at Liège University is summarized.

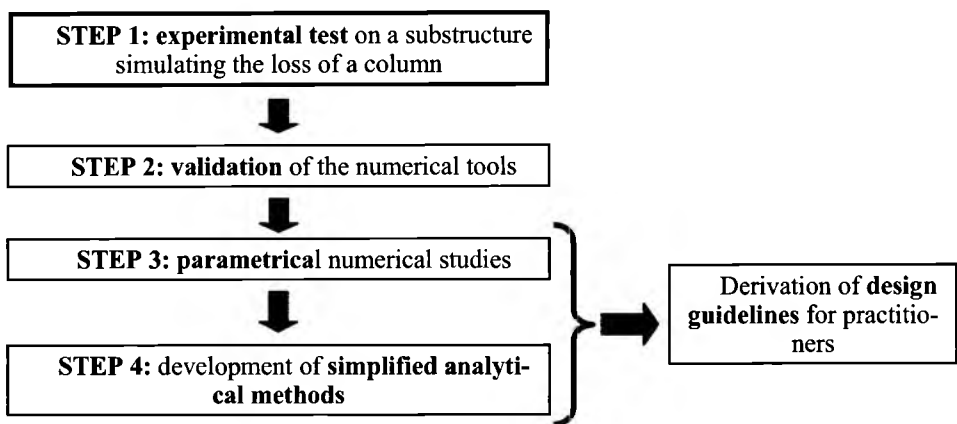


Figure 1: Global strategy followed in Liège.

In the next section, first analytical and numerical investigations performed at Liège University on “Event 1” (as a contribution to STEP 3 and 4 – see Figure 1) are described.

3 LOSS OF A COLUMN IN A BUILDING – FIRST ANALYTICAL AND NUMERICAL INVESTIGATIONS

3.1 Introduction

As mentioned in the previous section, analytical and numerical investigations have been conducted on “Event 1” dealing with the loss of a column in office or residential building frames, as illustrated in Figure 2.

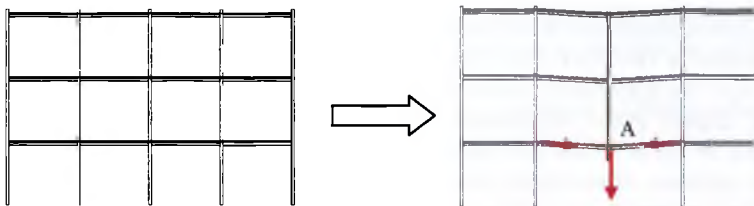


Figure 2: Loss of a column in a residential or office building frame.

At first, before the event, the beam-to-column joints and the beams are mainly subjected to bending moments and shear forces. When the column loses its carrying capacity (because it is impacted, for instance), catenary action develops in the beams (as illustrated in Figure 3); axial forces increase (because of loads transferred by the column stub located just over the impacted one) until the joint or the beam reaches a full plastic state (under moment and axial forces). The beam takes large transverse displacements and axial forces increase further while bending moments decrease; this loading path and the evolution of the bending moment and axial force in the beam-to-column joints (or in the beam) are qualitatively illustrated in Figure 4.

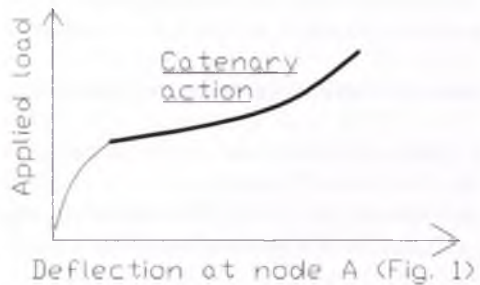


Figure 3: Development of a catenary action in the structure – “applied load/beam deflection” curve.

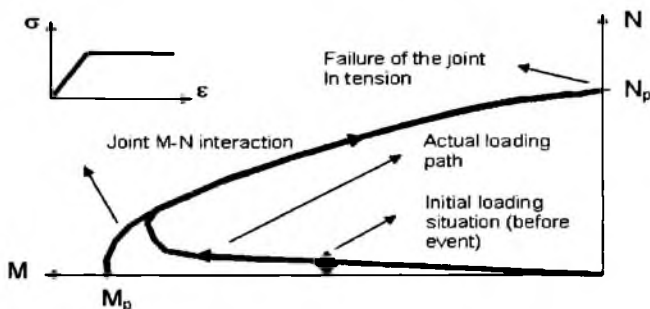


Figure 4: Actual loading in the joint or in the beam until failure.

At the end, the joints and the beam work mainly in tension. If the transverse forces applied to the beam (loads acting on the beam itself and loads from the upper storeys) is such that the value of N_p (axial resistance) is not reached in the joints or in the beam, the system has a sufficient robustness to face the event; if not, a lack of robustness has to be contemplated.

The scope of the previously mentioned project is to reach robustness through joint ductility. So, the frames under consideration possess partial-strength and semi-rigid beam-to-column joints; so the joints are the “weak” elements when catenary actions develop.

From the previous observation, requirements on the required joint tensile resistance may be derived; but it should not be forgotten that the joint will only be able to develop an adequate resistance all along the loading sequence if the ductility of the joint is sufficient to avoid a premature brittle failure inside the joint (welds, bolts, rebars in case of composite joints, ...). That is why the requirements have to be expressed in terms of resistance and ductility (as for some seismic design procedures), and not only, as it is the case in the few presently available design recommendations (e.g. BS 5950-1:2000, 2001 in UK), in terms of resistance.

The intention in Liège is to substitute the complex problem of the loss of a column in a frame by a far simpler one limited to the study of a single “two-beams” system (Figure 5), by referring to the definition of a K restraining coefficient.

The K spring simulates the restraint offered by the undamaged part of the frame to the development of very high transverse displacements at mid-span of the two-beams system when the column is impacted. Through this structural restraint K, a catenary action may develop in the system.

In order to validate this simplification, the following steps have to be crossed:

- proceed to the numerical simulation of the full non-linear response of the impacted frame;
- proceed to the numerical simulation of the full non-linear response of the “two-beams” simplified system;
- compare the good agreement between the numerical responses got respectively for the full frame and for the “two-beams” system.

And as a result, it may be concluded that by the study of the equivalent “two-beams” system may be adequately substituted to the study of the whole frame.

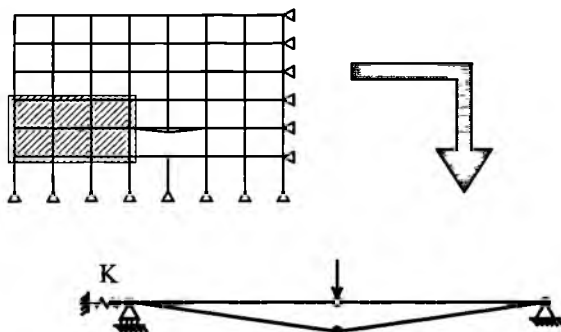


Figure 5: Global and local modelling of “event 1“ (loss of a column).

The final objective is to develop an analytical model, the use of which could allow the derivation of design requirements for robust structures, in case of the loss of a column.

Practically speaking, the influence of each of the main parameters on the response of the impacted system is studied and conclusions are drawn so as to see whether and how, at the end, these parameters have to be further contemplated.

In a first step, in order to understand how the various parameters influence the response of the “two-beams” system, an eleven-level parametrical study has been carried out. The latter is presented in the next section.

3.2 Parametrical study of the subsystem

So as to identify the parameters influencing the response of the subsystem under the considered exceptional event, an eleven-level parametrical numerical investigation has been performed on the subsystem previously defined.

The main parameters considered are the following ones:

- The beam response: the stiffness of the beams in bending (EI) and under axial force (EA) are varied, as well as the yield strength f_y of the constitutive material; a high value of EI allows to simulate “rigid” beams, while the adoption of high values of f_y enables to simulate a fully elastic response of the beam elements.
- The K restraint: the importance of the membrane effects in the beam increases with the K values, while the beam transverse displacements at failure decrease. For high values of K , high tying forces are obtained at beam ends, while demand in terms of rotational capacity is requested at beam ends when large displacements occur in the beam, i.e. for low values of K .
- The resistance properties of the beam end sections: in this preliminary study, no connection is assumed to act at beam ends; so possible plastic hinges develop in the beam itself for an axial force equal to N_p (tension resistance of the beam), for a bending moment equal to M_p (bending resistance of the beam cross-section) or under a combination of moment and axial forces. In the parametrical study, no interaction between axial forces and bending moments is first contemplated; then a non-linear interaction resistance curve characterizing the beam cross-section is considered.

The eleven considered levels are illustrated in Figure 6. The system is loaded by a uniformly distributed load; the total length of the system is equal to 4m.

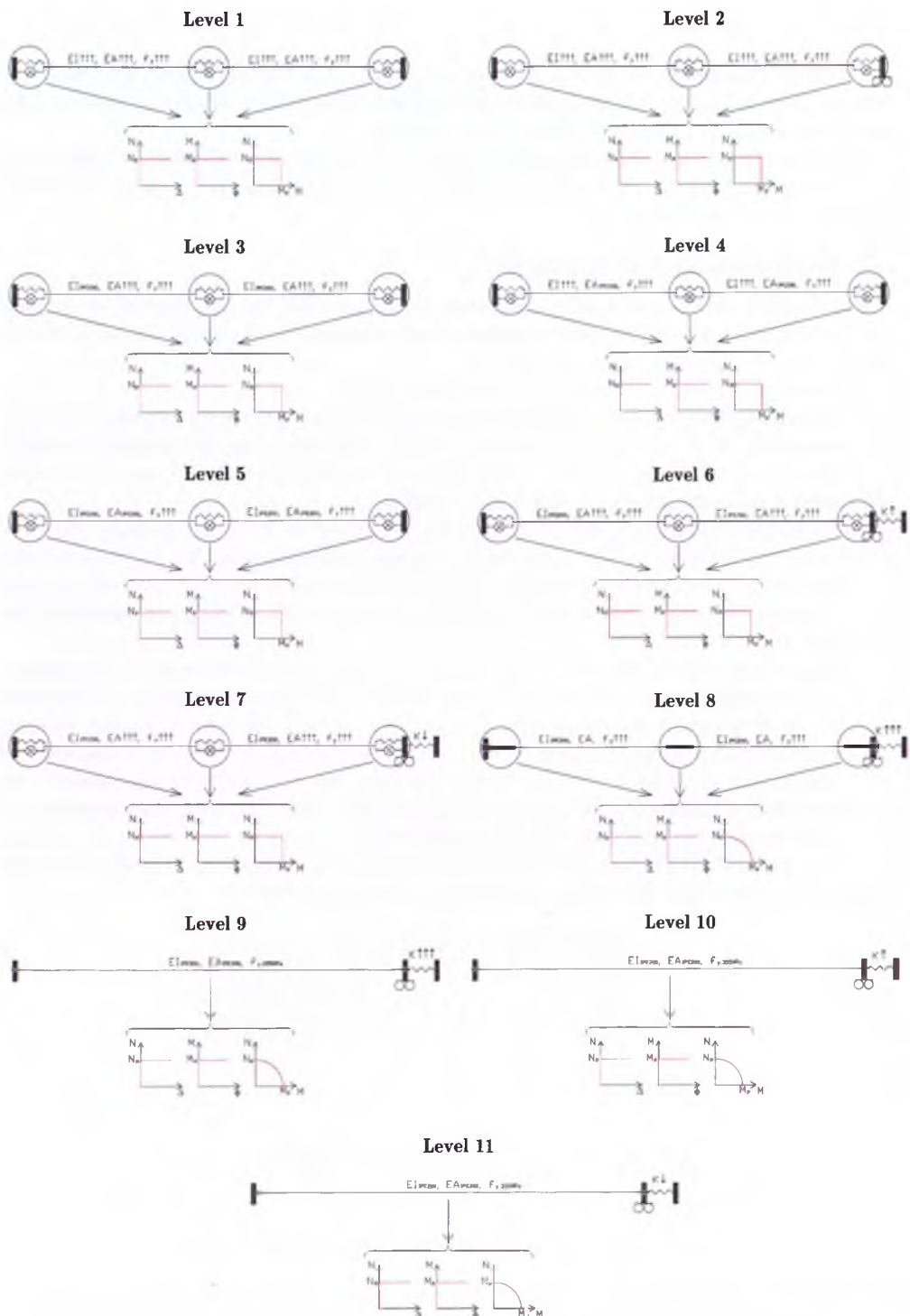


Figure 6: Investigated levels for the parametrical study of the subsystem

The numerical investigations are performed with the homemade finite element software FINELG developed at Liège University (ArGENCo Department) and at Greisch design office (Liège, Belgium).

Full 2-D non-linear analyses are performed, with due account of geometrical and material nonlinearities. The numerical technique implemented in FINELG enables to follow the behaviour of a structure under increasing external loading up to collapse or instability, and even beyond.

The scope of the presented study is to investigate the influence of different parameters on the development of the catenary action in the subsystem. So, in order to not to restrict the development of the catenary action in the numerical modelling, the plastic strain limitations have been deactivated in the software, as illustrated in Figure 7, i.e. it is assumed that the different members of the two-beams system have an infinite ductility. In conclusion, the collapse of the subsystem is assumed to be achieved when the axial forces in the system reach the axial resistance N_p .

The results obtained for the different levels are summarised in Figure 8.

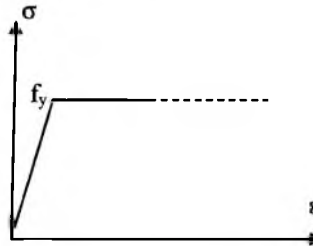


Figure 7. Infinite ductility assumption for steel material.

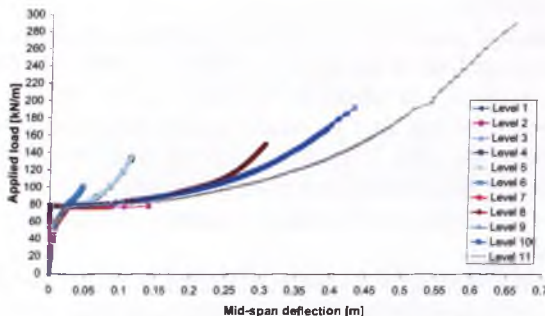


Figure 8. Obtained results for the different investigated levels – “applied load/mid-span beam deflection” curves.

From this parametrical study, interesting conclusions may be drawn:

- The development of the catenary action depends on the relative values of the axial beam stiffness EA/L and the stiffness of the spring K . In practical situations, it has been shown that the influence of the axial beam stiffness can be neglected. Additional parametrical investigations have also been performed to confirm this observation (Demonceau, 2006).

- The influence of the bending stiffness EI/L on the development of the catenary action may be neglected. This has also been confirmed through additional parametrical studies (Demonceau, 2006).
- The maximum applied load which can be reached, for the loading path described in Figure 3, depends of the value of K . It increases with decreasing values of K . Also, as previously predicted (see Section 3.1), the needs in terms of ductility increase also when the K value is decreasing.

These numerical analyses only represent the first step of the works carried out. As already said, the next steps to be reached are:

- the development of analytical formulations so as to predict the response of the “two-beams” sub-system;
- the derivation of design requirements in terms of resistance and ductility;
- the validation of the use of a “two-beams” sub-system.

The validation of the subsystem - through comparisons of its response with the one obtained by simulating the whole structure – requires the preliminary evaluation of the stiffness of the K restraint. This work has been carried out by the third author of the present paper and validated through few hundreds of numerical simulations. In his study, the position of the impacted column in the structure has been considered, as well as the braced/unbraced character of the structure. The analytical formulation of the K factor resulting from these investigations is intended to be published soon (Luu, 2008).

4 DESCRIPTION OF THE EXPERIMENTAL TEST ON A SUBSTRUCTURE (DEMONCEAU ET AL, 2006c)

4.1 Introduction

Within the RFCS European project, a test on a substructure simulating the loss of a column in a composite building has been performed in Liège. The aim is to validate the numerical tools used for the parametrical investigations.

To define the substructure properties, an “actual” composite building has been designed (Demonceau et al., 2006a) according to Eurocode 4 (NBN EN 1994-1-1, 2005), so under “normal” loading conditions (i.e. loads recommended in Eurocode 1 (EN 1991-1-1, 2002) for office buildings); the main properties of this building are briefly introduced in Section 4.2.

As it was not possible to test a full 2-D actual composite frame within the project, a substructure has been extracted from the actual frame described in Section 4.2; it has been chosen so as to respect the dimensions of the testing slab but also to exhibit a similar behaviour than the one in the actual frame (see Section 4.3).

Then, the loading path followed for the test is described in Section 4.4 and, finally, the main test results are presented in Section 4.5 where the main phenomena observed during the test are also described.

4.2 Description of the reference composite building

The building is composed of three main frames at a distance of 3m. Each frame has four bays (4m width each) and three storeys (3.5m height each); the general layout is given in Figure 9.

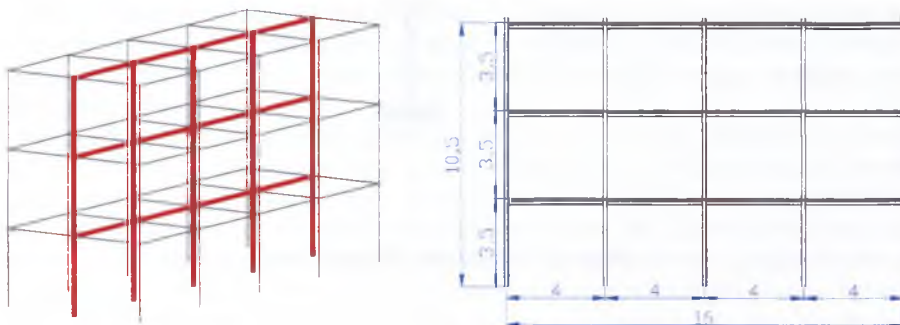


Figure 9: General layout of the reference composite building.

As previously said, the building has been designed according to Eurocode 4 and under normal loading conditions. Its structural characteristics are as follows:

- The slab is a reinforced concrete one (12cm thick and C25/30 concrete). The reinforcement is composed of two steel meshes: the upper one with 10mm rebars each 200mm and the lower one with 10mm rebars each 150mm. The steel grade for these rebars is S500C and the cover is equal to 25mm. The slab cross-section is shown in Figure 10.

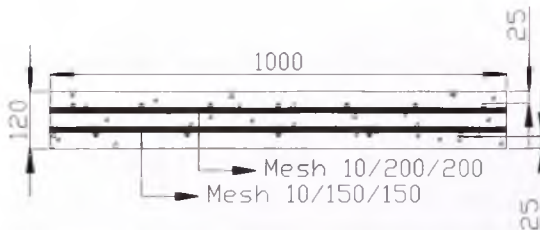


Figure 10: Slab properties

The composite beam cross-section is seen in Figure 11. A S355 IPE140 profile is used and a full shear connection is assumed between the steel profile and the concrete slab.

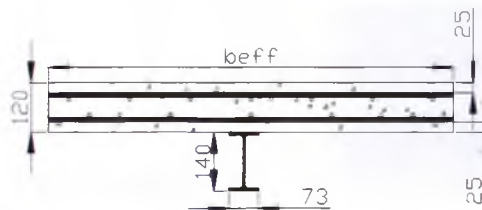


Figure 11: Composite beam cross-section.

- The columns are steel ones (S355 HEA160).
- Partial-strength and semi-rigid joints are considered (Figure 12 and Figure 13). The properties of these joints allow them to exhibit a ductile behaviour (with account of possible overstrength effects).

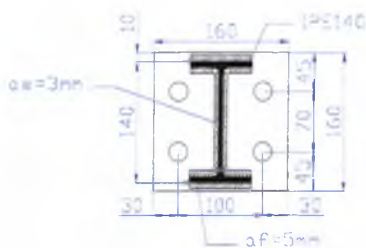


Figure 12: Dimensions of the end-plates.

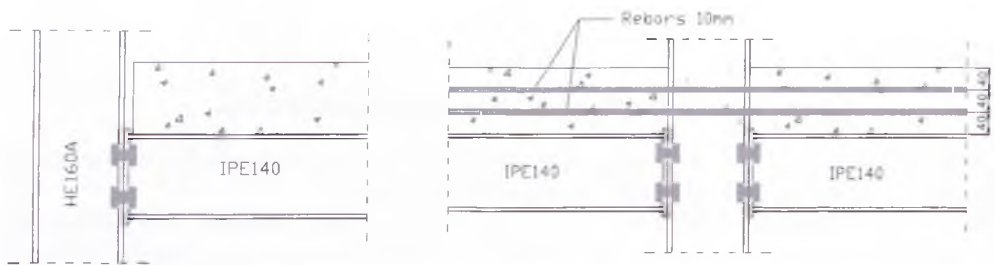


Figure 13: External steel joints and internal composite joints.

4.3 From the reference composite building to the tested substructure

Within the RFCS project, testing of the full reference composite frame may not be contemplated. So, a substructure has been extracted from the actual frame (Demonceau et al, 2006b). As previously mentioned, this substructure should conform to the dimensions of the testing slab but also exhibit a similar behaviour than the one which would be observed in the actual frame.

To achieve this goal, the bottom storey is isolated from the actual building, but the width of the external spans is then reduced, as illustrated in Figure 14.

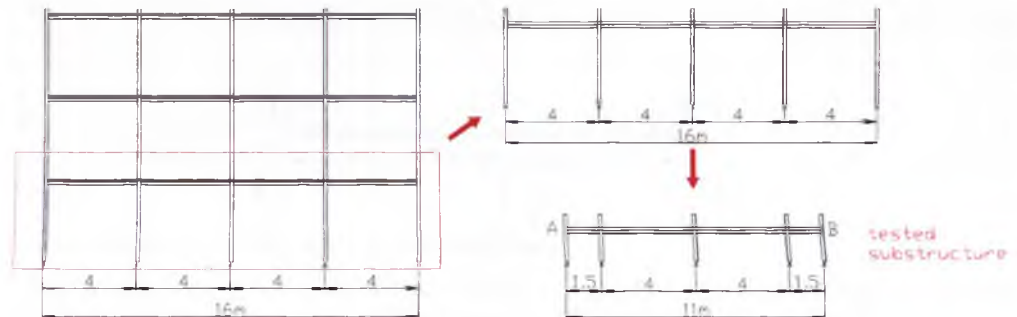


Figure 14: From the actual frame to the tested substructure

The width of the concrete slab is equal to 500mm. It is fixed so as to ensure that, during the loading, the distribution of the stresses in the concrete is as uniform as possible; in fact, 500mm corresponds to the value of the effective width of the concrete slab (under hogging moments) in the actual building, according to Eurocode 4.

The 10mm rebars used in the actual frame (see Section 4.2) are here substituted by 8mm ones; the objective is to increase the probability to develop a large number of small cracks in the slab, under hogging beam moments, instead of few big cracks and so to allow for more local ductility.

Besides that the distance between the first headed stud and the face of the column flange is larger than what is usually adopted and the amount of longitudinal reinforcement within this area is kept constant (see Figure 15); as a consequence, the slab is subjected to constant tension forces in this zone, what results in an especially high ductile behaviour. This specific detailing has been investigated at the University of Stuttgart (Kuhlmann et al, 2004) and its efficiency has been demonstrated.

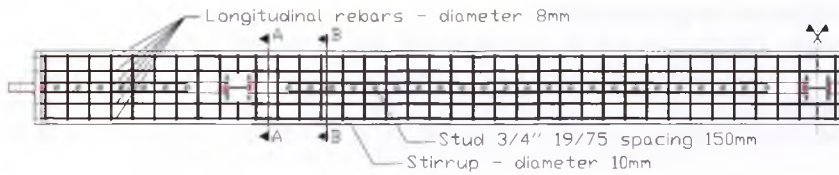


Figure 15: Reinforcement and studs layouts.

Column bases are assumed to be pinned (Figure 16). Teflon elements are used so as to limit the friction between the column steel supports and the pins during the loading.

The composite joints in the substructure are the same than in the actual building (Figures 12 and 13). Only the external beams are simply connected to the external columns (as shown in Figure 17) so as to limit the number of parameters which could influence the response of the internal beams during the test.



Figure 16: Actual hinges at the column bases.

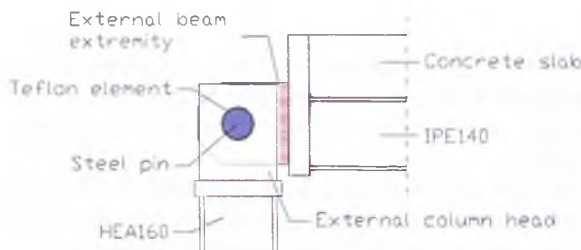


Figure 17: Actual hinges at the external beam-to-column joints.

As previously said, the response of the substructure should be as close as possible to the one of the reference frame. But by reducing the length of the external beam spans and placing hinges at the external joints, a key element is modified: the frame restraint (K factor) (see Section 3.1), which strongly influences the catenary action.

That is why lateral restraints are provided each side of the substructure (see point A and B in Figure 14) so as to simulate the actual frame restraints. Restraints are provided on both sides of the substructure in order to induce a symmetrical response of the substructure during the test (see Figure 18); this should facilitate the application of the loads and the measurements during the test.

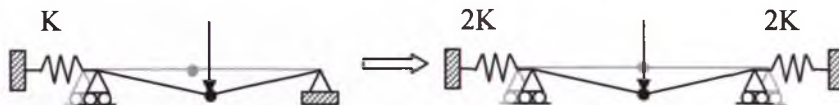


Figure 18: From the unsymmetrical actual behaviour to the symmetrical test behaviour.

In practice, the restraints will be brought by two horizontal calibrated jacks (Figure 19); the restraint will be assumed to be elastic until the end of the test.

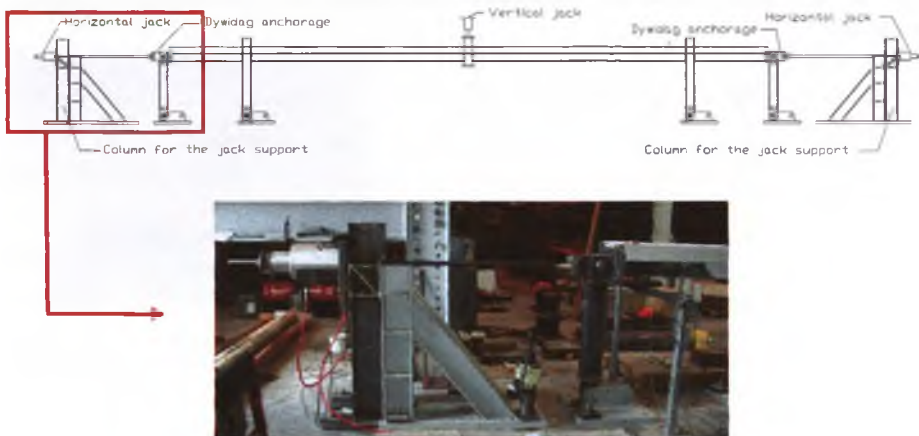


Figure 19: Configuration of the substructure test to be performed at Liège University

4.4 Loading path

The load path during the test is as follows:

- The substructure is first preloaded with an uniformly distributed load on the internal beams to simulate the reaction of the concrete slab on the main frame in the actual building (see Figure 9); during this preloading, two locked jack are placed at the middle of the substructure to simulate the presence of the column, as illustrated in Figure 20.
- In a second step, the support brought by the jacks is progressively removed by unlocking the jacks; when the latter are removed, the free deflection of the system is observed. The further procedure is to apply a vertical force with a jack on the column thus further deformation will occur (see Figure 21).

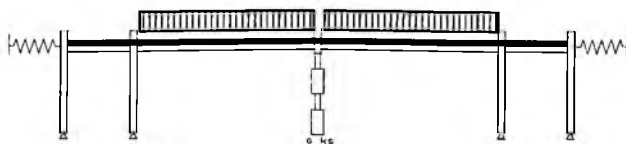


Figure 20: Column at the middle simulated by two locked jacks

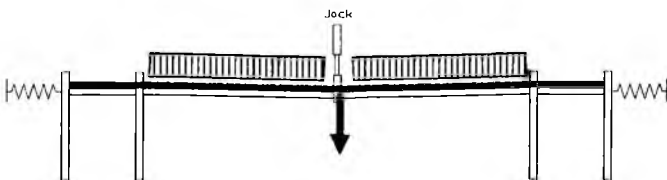


Figure 21: Application of a vertical load with a vertical jack until collapse

4.5 Experimental test results

As explained before, an uniformly distributed load is first applied on the substructure (by means of steel plates and concrete blocks). The vertical reaction which is associated to the uniformly distributed load and to the self-weight of the substructure is equal to 33,5kN as illustrated in Figure 22 (value of the load at point "O") presenting the evolution of the vertical displacement at the middle of the structure according to the vertical load. After the application of the uniform load, the jacks at the middle are unlocked and progressively removed. The system is completely released when a deflection of 29mm is reached. At this stage, first cracks at the vicinity of the external joints are observed and first steel yielding is seen in the column web panel of the internal composite joint. This first step of the test is illustrated by part "OA" of the curve presented in Figure 22; from the latter, it can be seen that the structure still be in the elastic range when "A" is reached.

Then, a vertical load is progressively applied until collapse of the tested specimen. During this stage, two "unloading-reloading" are performed as illustrated in Figure 22. From point "A" to "B", the substructure enters in the yielding stage to finally form a beam plastic mechanism at point "B" with formation of the plastic hinges at the joint level. During this stage, the cracks in the vicinity of the external composite joints are more pronounced and yielding of some steel components of the joints is observed (column web and beam flange in compression); also, for the internal composite joint, a detachment between the end-plate and the column flange at the bottom can be seen.

From point "B" to "C", a plateau is observed. During this stage, the concrete cracks in the vicinity of the external composite joints continue to develop and yielding spreads in the steel components; one important phenomenon to be mentioned is the concrete splitting in the vicinity of the internal composite joint during this stage. At point "C", membrane forces begin to develop as confirm by the shape of the curve "CD" in Figure 22.

When the point "D" is reached, the longitudinal rebars in the vicinity of the external composite joints are completely destroyed and the concrete at the internal joint is fully spited (Figure 23); at this moment, the joints work as steel ones. The yielding also spreads in the different steel components of the internal and external composite joints. At point "D", a loss of stiffness is observed which is linked to the loss of the longitudinal rebars in the vicinity of the external joints; indeed, when these rebars are lost, the tensile stiffness of the external joints decreases, phenomenon which affects the development of the membrane forces.

At the end of the test (point "E"), a maximum vertical displacement of 775mm is reached for an applied vertical load of 114kN; the deformation of the specimen at this stage is presented in Figure 24. The maximum horizontal displacement at each side of the structure is equal to 45mm for a horizontal load of 147kN. The main components which have been activated within the joints are:

- For the external composite joints: yielding of the column web in compression, the beam flange and web in compression, the column flange in bending.
- For the internal composite joint: yielding of the column web in tension (Luders bands) associated to the membrane forces, column flange in bending, beam flange and web in tension.

The test was stopped with the apparition of cracks at the bottom weld between the IPE140 profile and the end-plate at the internal composite joint for a maximum rotation of 190mRad.

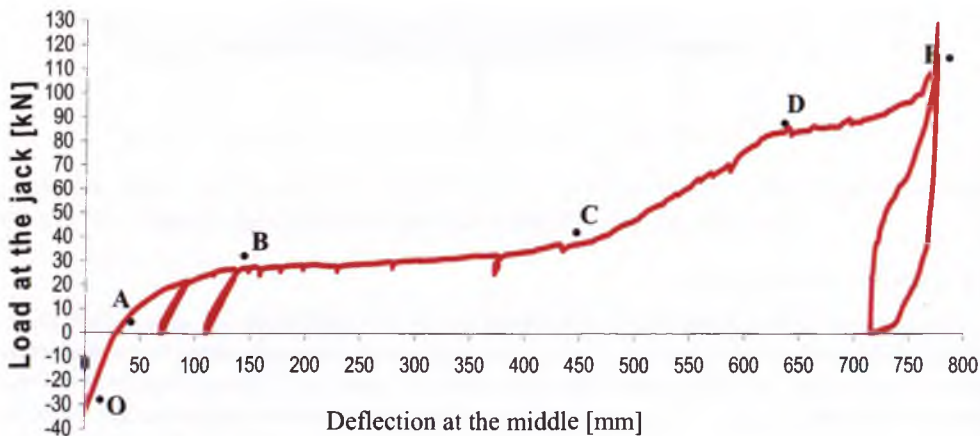


Figure 22: Vertical load at the middle/vertical displacement curve



Figure 23: Internal and external composite joints at point "D" of Figure 22



Figure 24: Deformation of the specimen at the end of the test.

Besides that, experimental tests in isolation have been performed at Stuttgart University on the composite joints of the substructure, respectively under hogging or sagging bending moments and tensile axial forces; finally tests on joint components have been realized at Trento University. So as to be able to compare the results obtained in the laboratories, all the steel elements (profiles, plates and rebars) were provided by the same companies and came from the same rolling. A unique chain of consistent experimental results is so obtained.

5 DEVELOPMENT AND VALIDATION OF AN ANALYTICAL PROCEDURE TO PREDICT THE RESPONSE OF COMPOSITE JOINTS SUBJECTED TO COMBINED MOMENTS AND AXIAL LOADS

As previously mentioned, the structural joints during the exceptional event are subjected to combined bending moments and axial loads. In the PhD thesis of Cerdantaine (Cerdantaine, 2003), an analytical procedure is proposed to predict the response of steel joints subjected to such a loading. The proposed method is based on the component method which is the recommended method in the Eurocodes for the design of joints subjected to bending moments.

In (Demonceau, 2008), this method is extended to composite joints. The particularity of composite joint configurations is the fact that two main additional components are activated if compared to steel ones: the slab rebars in tension and the concrete slab in compression. As the analytical procedure presented in (Cerdantaine, 2003) is based on the component method concept, the latter is easily extended to composite joint configurations by including the behaviour of the two additional components into the procedure. However, the characterisation of the component "concrete slab in compression" is not yet available in the actual codes; accordingly, an analytical method to characterise this component in terms of resistance and stiffness is proposed and validated in (Demonceau, 2008).

The extended method is validated through comparisons to results coming from experimental tests performed at Stuttgart University on the tested substructure joint configuration (Kuhlman & al., 2007). These results are compared in Figure 25 where two analytical curves are reported:

- one called "plastic resistance curve" which is computed with the elastic resistance stresses of the materials and;
- one called "ultimate resistance curve" which is computed with the ultimate resistance stresses of the materials.

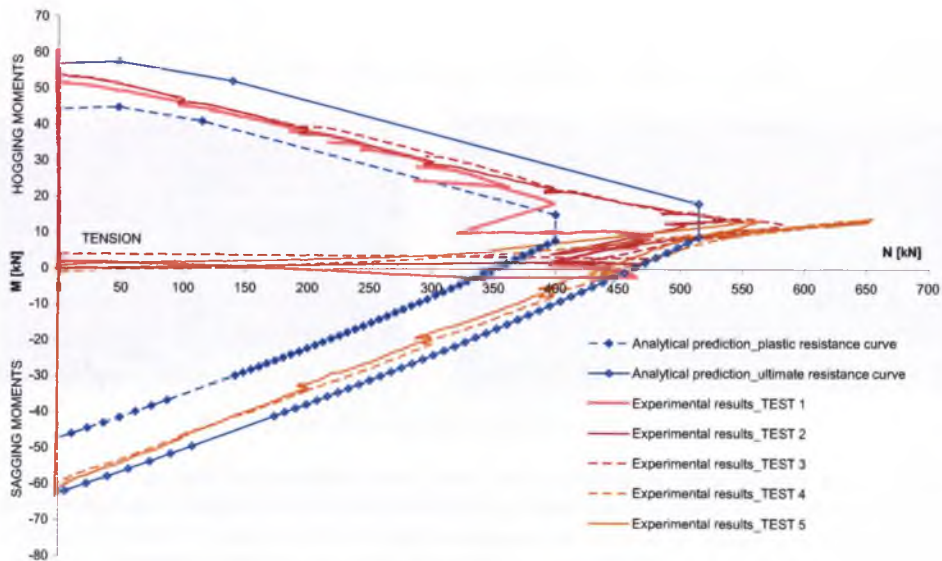


Figure 25: Comparison of the resistance interaction curves

According to Figure 25, the computed analytical curves are in very good agreement with the experimental results. Indeed, the experimental curves are between the plastic and ultimate analytical resistance curves what is in line with the loading sequence followed during the tests. The fact that the maximum tensile load reached during the experimental tests is higher than the one analytically

predicted can be explained by membrane forces developing in some joint components in bending, forces which are not taken into account in the analytical method.

6 DEVELOPMENT AND VALIDATION OF AN ANALYTICAL PROCEDURE TO PREDICT THE RESPONSE OF THE TWO-BEAMS SYSTEM

As explained earlier, the two-beams system (see Figure 5) may adequately reproduce the global response of a frame further to a column loss.

The objective is to develop an analytical procedure for the prediction of the response of the substructure in the post-plastic domain, i.e. after the formation of the beam plastic mechanism; as a direct consequence, the here-proposed analytical model is based on a rigid-plastic approach. Also, as the deformations of the substructure are significant and influence its response, a second-order analysis is conducted.

The parameters to be taken into account are presented in Figure 26:

- p is the (constant) uniformly distributed load applied on the storey modelled by the simplified substructure and the concentrated load Q is the force acting in the upper column;
- L is the total initial length of the simplified substructure;
- Δ_Q is the vertical displacement at the concentrated load application point;
- δ_K is the deformation of the horizontal spring simulating the lateral restraint coming from the indirectly affected part;
- δ_{N1} and δ_{N2} are the plastic elongations at each plastic hinges;
- θ is the rotation at the plastic hinges at the beam extremities.

In addition, the axial and bending resistances at the plastic hinges N_{Rd1} and M_{Rd1} for the plastic hinges 1 and 4 and N_{Rd2} and M_{Rd2} for the plastic hinges 2 and 3 have also to be taken into account (it is assumed that the two plastic hinges 1 and 4 and the two plastic hinges 2 and 3 - see Figure 26 - have respectively the same resistance interaction curves).

In order to be able to predict the response of the simplified substructure, the parameters K and F_{Rd} have to be known; these parameters depend of the properties of the indirectly affected part. As already said, analytical procedures are proposed in (Luu, 2008) to predict these structural characteristics.

The results obtained with the so-developed analytical procedure are compared to the substructure test results in Figure 27. In this figure, it can be observed that a very good agreement is obtained between the analytical prediction and the experimental results, what validates the developed method. More details about the developed method are available in (Demonceau, 2008).

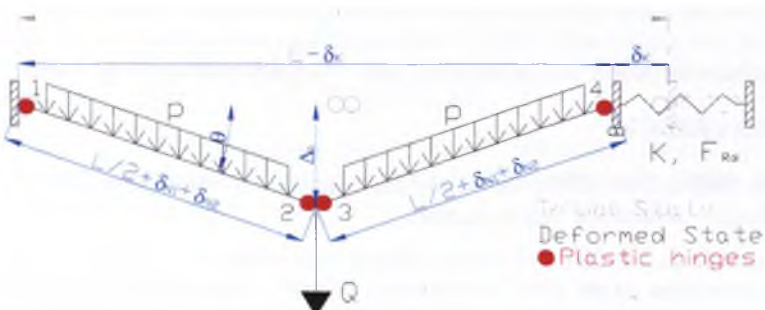


Figure 26: Substructure

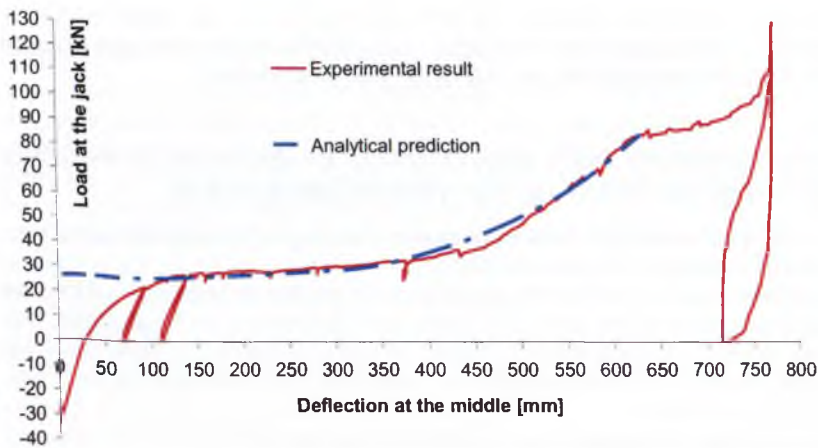


Figure 27: Comparison between analytical prediction and experimental test

7 CONCLUSIONS

In this paper, the global strategy defined at Liège University and adopted within the European project “Robust structures by joint ductility” is described for the study of the behaviour of steel and composite structures under exceptional events.

In this project, Liège University covers in particular the problems related to the loss of a column in a residential or office steel or composite building.

First numerical investigations have been achieved and the main results have been presented; the objective was to study the influence of some key parameters on the structural response of the building.

Also, an experimental test on a composite substructure simulating the loss of an internal column has been performed. This test has been described in details with the main obtained results. The performed test was successful and all the phenomena under investigations were registered. Indeed, the development of the catenary action in the system was observed and the registered curves confirmed the development of membrane forces in the beams. Also, the composite joints loaded by combined tensile forces and bending moments exhibited a ductile behaviour as expected.

Finally, analytical models aimed at predicting the full non-linear response of the structure further to the loss of a column have been developed and validated through comparisons with test results. The last step should now consist in deriving design requirements for robust structures, in the specific case of the loss of a column. This work is presently in progress in Liège.

8 REFERENCES

- [1] BS 5950-1:2000, 2001, “Structural use of steelwork in building – Part 1: Code of practice for design – Rolled and welded sections”.
- [2] Demonceau J.F, 2006, “Loss of a column in an office or residential building frame – Numerical investigation of the steel “two-beams” system”, internal report of the RFCS project “Robust structures by joint ductility - RFS-CR-04046”.

- [3] Demonceau J.F. & Jaspart J.P, 2006a, “*Predesign of the substructure to be tested at the University of Liège – draft 4*”, internal report of the RFCS project “Robust structures by joint ductility - RFS-CR-04046”.
- [4] Demonceau J.F. & Jaspart J.P, 2006b, “*From the “actual” composite building to the tested substructure – draft 1*”, internal report of the RFCS project “Robust structures by joint ductility - RFS-CR-04046”.
- [5] Demonceau J.F. & Jaspart J.P, 2006c, “*Experimental test simulating the loss of a column in a composite building – preliminary draft*”, internal report of the RFCS project “Robust structures by joint ductility - RFS-CR-04046”.
- [6] EN 1991-1-1, 2002, “*Eurocode 1: Actions on structures – Part 1-1: General actions – Densities, self-weight, imposed loads for buildings*”, April 2002.
- [7] ENV 1991-2-7, 1998, “*Eurocode 1: Basis of design and action on structures – Part 2-7 : Accidental actions due to impact and explosions*”, final draft, June 1998.
- [8] Kuhlmann U. & Schäfer M, 2004, “*Innovative verschiebbliche Verbund-Rahmen mit teiltragfähigen Verbund-Knoten*”, Forschung für die Praxis P 505, Forschungsvereinigung Stahlanwendung e.V. im Stahl-Zentrum, 2004.
- [9] NBN EN 1994-1-1, 2005, “*Eurocode 4: Calcul des structures mixtes acier-béton – Partie 1-1: Règles générales et règles pour les bâtiments*”, February 2006.
- [10] prEN 1991-1-7, 2004, “*Eurocode 1 – Action on structures – Part 1-7: General actions – Accidental actions*”, final project team draft (stage 34), 9 July 2004.
- [11] UFC 4-023-03, 2005, “*Unified Facilities Criteria (UFC) - Design of buildings to resist progressive collapse*”, Department of Defence, USA, 25 January 2005.
- [12] Demonceau J.F., 2008, “*Steel and composite building frames: sway response under conventional loading and development of membrane effects in beams further to an exceptional action*”, PhD Thesis to be presented in spring 2008 at Liège University, 2008.
- [13] Demonceau J.F., 2008, “*Steel and composite building frames: sway response under conventional loading and development of membrane effects in beams further to an exceptional action*”, PhD Thesis to be presented in spring 2008 at Liège University, 2008.
- [14] Luu H.H.N., 2008, “*Structural response of steel and composite building frames further to an impact leading to the loss of a column*”, PhD Thesis to be presented in summer 2008 at Liège University, 2008.
- [15] Cerfontaine F., 2003, “*Study of the interaction between bending moment and axial force in bolted joints (in French)*”, PhD Thesis, Liège University, 2003
- [16] Kuhlman U., Rölle L., Jaspart J.P. and Demonceau J.F., 2007, “*Robust structures by joint ductility*”, COST C26 European Action “Urban habitat constructions under catastrophic events”, Proceedings of the Workshop in Prague, March 2007.

PROGRESSIVE COLLAPSE SIMULATION TECHNIQUES FOR RC STRUCTURES

Ph. Bouillard¹, K. Menchel¹, B. Santafé² and T. J. Massart¹

¹Université Libre de Bruxelles, BATir
50 Avenue F. Roosevelt, 1050, Brussels, CP 194/2
e-mail: {kmenchel, thmassar, pbouilla}@batir.ulb.ac.be

²Royal Military School, Civil and Materials Engineering Dept
Avenue de la Renaissance 30, B-1000 Brussels
e-mail: Bertha.Santafe@rma.ac.be

Keywords: Progressive collapse, plastic hinge, frame.

Abstract. *Throughout recent history, well documented records of building failures may be found, unfortunately accompanied by great human loss and major economic consequences. One of the mechanisms of failure is referred to as 'progressive collapse': one or several structural members suddenly fail, whatever the cause (accident or attack). The building then collapses progressively, every load redistribution causing in turn the failure of other structural elements, until the complete failure of the building or of a major part of it. Various procedures are proposed in the literature in order to simulate the effects of this phenomenon, all of them based on different specific assumptions, such as the independence of the procedure with respect to the cause of the initial failure, or the sequence in which the loads are applied. Since the degree of approximation induced by these assumptions is not discussed in these contributions, the aim of this paper is to assess it. A more complete yet still simplified approach, avoiding some of these assumptions, is devised, based on a finite element large displacement code, using plastic hinges associated to beam finite elements. Comparisons are established between these results and those obtained with four quasi-static procedures already present in the literature. A discussion based on the results of a large-scale example, provides an assessment of their degree of validity. Discrepancies appear in some cases between the results obtained with the procedures taken from the literature and the reference solutions obtained with the more complete approach. As a result, the better procedures out of those studied can thus be singled out.*

1 INTRODUCTION

Throughout recent history, famous records of building failures may be found, unfortunately accompanied by great human loss and major economic consequences. One of the mechanisms of failure is referred to as ‘progressive collapse’: one or several structural members suddenly fail, whatever the cause (accident or attack). The building then collapses progressively, every load redistribution causing the failure of other structural elements, until the complete failure of the building or of a major part of it. The civil engineering community’s attention to this type of event was first drawn by the progressive collapse of the building called Ronan Point, following a gas explosion in one of the last floors. Different simplified procedures for simulating the effects of progressive collapse can now be found in the literature [1-9], some of them described in detail. However, to the best of the author’s knowledge, no extensive study can be found, in which these procedures are compared to more complete approaches for progressive collapse simulation, aiming at the comparison of the assumptions underlying them. To further contribute to the elaboration of design codes for progressive collapse, such a study would therefore be of great interest for practitioners. This constitutes the aim of the present paper.

A classification of progressive collapse design strategies is proposed in [10]. This classification unfolds as follows:

- a) High safety against local failure: specific local resistance of key elements (direct design), and non-structural protective measures (event control)
- b) Design for a load case consisting of a local initial failure
- c) Prescriptive design rules (indirect design)

The present paper focuses on the procedures for design strategy b), where there is no attempt to prevent the collapse triggering event, but rather to prevent or limit further damage from occurring in the structure. The different procedures proposed in the literature in order to account for this phenomenon are based on different assumptions, such as the independence of the procedures with respect to the cause of the initial failure [1-9], or their independence with respect to the sequence in which the loads are applied [3,4,8,9]. The aim of this paper is to assess the discrepancies induced by these assumptions based on comparisons on a large scale structure. For this purpose, a more complete yet simplified approach, avoiding some of these hypotheses, is developed, based on a finite element large displacement code with plastic hinges associated to elastic beam elements. This study focuses on reinforced concrete structures, where, in contrast with steel structures, assembly parts do not play a major role during collapse.

The paper is structured as follows: the next section further sets the framework for this paper, and gives a description of the progressive collapse simulation procedures investigated in the paper, focusing on the simplifying assumptions that are discussed subsequently. The key features of each procedure are underlined. The following section describes the plastic hinge element used for all the computations presented in the paper, followed by a short section that briefly describes the corotational approach used to account for large displacements in the beam finite elements. Then, the completed approach, which allows the assessment of the validity of the different features underlying the studied progressive collapse simulation procedures, is presented. It is followed by numerical results obtained for the analysis of a ten-bay eight-floor structure, and their comparison with the other approaches. Finally, the last section sums up the conclusions, and draws main lines of prospective research.

2 NUMERICAL PROCEDURES INVESTIGATED

2.1 Introduction

Different approaches can be found in the literature for progressive collapse simulation. These can be classified in two groups: the probabilistic (or semi-probabilistic) approaches [1,6,7,11] and the deterministic ones [2-5,8-9]. The papers discussing the probabilistic approaches evaluate the failure probability of structures as a function of the occurrence probability of the cause of initial failure. They are therefore of interest for the definition of design codes, with a view to specifying the maximal admissible failure probability. Since every probabilistic approach is based on a deterministic model, the validity of which is not assessed in these papers, the present paper focuses on the assessment of the level of approximations present in different deterministic models.

The focus is set on an analysis of the procedures based on quasi-static computations. As highlighted in the next paragraphs, these quasi-static procedures are based on different simplifying approximations. Although dynamic effects should be accounted for in a complete version of a progressive collapse design tool, as shown in [5], the purpose of the present paper is not to investigate and discuss the techniques with which the investigated procedures take into account dynamic effects, so that the focus is set on the other features of the investigated procedures. This section provides a description of these procedures, with their inherent features.

2.2 Sequence Inversion Procedures

These procedures are based on a computation beginning with the unloaded structure, from which the initially failing elements have been removed. The design loads are then applied to the structure through different types of computations, depending on the phenomena to be taken into account: cross section plastification, choice of yield criterion (stress or strain), quasi-static or dynamic analysis, etc...

The distinctive feature for this class of procedure is that the sequence of events is disregarded. Whereas in reality, the design loads are first applied to the structure, before an external action causes the failure of at least one structural element, these procedures reverse the loading sequence by first removing the initially failing elements, and then loading the structure. In essence, this approach neglects any path dependency effects.

Examples of application of such procedures can be found in [4,5,8,9].

2.3 GSA Static Linear Procedure

In June 2003, the General Services Administration (GSA) issued guidelines [8] for progressive collapse prevention for steel and reinforced concrete structures. It provides a flowchart methodology to determine whether the facility under consideration requires detailed consideration for progressive collapse. If the risk of progressive collapse needs to be further considered, the document provides a threat independent procedure, following the design strategy for a load case consisting of a local initial failure (alternate load path). The document allows for sophisticated nonlinear and/or dynamic procedures, but advocates, and therefore describes in detail, a static linear procedure for progressive collapse mitigation (page 4.12 in [8]).

This static linear procedure introduces the notion of demand to capacity ratios (DCR), and specifies the DCR limit values to be used, depending on the cross-sectional dimensions and on the construction materials (reinforced concrete or steel). In all cases, these limit values are higher than one, in order to account for the structure's ability to redistribute stresses. The pro-

cedure also specifies the size of the portion of the structure in which damage is allowed (called the allowable collapse region in the document)

The load level to be applied to the structure is specified, and consists of the dead loads, and 25% of the live loads. These loads are multiplied by a load factor of 2, accounting for inertial dynamic effects.

The step-by-step procedure given in section 4.1.2.4 (page 4-12) of [8] shows that this linear static procedure falls into the sequence inversion category. Indeed, Step 1 prescribes the removal of a vertical support, followed by a linear static analysis in order to determine the DCR values. Steps 2 and 3 then prescribe geometrical changes to be performed based of the results of step 1, at the locations where the limit DCR values are exceeded. These changes consist in either the removal of the element from the model, or the introduction of a hinge. Step 4 specifies the application of equal-but-opposite moments at the ends of the newly introduced hinges, thus introducing effective plastic hinges. Steps 1 to 4 are to be repeated until no limit DCR value is exceeded in the allowable collapse region, at which point the analysis is complete. No limit DCR value exceeded in the allowable collapse region thus constitutes the exiting criterion from the loop on steps 1 to 4. Then, if no limit DCR value is exceeded outside of the allowable collapse region, the construction is considered to have a low potential for progressive collapse. Otherwise, the structure has to be redesigned.

Specific assumptions of the linear static GSA procedure

1. Since the static linear procedure described in the GSA document prescribes the introduction of hinges while applying equal-but-opposite constant moments, it is a stepwise linear procedure with sequence inversion.

2. While looping on steps 1 to 4, step 1 consists of computations that are started from the unloaded/undeformed structure, in which some geometrical changes are introduced at once. Except for the hinge corresponding to the highest DCR value, this does not take into account the stress redistributions associated with the successive appearance of hinges.

3. Allowing DCR values higher than 1 is probably used to account for stress redistribution potential by the structure. However, choosing fixed limit DCR values for all structures belonging to the same category induces approximations in the stress redistribution potential estimation with respect to computations in which the structural elements yield strengths are explicitly taken into account (i.e. limit DCR values set to 1).

4. The live loads to be applied are set to a 25% of the design live loads. As shown below, the guidelines issued by the Department of Defense specify a value that is twice higher, which may influence the level of validity of the assumptions mentioned above.

2.4 DoD Linear Static Procedure

In June 2005, the American Department of Defense issued guidelines [9] for progressive collapse prevention. Buildings are separated into categories depending on the required level of protection. When a very low or low level of protection is required, the safety of the structure is ensured through horizontal and vertical ties, while an alternate path approach is prescribed, in addition to the ties for higher protection levels. A step-by-step procedure is provided for a linear static analysis, for a nonlinear static analysis, and for a nonlinear dynamic analysis. The nonlinear dynamic procedure is not discussed here, since the present paper focuses on quasi-static approaches.

The DoD step-by step procedure for linear static analysis is similar to the GSA procedure in its general philosophy. The first step consists in the removal of a vertical load bearing element, and the application of the specified loads, showing that this is also a sequence inversion procedure (page 3-19 in ref [9]). The following steps consist in the introduction of geometri-

cal changes (element removal or effective plastic hinge introduction), and the analysis is repeated, starting from the unloaded/undeformed condition. These steps are repeated until no element violates the acceptability criteria, at which point the procedure is complete. The exiting criterion from the analysis – geometrical modification – analysis loop is therefore that no new geometrical modification needs to be performed following the latest analysis. Then, if the collapsed floor area is restricted to the allowable collapse area specified in the document, the structure is deemed safe with respect to progressive collapse. Otherwise, the structure needs to be redesigned.

However, unlike the GSA procedure, the linear static DoD procedure does not allow for DCR values higher than 1. The loads specified are also different, and are given by the following equation:

$$2[(0.9 \text{ or } 1.2) \text{ dead loads} + (0.5 \text{ live loads or } 0.2 \text{ snow load})] + 0.2 \text{ wind load}$$

Finally, the set of criteria prescribing whether a structural element should be removed, or a plastic hinge be introduced, is more detailed in the DoD document than in the GSA one.

Specific assumptions of the DoD linear static procedure

The assumptions introduced by the DoD linear static procedure are the same as those described for linear static GSA procedure, with the exception of assumption number 3, which is avoided since the DCR values are not allowed to exceed 1. Keywords

2.5 DoD Nonlinear Static Analysis Procedure

This procedure is in fact very close to the DoD linear static procedure, the main difference being that following every geometry change, the analysis is restarted from the point in the load history at which the model was modified. If, during computation, the collapse floor area is no longer restricted to the allowable collapse area, the analysis is complete, and the structure needs to be redesigned. If the total load is applied, and the collapse floor area is restricted to the allowable collapse area, the analysis is complete, and the design is considered adequate.

Specific assumptions of the DoD nonlinear static procedure

The introduction of geometrical changes one by one along the analysis enables the procedure to avoid assumption number 2 mentioned above for the GSA linear static procedure (on top of hypothesis number 3 already avoided by the DoD linear static procedure), but this nonlinear static procedure remains a sequence inversion procedure.

2.6 Load history dependent procedure (LHD procedure)

This type of computation, similar in principle to the one that can be found in [2], is carried out in two steps. First, a computation is performed in order to determine the cross sectional resultant forces at the ends of the initially failing element, when the structure is submitted to the design loads (i.e. gravity, service loads...). A second computation is then performed, in which the initially failing element has been removed. The design loads and the previously calculated cross sectional resultant forces are simultaneously applied, as if the failed element was present. In a second phase, the design loads are maintained constant while the cross sectional resultants of the initially failing element are gradually decreased proportionally, thus causing stress redistributions in the structure. The second step of the procedure is carried out taking into account plastic yielding of structural elements.

This procedure does not introduce the notion of an allowable collapse area, contrary to the GSA and DoD procedures, and also does not consist in successive re-analyses of the structure.

The acceptability criterion for thus procedure is that if the sectional resultants representing the initially failing element can be fully decreased, the structure is considered safe with respect to progressive collapse. Otherwise, it has to be redesigned.

Specific assumption of the LHD procedure

Replacing the initially failing element by its decreasing cross sectional resultant forces assumes that the failing element does not contribute to the overall structural stiffness as of the start of this second phase, while the stiffness degradation is actually not instantaneous, but rather evolves with the decrease of the cross sectional resultant forces.

Furthermore, within a failing element, the cross sectional resultant forces do not necessarily decrease at the same rate. Although controlling the computation by decreasing the cross sectional resultant forces at different relative rates poses no particular implementation problems, no data providing these correct relative rates is present in the model, the failing element having been removed from the model.

2.7 Common notion of independence with respect to the cause of the initial failure

A central assumption common to all these procedures lies in their independence with respect to the cause of the initial structural failure. All of them only require the knowledge of the initially failing elements. The use of such an independency assumption can be understood, the initial cause being usually unknown and potentially difficult to simulate. This, however, might lead to approximations, since there is no certainty that the structure reacts globally in the same way to different causes of failure for the same initially failing structural elements.

3 2-D PLASTIC HINGE MODEL FORMULATION

3.1 Reinforced concrete model chosen for the present study

Many different models are available in the literature for reinforced concrete simulation, ranging from micro models, where concrete and reinforcement are modeled separately, to macro models with lumped plastic hinges coupled with linear elastic beams. The advantage of macro models lies in their moderate computational cost, as well as their ease of implementation.

Since the aim of the present study is to compare progressive collapse simulation procedures, a macro model with lumped plastic hinges allowing for plastification in bending only will be used. Note that this does not impede the generality of the conclusions reached through the comparisons. The only axial-flexure coupling feature taken into account is that the value for the yield moments of such hinges are chosen in accordance to the axial load expected at the section during the design stage.

The plastic hinge formulation described in this section is based on [12], and allows sectional plastification, and hence stress redistribution, to be taken into account during the computations. The element presented can only account for plastification in bending, but its extension to plastification with interactions between bending and axial straining may be considered. However, the implementation is then more complex since composite yield surfaces have then to be identified, as well as the numerical length of the plastic hinge.

3.2 Kinematic formulation

As in design beam formulations, the displacement field is discretized using three degrees of freedom per node. For a given hinge element, the displacements are collected in a vector \mathbf{u} ,

$$\mathbf{u} = \{u_1 \ v_1 \ \varphi_1 \ u_2 \ v_2 \ \varphi_2\}^t \quad (1)$$

where u_i , v_i and φ_i denote respectively the axial and transverse displacements, and the rotation at node i. The generalized strain vector is given by

$$\boldsymbol{\varepsilon} = \begin{Bmatrix} u_2 - u_1 \\ v_2 - v_1 \\ \varphi_2 - \varphi_1 \end{Bmatrix} = \mathbf{B}\mathbf{u} \quad (2)$$

where the matrix \mathbf{B} which allows the computation of the generalized strains from the nodal displacements is given by

$$\mathbf{B} = \begin{pmatrix} -1 & 0 & 0 & 1 & 0 & 0 \\ 0 & -1 & 0 & 0 & 1 & 0 \\ 0 & 0 & -1 & 0 & 0 & 1 \end{pmatrix} \quad (3)$$

The conjugated generalized stresses, representing the forces transferred between the two nodes (axial and transverse forces, and one bending moment) are denoted

$$\boldsymbol{\sigma} = \begin{Bmatrix} F_x \\ F_y \\ M_z \end{Bmatrix} \quad (4)$$

The tangent relation between the generalized stresses and strains is

$$\Delta\boldsymbol{\sigma} = \mathbf{H}_t \Delta\boldsymbol{\varepsilon} \quad (5)$$

Where

$$\mathbf{H}_t = \begin{pmatrix} k_1 & 0 & 0 \\ 0 & k_2 & 0 \\ 0 & 0 & k_3(\Delta u) \end{pmatrix} \quad (6)$$

The tangent stiffness $k_3/\Delta u$ indicates that this value is not constant, as plastification occurs in bending. k_3 depends on the properties of the considered cross section. The two other diagonal terms are constant, and can be seen as penalty coefficient.

The discretized tangent stiffness matrix and the internal forces vector are given by the usual relations (7) and (8), where no spatial integration is needed on the element domain (hinge with null length).

$$\mathbf{K}_t = \mathbf{B}^t \mathbf{H}_t \mathbf{B} \quad (7)$$

$$\mathbf{f}_{int} = \mathbf{B}^t \boldsymbol{\sigma} \quad (8)$$

3.3 Generalization of the theory of plasticity

The generalized strains are split into an elastic and a plastic contribution, as classically postulated in plasticity.

$$\boldsymbol{\varepsilon} = \boldsymbol{\varepsilon}_e + \boldsymbol{\varepsilon}_p \quad (9)$$

Since the axial and transverse behaviour of the hinge element are assumed to remain elastic, equation (9) reads

$$\begin{cases} \varepsilon_n = \varepsilon_{n,e} \\ \varepsilon_t = \varepsilon_{t,e} \\ \varphi = \varphi_e + \varphi_p \end{cases} \quad \text{where} \quad \begin{cases} \varepsilon_n = u_2 - u_1 \\ \varepsilon_t = v_2 - v_1 \\ \varphi = \varphi_2 - \varphi_1 \end{cases} \quad (10)$$

Since no stiffness degradation is considered, the elastic strains are related to the stresses through a constant operator by

$$d\varepsilon_e = H_e^{-1} d\sigma \quad (11)$$

With plastification occurring in bending only, the yield surface is represented by two limits in a one-dimensional space consisting of the bending moment axis. The yield values correspond to the maximal and the minimal bending moments M_{lim+} and M_{lim-} . Since this is a composite yield surface, it is necessary to detect whether plastification occurs through positive or negative bending. In the case of positive bending for instance, the following expression is adopted for the yield surface

$$f(M) = M - M_{lim+} \quad (12)$$

In order to take into account hardening or softening evolution laws, a historic parameter κ is introduced, and the general stress yield values, M_{lim+} and M_{lim-} , are made functions of this parameter. The plastic flow rule is trivial in this case, as plastification is allowed along one dimension only. We therefore have

$$d\varphi_p = d\kappa \quad (13)$$

For a given hinge element, the system of equations to be solved in order to update the stress level corresponding to given displacement increments (return mapping procedure) is given in equation (14)

$$\begin{aligned} (a) \quad & \Delta\varphi = \Delta\varphi_e + \Delta\varphi_p \\ (b) \quad & \Delta\varphi_p = \Delta\kappa \\ (c) \quad & \Delta\varphi_e = H_e(3,3)^{-1} \Delta M \\ (d) \quad & f(M(\kappa)) = 0 \end{aligned} \quad (14)$$

Such a system can be non linear, depending on the nature of the hardening-softening rule, in which case it is solved using a standard Newton-Raphson procedure.

To evaluate the discretized tangent stiffness defined by equation (7), the material tangent operator $[H_e]$ defined by equation (5) should be available. This operator should result from a consistent linearization of the stress update equations to ensure an asymptotically quadratic convergence of the structural Newton-Raphson scheme [13]. This can be achieved by substituting the second and third equations of system (14) into the first one, yielding

$$\begin{aligned} H_e(3,3)^{-1}(M_{n+1} - M_n) + \Delta\kappa &= \Delta\varphi_{n+1} \\ f(M_{n+1}) &= 0 \end{aligned} \quad (15)$$

By using this system to solve the return mapping problem, its linearization yields

$$\left[J(M, \varphi_p) \right] \begin{Bmatrix} \delta M \\ \delta\kappa \end{Bmatrix} = \begin{Bmatrix} \delta\varphi \\ 0 \end{Bmatrix} \quad (16)$$

where the upper left part of the inverse of the Jacobian provides the operator that links stress increments with total strain increments, which is the consistent tangent operator.

4 COROTATIONAL BEAM ELEMENT USING KIRCHHOFF THEORY

In order to take into account the correct behaviour under buckling of the failing columns, as well as accounting for potential catenary effects, a large displacements formulation is adopted for the beam finite elements, based on a corotational approach [14]. This approach consists in decomposing the strains into a rigid body motion contribution, and a small strain one. It is suggested by the fact that all plastic phenomena, including potentially large rotations, are concentrated in the plastic hinges, the beam elements remaining elastic.

The decomposition into a rigid body motion contribution and the rest of the displacements is illustrated in Figure 1. Once the rigid body contribution has been subtracted from the total displacements, it is assumed that the remainder of the displacements leads to small strains in the updated local axis system of the beam.

The total displacements in global axes are given by

$$\mathbf{u} = \{u_1 \ v_1 \ \theta_1 \ u_2 \ v_2 \ \theta_2\}^t \quad (17)$$

whereas the local displacement are given by

$$\mathbf{u}_l = \{\bar{u} \ \bar{\theta}_1 \ \bar{\theta}_2\}^t \quad (18)$$

where

$$\begin{cases} \bar{u} = \text{final beam length} - \text{initial beam length} \\ \bar{\theta}_1 = \theta_1 - \alpha \\ \bar{\theta}_2 = \theta_2 - \alpha \end{cases} \quad (19)$$

where α is defined in Figure 1.

Based on Equations (17) to (19), the relation between the internal forces expressed in global axes and the total displacements, as well as the tangent stiffness operator, are obtained as described in [14].

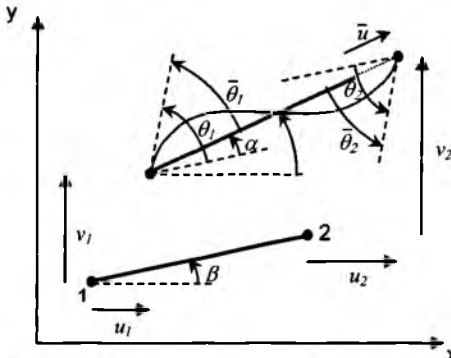


Figure 1: Displacement decomposition for the corotational approach (reproduced after Crisfield 1991)

5 NUMERICAL RESULTS AND COMPARISONS

In this section, the completed approach that allows for the construction of reference solution is first described, followed by a description of the ten-bay eight-floor structure studied in this paper. The results obtained with the GSA linear static procedure are shown, along with a discussion of the key features underlying this procedure. The DoD linear static procedure results are then discussed, followed by the results obtained with the DoD nonlinear static proce-

dure. All along this section, results are also compared with those provided by the LHD procedure.

5.1 Completed approach

In order to assess the validity of the assumptions described in Section 2, a more complete approach, avoiding them, has to be devised. This is achieved by the simulation of a situation for which the initial cause for the failure is known, which allows for avoiding the assumption common to all the investigated procedures. The computation is carried out in two steps:

- (i) The design loads are applied
- (ii) While maintaining these design loads constant, a second loading phase, representing the cause of the initial failure, is applied

In this way, the sequence of events and the behaviour of the initially failing element are taken into account. No assumption is introduced through an instantaneous elimination of the initially failing element, nor through an independence with respect to the cause of the failure. This approach enables the production of results that, within the context of the present paper, can be considered as reference solutions and will therefore be referred to as the ‘reference solution’ in all following paragraphs and sections. The plastic hinge element described in Section 3 is used to account for cross section plastification, and an elasto-plastic perfectly plastic behaviour law is used, where no strain yield criterion is taken into account.

It is emphasized that a cause for the initial failure is only to avoid the common assumption of independence with respect to the cause. It is clear that if the practitioner is aware of the nature of this triggering event, designing the column to withstand the triggering event would be a much more efficient way to prevent progressive collapse than allowing it to fail, and, through the use of an alternate path analysis, designing the rest of the structure to withstand the column loss.

5.2 Studied structure

The studied structure consists of an eight-floor ten-bay building, where the first floor was designed with a span and a height twice that of the other floors. All details related to the dimensions of the beams and columns, reinforcement, material behaviour and loads can be found in appendix A. They were obtained according to the Eurocode construction codes. Although the model accounts for plastification in bending only, the ultimate bending moment for every plastic hinge element was calculated taking into account the axial load level corresponding to the application of the design loads, without any removed element. In the beams, the axial load effect is negligible, but for the columns, the ultimate bending moment is substantially affected by the presence of the “design” axial load. Figure 2 shows the structure as well as portions of different sectional properties (either due to different dimensions or to different steel reinforcement). The third bottom column from the left is considered as the initially failing element.

6	7	6	6	7	6	6	7	6	6	7	6	6	7	6	6	7	6	6	7	6		
10	5	4	3	4	5	4	3	4	5	4	3	4	5	4	3	4	5	4	3	4	5	4
10	5	4	3	4	5	4	3	4	5	4	3	4	5	4	3	4	5	4	3	4	5	4
10	5	4	3	4	5	4	3	4	5	4	3	4	5	4	3	4	5	4	3	4	5	4
10	5	4	3	4	5	4	3	4	5	4	3	4	5	4	3	4	5	4	3	4	5	4
10	5	4	3	4	5	4	3	4	5	4	3	4	5	4	3	4	5	4	3	4	5	4
10	5	4	3	4	5	4	3	4	5	4	3	4	5	4	3	4	5	4	3	4	5	4
10	5	4	3	4	5	4	3	4	5	4	3	4	5	4	3	4	5	4	3	4	5	4
10	2	3	2	2	3	2	2	2	3	3	2	2	2	3	3	2	2	2	3	3	2	10
10		3		3		3		3		3		3		3		3		3		3		10

Figure 2: Portions of different sectional dimensions and/or reinforcement (all data given in Appendix A)

In all the analyses performed, resistance criteria relative to the shear effort are neglected, despite the GSA and DoD documents prescribing element removal when the DCR shear limit value (for the GSA procedure) or the yield shear value (for the DoD procedure) is reached. This implies that only the ability to take into account stress redistribution for bending effects is investigated. Also, as explained above, the techniques used by the different procedures to account for dynamic effects are not investigated in this paper. Therefore, no dynamic loading factor was applied to the loads, even if the investigated procedure actually specifies one.

Reference solution

To compute the reference solutions for the next paragraphs, the design loads first are applied to the structure. The second loading phase consists in a horizontal load applied at the third of the height of the initially failing column. A large displacement analysis is performed, in order to account for the buckling of the initially failing column. Since this buckling may lead to a decrease of the horizontal load while the horizontal displacement at its application point increases, the computation is carried out by controlling the displacement level, rather than the load level. The computation is stopped when equilibrium can no longer be obtained for further increase of that horizontal displacement. For all other computations, it was noticed that catenary effects could not come into action before the capacity to redistribute stresses is exhausted. Therefore, small and large displacements formulation based computations yield similar results.

5.3 GSA linear static procedure

In some references [15], the authors provide a simplified interpretation of the linear static GSA procedure: a single linear elastic analysis is performed on the structure bereft of the initially failing element. Based on these results, the DCR values are calculated, and the structure is deemed safe with respect to progressive collapse if no limit DCR value is exceeded anywhere in the structure. In this section, the linear static procedure described in GSA 2003 is followed more strictly, in that the effective plastic hinges are introduced as specified, and that the allowable collapse region is taken into account. After several design-strengthening iterations, Figure 3 shows the results obtained for a structure designed to resist progressive collapse, according to the GSA linear static procedure (only the portion of the structure where plastic hinges appear is shown). The transfer girder and floor beams (not the roof beam) were strengthened by a factor of roughly 1.5, and the non lateral floor columns reinforcement was increased by roughly ten percent (all details in Appendix B). The application of the GSA procedure leads to the introduction of three groups of plastic hinges, with limit DCR value of 1.5, as specified in GSA 2003 for an atypical structural configuration (structures with transfer

girders are considered to belong to this category, according to GSA 2003). Following the introduction of the third group (red groups on Figure 3), DCR limit values are no longer exceeded in the allowable collapse region (red dashed rectangle on the figure), and DCR limit values are not exceeded outside the allowable collapse region either. The analysis is therefore complete, and the design is considered safe with respect to progressive collapse, based on the GSA linear static procedure criteria.

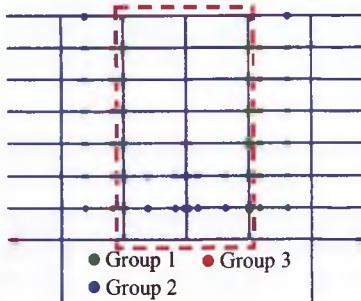


Figure 3: GSA procedure, groups of introduced plastic hinges

Figure 4 shows the plastic hinge appearance scheme obtained for this design when studied with the LHD procedure (left). The sectional resultant forces of the initially failing column can only be decreased by 85%, which means that based on the acceptability criterion associated with this procedure, the structure is not safe with respect to progressive collapse. Figure 4 also shows the reference solution for this design (right).

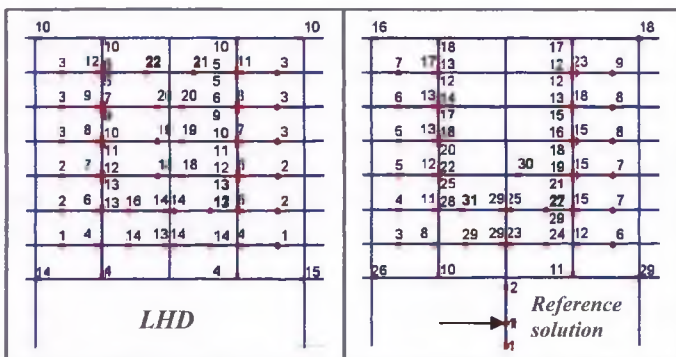


Figure 4: Structure designed to resist progressive collapse based on the GSA linear static procedure, LHD procedure results on the left, reference solution on the right

Discussion

The acceptability criteria for the GSA linear static procedure and the LHD procedure are different, mainly in that the GSA procedure takes into account an allowable collapse region, while the LHD procedure does not. Therefore, even if both procedures were to provide the exact same level of accuracy for the stress redistribution, it should not necessarily be expected that both procedures provide the same conclusion with respect to progressive collapse safety. However, the reasons for the difference in the results can be investigated more thoroughly, and be shown to be due to more than just the different acceptability criteria. Figure 5 depicts the flowchart of the GSA linear static procedure. The steps depicted by the red arrows represent the loops performed due to the geometrical changes introduced following every analysis,

as long as the DCR limit values are still exceeded in the allowable collapse region. Given that the GSA procedure belongs to sequence inversion family, that several geometrical changes (i.e. plastic hinge introduction) are performed at once, and that DCR values are allowed to exceed 1 in order to account for stress redistribution capacity by the structure, approximations may result in the locations and number of plastic hinges introduced. The LHD procedure, on the other hand, takes into account the loading sequence, and hinges appear one by one where and when the yield bending moment is reached. For these reasons, the locations and number of plastic hinges can not be detected less accurately by the LHD procedure, in comparison with the GSA procedure.

On the left in Figure 4, the plastic hinge configuration corresponds to the instant beyond which the sectional resultant forces representing the initially failing column can no longer be decreased. As explained above, and based on the assumptions used in this paper, this plastic hinge configuration cannot be less accurate than the one gradually detected by the loops depicted by the red arrows in Figure 5. For comparisons purposes, one can therefore consider

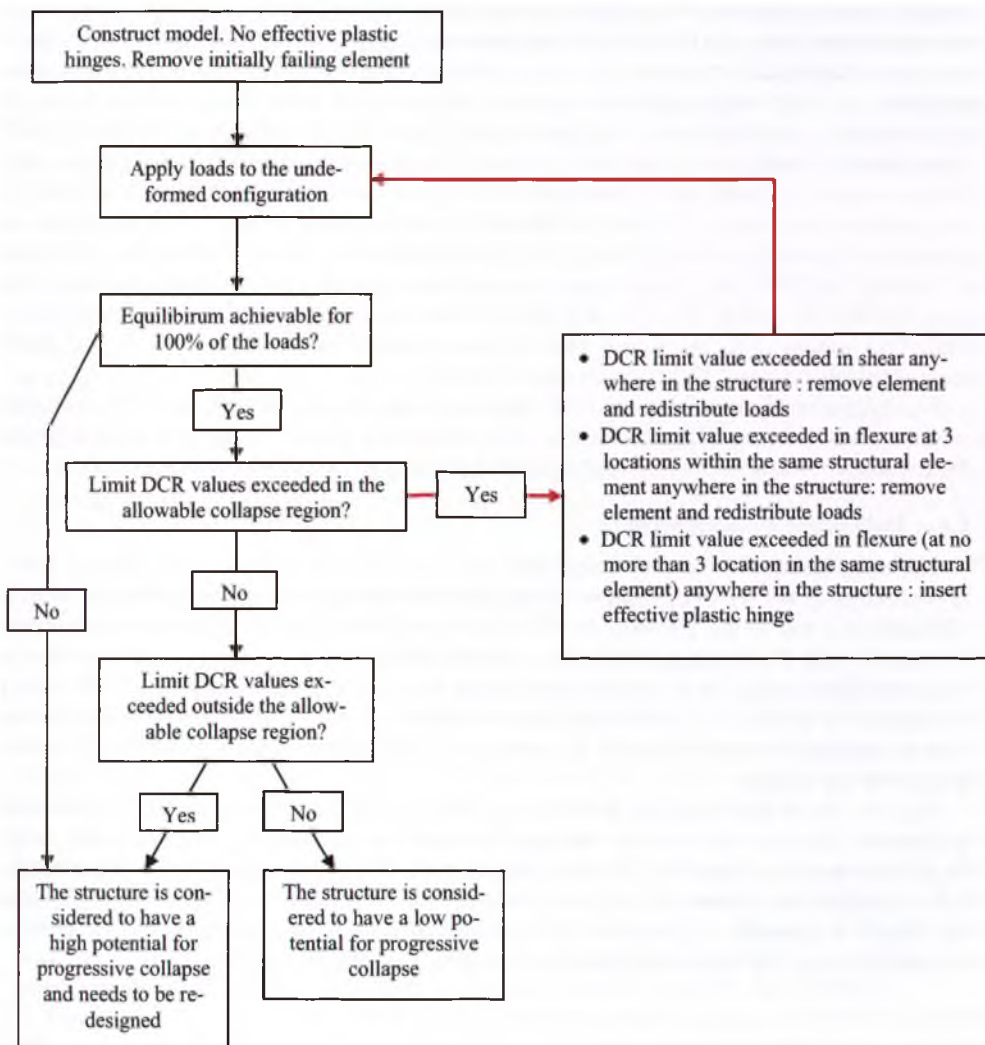


Figure 5: GSA linear static procedure flowchart

using the GSA linear static procedure, starting the procedure with a structure in which the hinges shown in Figure 4 (left figure) are inserted. This equates to replacing the topmost box in the flowchart of Figure 5 by the caption ‘Construct model, insert plastic hinges detected by a LHD procedure, remove initially failing element’. Such an analysis was performed, and following the insertion of the hinges detected by the LHD procedure, only 72% of the loads could be applied before equilibrium could no longer be reached, indicating that the structure needs strengthening.

The considerations detailed above show that the different acceptability criteria are not the only reasons for the difference in the results provided by the GSA linear static procedure and the LHD procedure, and that the different features of the GSA linear static procedure induce approximations leading, for the studied structure, to insufficient strengthening. Despite this conclusion, the authors are aware that the GSA linear static procedure should probably be seen as a procedure that provides an indication of the inherent redundancy of a structure, should a key component fail. It could therefore be reliable enough for the comparison of the relative vulnerabilities of two designs. It nevertheless remains interesting to note that for the structure studied here, the GSA linear static procedure leads to insufficient (rather than excessive) strengthening. Furthermore, the GSA guidelines do allow for the use of the linear static procedure to ensure safety against progressive collapse for a given design, so that the use of this procedure is not restricted to the purpose of determining the relative vulnerability of different designs. Conclusions obtained with the GSA linear static procedure thus carry a more absolute aspect. It should also be emphasized that given that the structure belongs to the atypical configuration category, it is less surprising to reach the conclusion that a nonlinear procedure should probably be used, as suggested by the GSA guidelines. Nevertheless, the feature of allowing for DCR values larger than 1 is specific to the GSA linear elastic procedure, and the guidelines do specify the allowable DCR values for atypical structural configurations as well. This suggests that the linear static procedure can be used for such structures, which seems debatable in view of the results obtained here.

Finally, Figure 4 shows that the LHD procedure provides results that match the reference solution fairly well. Similar conclusions were observed when the horizontal load triggering the collapse for the reference solution is applied towards left (and not towards the right).

5.4 DoD linear static procedure

The main features of the DoD linear static procedure (on top of it being a sequence inversion procedure) are the ones relative to the procedure actually consisting of a succession of computations, and to the introduction of several geometrical changes simultaneously, rather than one by one. These assumptions are somewhat linked. Indeed, as far as the introduction of effective plastic hinges is concerned, performing successive computations while introducing the hinges one by one (i.e. introducing only one hinge, at the location where the yield moment is most exceeded) would allow for the detection of the correct locations and appearance sequence for the hinges.

Figure 6 shows the results for the reference solution, LHD procedure and DoD linear static procedure, after the structure was designed to withstand progressive collapse based on the DoD linear static procedure (all details in Appendix C). The beams yielding moments needed to be multiplied by a factor of roughly 2, with their flexural stiffness correspondingly updated (all details in appendix C), and the non-lateral floor columns size (initially 50 cm) were increased by 5 cm. The three configurations in Figure 6 show very close results.

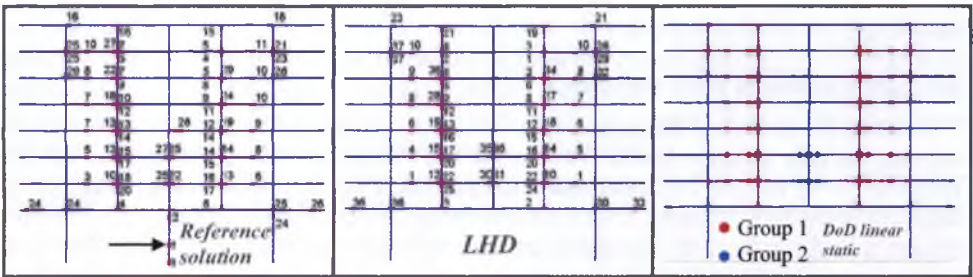


Figure 6: Structure strengthened to withstand progressive collapse based on the DoD linear static procedure. Plastic hinge appearance scheme, from left to right: reference solution, LHD and DoD linear static procedure

Remark

The DoD linear static procedures ends when the results of the last analysis show that no new geometrical changes need to be introduced. If the extent of the collapsed floor area is restricted to the allowed collapse area defined in DoD 2005, the structure is deemed safe with respect to progressive collapse. Since in the context of this paper, shear effects and strain yield criteria are not taken into account, no collapse floor area can be detected, so that the analysis is complete when no new hinges need to be introduced. Nevertheless, the ability of the DoD linear static procedure to correctly assess moments redistributions is investigated.

Discussion

On top of the DoD linear static procedure being based on a sequence inversion procedure, one of its features consists in the fact that several plastic hinges are introduced at once, following every analysis (until an analysis shows that no new geometrical changes need to be introduced). Checking exclusively whether the introduction of several hinges at a time leads to an approximation can be achieved by comparing the results of the DoD linear static procedure to those obtained by what is referred to in this paragraph as a nonlinear sequence inversion procedure. This procedure consists in removing the initially failing column from the model, applying the loads to the undeformed configuration (i.e. sequence inversion), and introducing the plastic hinges one by one, when and where the yield moment is reached. In this way, independently of the validity of the sequence inversion hypothesis (which will be discussed in the next section), the only different feature between the two procedures has to do with the hinges being introduced one by one, or several at once.

These comparisons were carried out, and it was noted that if the non-lateral floor column size is not increased by 5 cm, both analyses show that the structure just about fails to withstand the loads applied: with a nonlinear sequence inversion procedure, equilibrium can no longer be ensured when 99.57% of the loads are applied, and the DoD linear static procedure shows that, following the introduction of two groups of hinges, equilibrium can no longer be ensured for a similar loading percentage. Furthermore, if the column size is increased by only 1 cm (a non-realistic increase for reinforced concrete from a practical point of view, but numerically possible nonetheless), the nonlinear sequence inversion procedure shows that the structure can withstand 100% of the loads. In this case, the DoD linear static procedure also ends after the introduction of the second group of hinges (i.e. no new hinge needs to be introduced following the analysis carried out with the first two groups). This shows that not only does the DoD linear static procedure provide a good assessment of the plastic hinge locations, but that it also provides a correct value for the limit loads the structure can withstand.

Finally, Figure 6 also shows that the LHD procedure provides results that match the reference solution very closely. Similar conclusions were observed when the horizontal load trig-

gering the collapse for the reference solution is applied towards left (and not towards the right).

5.5 DoD nonlinear static procedure

Since in the context of this paper, shear effects and strain yield criteria are not taken into account, the only different feature between the DoD nonlinear static procedure and the LHD procedure is the fact the DoD nonlinear static procedure disregards the loading sequence (i.e. sequence inversion). Although from a rigorous point of view, the loading sequence should be respected in the context of a nonlinear analysis, this does not necessarily imply that the sequence inverted nature of the DoD nonlinear static procedure will lead to unacceptable approximations. Indeed, when a model taking plasticity into account is used, sequence inversion procedures might be expected to yield results with satisfactory accuracy, provided the structure has a sufficient elastic resistance reserve, making it less sensitive to the loading history. This is confirmed by the results shown in Figures 7 and 8. For the results of Figure 7, all design loads, including the dead loads, were multiplied by a factor of 1.2 in order to artificially reduce the load level where the first plastic hinges appear. For figure 8, the structure was redesigned to resist progressive collapse based on a DoD nonlinear static procedure (details in Appendix C): following the removal of the initially failing column, the structure can withstand the total loads. Applying the LHD procedure to the same design also shows that it can withstand progressive collapse (it can therefore withstand the full decrease of the sectional resultant forces representing the initially failing element). The figures depict the plastic hinge appearance schemes (only the portion of the structure where plastic hinges appear is shown) for the reference solution, the LHD procedure results and the DoD nonlinear static results. As can bee seen in Figure 7, the results corresponding to the reference solution and LHD procedures are very close to one another, but different from those corresponding to the DoD nonlinear static procedure. On Figure 8, however, where the structure has a larger elastic resistance reserve, thus postponing the loading point as of which the stresses have to be redistributed, the three plastic hinge appearance schemes are nearly identical.

5.6 DoD nonlinear static procedure

Since in the context of this paper, shear effects and strain yield criteria are not taken into account, the only different feature between the DoD nonlinear static procedure and the LHD procedure is the fact the DoD nonlinear static procedure disregards the loading sequence (i.e. sequence inversion). Although from a rigorous point of view, the loading sequence should be respected in the context of a nonlinear analysis, this does not necessarily imply that the sequence inverted nature of the DoD nonlinear static procedure will lead to unacceptable approximations. Indeed, when a model taking plasticity into account is used, sequence inversion procedures might be expected to yield results with satisfactory accuracy, provided the structure has a sufficient elastic resistance reserve, making it less sensitive to the loading history. This is confirmed by the results shown in Figures 7 and 8. For the results of Figure 7, all design loads, including the dead loads, were multiplied by a factor of 1.2 in order to artificially reduce the load level where the first plastic hinges appear. For figure 8, the structure was redesigned to resist progressive collapse based on a DoD nonlinear static procedure (details in Appendix C): following the removal of the initially failing column, the structure can withstand the total loads. Applying the LHD procedure to the same design also shows that it can withstand progressive collapse (it can therefore withstand the full decrease of the sectional resultant forces representing the initially failing element). The figures depict the plastic hinge appearance schemes (only the portion of the structure where plastic hinges appear is shown)

for the reference solution, the LHD procedure results and the DoD nonlinear static results. As can bee seen in Figure 7, the results corresponding to the reference solution and LHD procedures are very close to one another, but different from those corresponding to the DoD nonlinear static procedure. On Figure 8, however, where the structure has a larger elastic resistance reserve, thus postponing the loading point as of which the stresses have to be redistributed, the three plastic hinge appearance schemes are nearly identical.

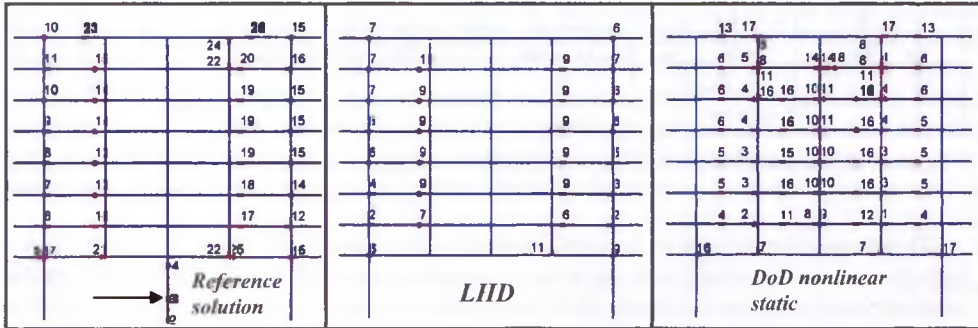


Figure 7: Dimensioning loads multiplied by 1.2. Plastic hinge appearance scheme, from left to right: reference solution, LHD procedure, DoD nonlinear static procedure.

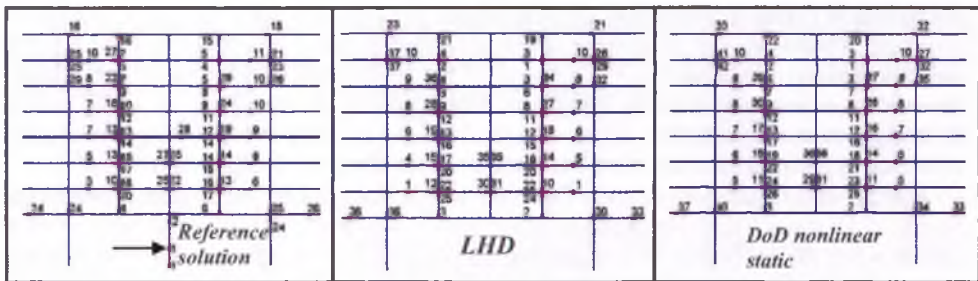


Figure 8: Structure designed to withstand progressive collapse using the DoD nonlinear static procedure. Plastic hinge appearance scheme, from left to right: reference solution, LHD procedure, DoD nonlinear static procedure.

The same comparisons can be performed for the structure that was designed to resist the design loads under normal circumstances (no missing column), and submitting it to the DoD live load level (50% of the design live loads). Based on Figures 7 and 8, the results of these comparisons are expected to be in between those shown in Figures 7 and 8. This is confirmed by Figure 9, where the results appear closer to one another than on Figure 7, but not as close as on Figure 8.

For this design, the reference solution shows that the lateral displacement imposed on the bottom column can no longer be increased before the axial effort in the column is nullified, indicating that the structure will not withstand progressive collapse. The LHD procedure shows that the sectional resultant forces replacing the initially failing column can not be decreased by more than 52%, leading to the same conclusion, similarly to the DoD nonlinear static procedure that indicates a limit load of 57% of the total loads.

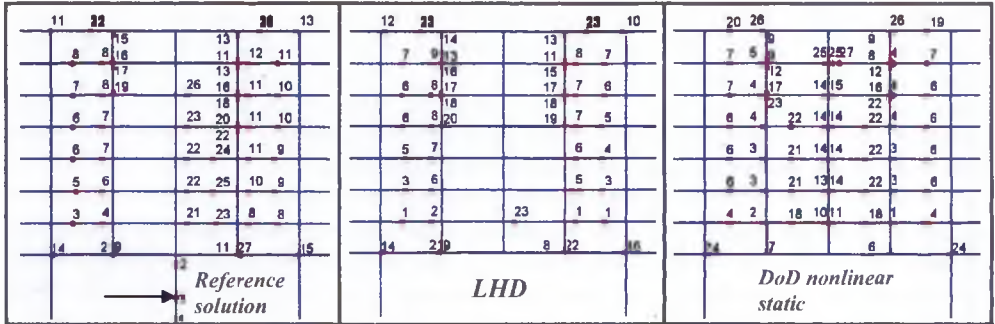


Figure 9: Structure not strengthened to withstand progressive collapse, submitted to the DoD live loads. Plastic hinge appearance scheme, from left to right: reference solution, LHD procedure, DoD nonlinear static procedure

The comparisons shown in Figures 7 to 9 show that the validity of the sequence inversion hypothesis increases along with the elastic resistance reserve of the structure. Based on these considerations, and on the results shown in Figure 9, it appears that the sequence inversion nature of the DoD nonlinear static procedure does not induce an unacceptable level of approximation. Indeed, under the live load level specified by the DoD guidelines, and for the structure that has not yet been strengthened specifically for progressive collapse mitigation, the results in Figure 9 would lead the practitioner to strengthen the same group of structural elements, whichever type of analysis (reference solution, LHD procedure or DoD nonlinear static procedure) is carried out. For instance, if the practitioner opts for the strengthening of the structural elements where the first plastic hinges appear, all three analyses would lead him to strengthen the floor beams. Then, as a result of the iterative strengthening, the sequence inversion hypothesis becomes more and more accurate along the design iterations.

Another conclusion derived from Figures 7 to 9 is that the LHD procedure provides good results in all cases, when compared to the reference solutions. Similar conclusions were observed when the horizontal load triggering the collapse for the reference solution is applied towards left (and not towards the right).

6 CONCLUSIONS

In order to investigate different quasi static progressive collapse simulation techniques, a zero-length plastic hinge element accounting for inelastic rotations was used. Two dimensional beam-column structures accounting for cross sectional plastification were studied. These models enable the assessment of four progressive collapse simulation procedures: the linear static GSA procedure, the linear static DoD procedure, the nonlinear static DoD procedure and the LHD procedure. These procedures are based on implicit assumptions such as the independence of the computational procedure with respect to the cause of the initial failure, the sequence in which the loads are applied or several geometrical changes introduced at once (rather than one by one). In order to assess the level of approximation that these assumptions induce, a more complete approach avoiding them was used. Computations were carried out neglecting dynamic effects, and also neglecting shear effort and strain based yield criteria, so that only the ability of the structure to redistribute moments is taken into account.

The comparisons between the results obtained with the more complete approach and those obtained with the four investigated techniques show non-negligible differences in some cases. The advanced LHD procedure appears to be the most accurate. Although the presented results do not constitute an extensive study of the event triggering independence hypothesis, and more comparisons on different structures should be performed before definite conclusions can

be reached, they suggest that the simplifying assumptions inherent to the LHD procedure, relative to the absence of the initially failing element from the model, do not affect the obtained results.

The comparisons performed for the three other investigated procedures allow for separate conclusions relative to their different features. The comparisons performed with the DoD nonlinear procedure indicate that the sequence inversion nature of the procedure does not induce unacceptable approximations, when the structure is submitted to the live load level specified by the DoD guidelines, due to the corresponding elastic resistance reserve. It was also shown that for lower load levels, the sequence inversion assumption leads to more accurate results. Therefore, the sequence inversion assumption is also probably valid for the GSA linear elastic procedure, since the live load level specified by the GSA guidelines is twice lower than the one specified by the DoD guidelines. The comparisons performed with the DoD linear static procedure indicate that the introduction of several plastic hinges at once still yields accurate results. Finally, these conclusions indicate that setting the DCR limit values at 1.5 for atypical structural configurations, as specified by the GSA linear static procedure, does not always provide a good assessment of moments redistribution potential by the structure, and may lead, as is the case for the structure studied in this paper, to insufficient strengthening of the structure to ensure safety with respect to progressive collapse.

7 ACKNOWLEDGEMENTS

The first author would like to acknowledge the financial support of FRIA (Fonds pour la formation à la Recherche dans l'Industrie et dans l'Agriculture), as well as the industrial partners Bagon and Seco, and Pr. Bernard Espion for enriching interactions.

REFERENCES

- [1] B. Ellingwood and E. Leyendecker, Approaches for design against progressive collapse. *J. Struct. Div. ASCE*, 104 (ST3), 413-423, 1978.
- [2] J. Gilmour and K.S. Virdi, Numerical modelling of the progressive collapse of framed structures as a result of impact or explosion. *2nd Int. PhD Symposium in Civil Engineering Budapest*, 1998.
- [3] H. Choi and T. Krauthammer, Investigation of progressive collapse phenomena in a multistory building. *International Symposium of Interaction of Munitions Effects with Structures*, 2003.
- [4] D.E. Grierson, L. Xu and Y. Liu, Progressive-failure analysis of buildings subjected to abnormal loading. *Computer-aided Civil and Infrastructure Engineering*, 20, 155-171, 2005.
- [5] G. Kaewkulchai and E. Williamson, Beam element formulation and solution procedure for dynamic progressive collapse analysis. *Computers and Structures*, 82, 639-651, 2004.
- [6] D.V. Val and E.G. Val, Robustness of frame structures. *Structural Engineering International*, 16 (2), 108-112, 2006.
- [7] J. Agarwak, J. England and D. Blockley, Vulnerability analysis of structures. *Structural Engineering International*, 16 (2), 124-128, 2006.

- [8] United States General Services Administration (GSA), *Progressive Collapse Analysis and Design Guidelines for New Federal Office Buildings and Major Modernization Project*, Washington DC, 2003.
- [9] Department of Defense (DoD), *Unified Facilities Criteria (UFC): Design of Structures to Resist Progressive Collapse*, Washington, D.C, 2005.
- [10] K. Starossek, Progressive collapse of structures: nomenclature and procedures. *Structural Engineering International*, 16 (2), 113-117, 2006.
- [11] B. Ellingwood, Mitigating risk from abnormal loads and progressive collapse. *J. Perform. Constr. Facil.*, 20 (4), 315-323, 2006.
- [12] M. Jirasek, Analytical and Numerical Solutions for Frames with Softening Hinges." *Journal of Engineering Mechanics*, 123 (1), 8-14, 1997.
- [13] J.C. Simo and R.L. Taylor, Consistent tangent operators for rate independent plasticity. *Computer Methods in Applied Mechanics and Engineering*, 48, 101-118, 1985.
- [14] M. A. Crisfield, *Non-linear Finite Element Analysis of Solids and Structures – Volume I*, John Wiley & Sons Ltd, Chichester,, Pages 211 to 219, 1991.
- [15] S. Marjinashvily and E. Agnew, Comparison of various procedures for progressive collapse analysis. *J. Perform. Constr. Facil.*, 20 (4), 365-374, 2006.
- [16] B. Espion, *Aspects approfondis du calcul des constructions en béton CNST 324 (1^{re} partie)*, Presses universitaires de Bruxelles, Brussels, 3ème édition 2000-01/1, Pages 4-6, 2000.
- [17] B. Espion, *Aspects fondamentaux du calcul des constructions en béton CNST 212 (1^{re} partie)*, Presses universitaires de Bruxelles, Brussels, 1ère édition 1999-2000/3, Page 78, 1999.

Appendices

Appendix A

Figure 10 shows the structure studied in the paper. The span for the floor is of 6m, except for the bottom floor where the span is 12m. The floor height is of 3m, except for the bottom floor where it is 6m. The beam span in the direction perpendicular the plane of the figure is of 6 meters. The width of the slabs is of 0.2m, with an additional concrete screed of 10cm.

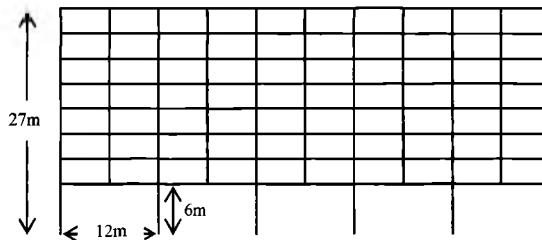


Figure 10: Eight-story ten-bay structure studied in the paper

Table 1 details the section sizes of all the beams and columns of the structure.

	Lateral columns	Bottom central columns	Central floor columns	Transfer girder	Floor beams	Roof beam
Area (m*m)	0.5 * 0.5	0.7 * 0.7	0.5 * 0.5	1.5 * 0.9	0.8 * 0.5	0.6 * 0.4

Table 1: sections of all beams and columns of the structure

The gravitational load of the columns is not neglected, and the specific weight of concrete is 24 kN/m³. The loads applied to the bottom and floor beams are:

- Service loads: $3 \text{ kN/m}^2 * 6\text{m} = 18 \text{ kN/m}$
- Slab weight: $24 \text{ kN/m}^3 * 6\text{m} * 0.2\text{m} = 28.8 \text{ kN/m}$
- Add. concrete layer: $24 \text{ kN/m}^3 * 0.1\text{m} * 6\text{m} = 14.4 \text{ kN/m}$
- Beam weight: $24 \text{ kN/m}^3 * \text{section area (m}^2\text{)}$

For the roof beam, there are no service loads, and for the columns, only the self-weight needs to be taken into account.

Figure 11 shows the portions of different reinforcement along the first span (i.e. first twelve meters, starting from the left) of the transfer girder, the same pattern being repeated five times along the beam. For the floor and roof beams, the reinforcement layout is similar, except that the lengths of portions 1 and are of 2.1m and 1.8m respectively, and the sequence is to be repeated 10 times.

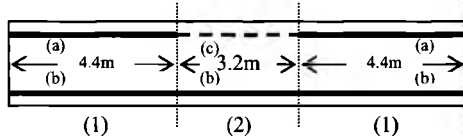


Figure 11: Reinforcement portions for the transfer girder

The distance between the reinforcement bars and the top or bottom face of the beam is of 5cm. If $\alpha \phi \delta$ means α bars of diameter δ in mm, then for the transfer girder, (a) corresponds to 15 ϕ 30, (b) to 13 ϕ 30 and (c) to 9 ϕ 10.

For the floor beam, (a) corresponds to 10 ϕ 16, (b) to 5 ϕ 12 and (c) to 3 ϕ 10, and for the roof beam, (a) corresponds to 7 ϕ 16, (b) to 4 ϕ 12 and (c) to 3 ϕ 10

The tri-linear idealization of the flexural behaviour of a reinforced concrete section is shown in figure 12.

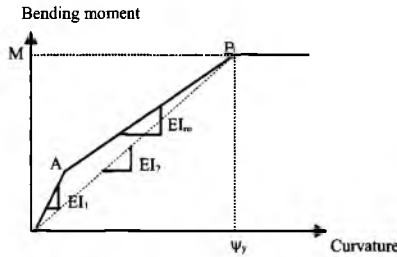


Figure 12: Tri-linear idealization of the flexural behaviour of reinforced concrete sections

Since the portion leading to point A on figure 12 (flexural stiffness EI_1) is very short in practice (much shorter than on the figure), EI_2 is very close to EI_m , and thus provides a very

good approximation of the flexural stiffness of the section (which is thus considered to constantly be in a cracked state). In order to find EI_2 , the coordinates of point B have to be calculated. Equation 20 provides the ultimate bending moment M_{lim}

$$M_{\text{lim}} = 0.9 f_y A_s d \quad (20)$$

where f_y is the elastic yield of the reinforcement steel, A_s is the total reinforcement area of the layer loaded in tension due to the bending moment, and d is the distance between the reinforcement layer and the farthest beam face.

The corresponding curvature is given by equation (21)

$$\psi_y = \frac{\varepsilon_y}{d(1-\xi)} \quad (21)$$

where ξ is given by the solution of equation (22).

$$\xi^2 + 2\alpha\rho\xi - 2\alpha\rho = 0 \quad (22)$$

$$\text{where } \alpha = \frac{E_s}{E_c} \quad ; \quad \varepsilon_y = \frac{f_y}{E_s} \quad ; \quad \rho = \frac{A_s}{bd}$$

A_s , f_y and d have been defined above (equation 20), E_s and E_c are the Young's moduli of the reinforcement steel and concrete respectively, and b is the beam width. The flexural stiffness EI_2 is therefore given by the ratio between M_{lim} and ψ_y . This procedure is derived from [16]. The Young's moduli of the steel and concrete are of 200GPa and 30GPa respectively, and the steel elastic yield is of 500MPa.

The ultimate bending moments and the flexural stiffness for the three reinforcement type portions of the transfer girder can thus be calculated using equations (20) to (22), and are given in Table 2.

Portion Properties	Transfer girder		Floor beam		Roof beam	
	(1)	(2)	(1)	(2)	(1)	(2)
$M_{\text{lim+}}$ (Nm)	5995926	5995926	190852	678584	111966	348340
$M_{\text{lim-}}$ (Nm)	6918376	461225	190852	79522	111966	58316
Flexural stiffness (Nm ²)	2727202106	2562875556	155936971	49692121	57283862	16008386

Table 2: Ultimate bending moments and inertias for the bottom, floor and roof beams

The columns are assumed to be in uncracked regime due to the compressive axial load. Their inertia can thus be calculated as $h^4/12$, where h is the side of the square section (all columns in the structure have square sections). The ultimate bending moment was calculated by taking into account the design axial load, using equation 23, derived from [17], adapted for symetrically reinforced sections.

$$M_{\text{lim}} = -0.9 N d + A_s f_y (d - d_e) + N (d - d_e) / 2 \quad (23)$$

where N is the design axial load (counted positively in tension), d is the distance between one of the reinforcement layers and the farthest face, A_s is the total reinforcement area of one of the layers, f_y is the steel elastic yield, and d_e (=5cm for all columns) is the distance between the reinforcement layer and the closest face.

The lateral columns reinforcement consists of two symmetrical layers of seven 16mm diameter bars for each layer. The bottom central columns reinforcement consists of two symmetrical layers of seven 14mm diameter bars for each layer, and the central floor columns reinforcement consists of two symmetrical layers of five 14mm diameter bars for each layer.

Appendix B

For this design, the floor beam's width is increased to 0.6m. For the transfer girder, (a) corresponds to 22 ϕ 30 (on two layers), (b) to 20 ϕ 30 (on two layers) and (c) to 9 ϕ 10. For the floor beam, (a) corresponds to 15 ϕ 16, (b) to 8 ϕ 12 and (c) to 3 ϕ 10. This provides the yield moments and flexural stiffness values given Table 3.

Portion Properties	Transfer girder		Floor beam		Roof beam	
	(1)	(2)	(1)	(2)	(1)	(2)
M_{lim+} (Nm)	9383545	9383545	305363	305363	111966	111966
M_{lim-} (Nm)	10321899	461225	1017876	79522	348340	58316
Flexural stiffness (Nm ²)	3813802822	3666849657	226709560	77787275	57283862	16008386

Table 3: Ultimate bending moments and inertias for the bottom, floor and roof beams

For the central floor columns, the reinforcement consists of two symmetrical layers of two 13mm diameter bars and three 16mm diameter bars each.

Appendix C

For this design, the transfer girder's depth is increased to 1.6m, while the floor beams depth and width are increased to 1m and 0.7m respectively. For the transfer girder, (a) corresponds to 30 ϕ 30 (on two layers), (b) to 26 ϕ 30 (on two layers) and (c) to 9 ϕ 10. For the floor beam, (a) corresponds to 15 ϕ 16, (b) to 10 ϕ 12 and (c) to 4 ϕ 10. This provides the yield moments and flexural stiffness values given Table 4.

Portion Properties	Transfer girder		Floor beam		Roof beam	
	(1)	(2)	(1)	(2)	(1)	(2)
M_{lim+} (Nm)	12818876	12818876	483491	483491	111966	111966
M_{lim-} (Nm)	14791011	493033	1289310	134303	348340	58316
Flexural stiffness (Nm ²)	5867906725	5242374817	383365012	158064752	57283862	16008386

Table 4: Ultimate bending moments and inertias for the bottom, floor and roof beams

The central floor columns size is increased to 0.55m by 0.55m.

THE MILLAU VIADUCT: AN OUTSTANDING STRUCTURE. THE SAFETY DURING THE DECK LAUNCHING

V. de Ville de Goyet, J.-M. Crémer, and J.-Y. Del Forno

Bureau Greisch
Liège Science Park, allée des noisetiers, 25, Liège, Belgium
{vdeville, jmcremer, jydeforno}@greisch.com

Keywords: Structural Design, Exceptional Actions, Safety, Building procedures

Abstract. *The Millau viaduct is the tallest civil engineering structure. But, as, often for a bridge, the difficulties of the design do not concern the structure during its life but during its building. One of them is to imagine a solution to minimize the costs and the building time, to maintain the safety of the workers. Another one, undoubtedly the most complex, is the control of the structure design during all its building stages taking account of several accidental configurations. For Millau, it can be considered that 80 % of time was devoted to the design of the building operations. This paper describes the state of mind in which that was done.*

1 INTRODUCTION

1.1 The structure

The Millau viaduct, the biggest civil engineering structure on the A75 motorway, carries the latter over the Tarn valley between the Causse Rouge to the north and the Causse of the Larzac to the south, 5 km west of the town of Millau.

The viaduct, 343 m high to the top of the pylons, is the last link in the A75 Clermont Ferrand-Béziers motorway in the South of France. The search for an aesthetically pleasing structure led to the choice of a multi cable-stayed viaduct with slender piers and a very light deck, touching the valley at only seven points.



Figure 1. – The Millau Viaduct

The Millau viaduct is 2460 m long, slightly curved in plan on a radius of 20,000 m and with a constant upward slope of 3.025 % from north to south.

The structure is continuous along its eight cable-stayed spans: two end spans of 204 m each and six central spans of 342 m each.

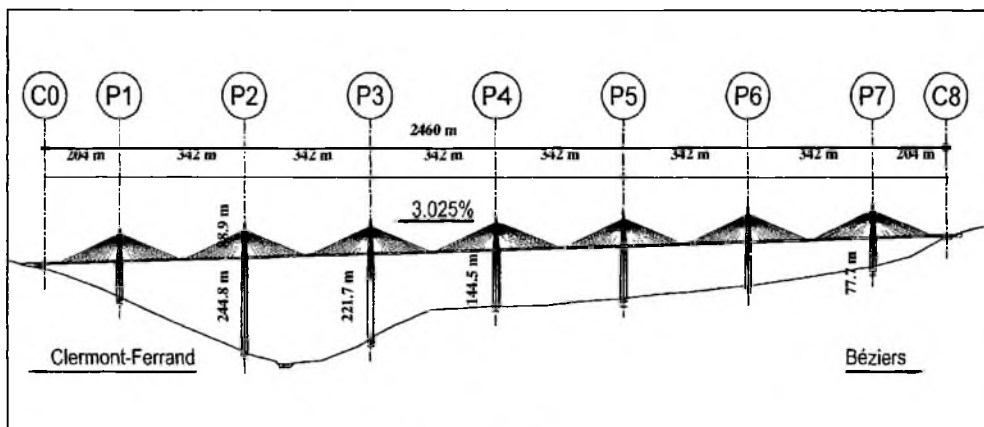


Figure 2 – Elevation view

The cross-sectional profile of the motorway consists of a dual carriageway, each carriageway bordered by a 3 m emergency lane and a 1 m shoulder next to the central reservation. The cross-sectional profile resulting has a width of 27.75 m.

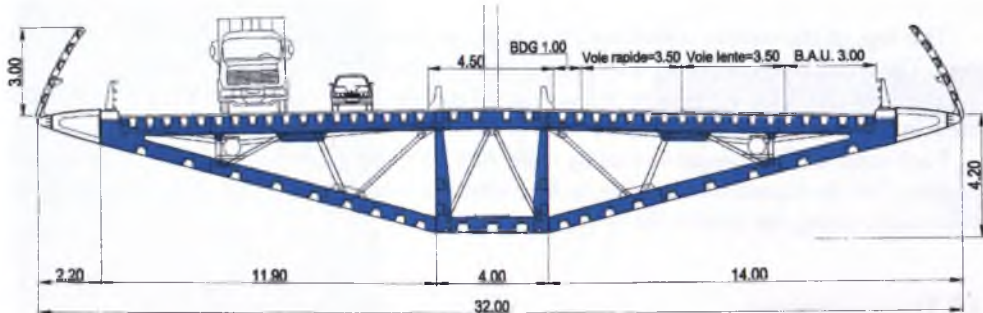


Figure 3: Functional cross-section of the deck

The deck is supported by seven piers; the P2 (height 245 m) and P3 (height 223 m) ones are the two highest piers ever built in the world today; the top 90 m of the shafts of the piers are split into two.



Figure 4
Elevation of the pier P2

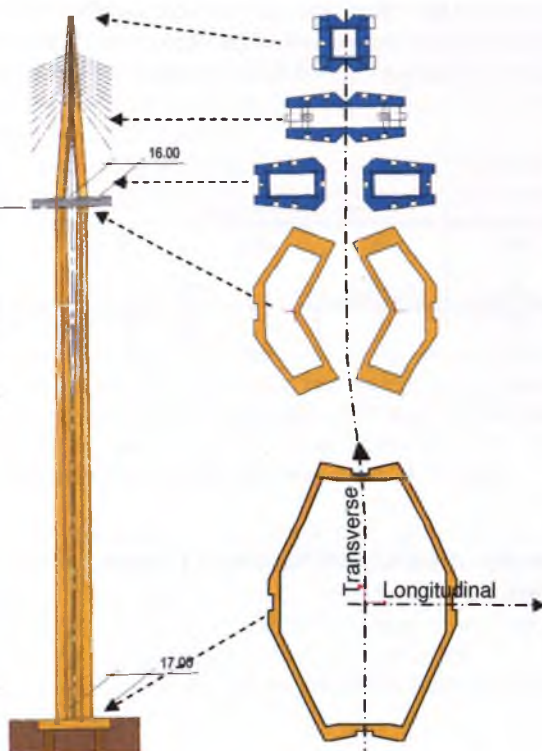


Figure 5
Cross-sections of a pier and pylon



Figure 6:
Elevation of a pylon

The pylons are set into the deck:

- Longitudinally, continuity is ensured between the metal sheets of the webs of the central box girder and those of the walls of the pylons legs.
- Transversely, rigidity is provided by a frame which covers the bearings found on each pier shaft.

The legs of the pylons, which are 38 m high, are composed of two stiffened metal box girders. These are surmounted by a 49 m high mast onto which the cables are anchored.

The concrete piers P2 (height 245 m) and P3 (height 223 m) are the two highest piers ever built in the world to date and the top 90 m of the shafts of each pier is split into two.

Each split shaft is prestressed using eight 19 T 15 Super cables using the DYWIDAG procedure. The deck rests on each pier by four spherical bearings, two on each column half, thus effectively fixing the deck to the pier.

1.2 The construction

After the building of the abutments, the piles were constructed.

Between consecutive concrete piers, excepted between P2 et P3 over the Tarn river, steel temporary piers have been erected. The distance between each support was equal to 171 m.

The steel deck was assembled behind the abutments. When 171 m of the deck was constructed, the deck was launched from one support to the following one, from a pier to a temporary pier or vice-versa. The first pylon was launched with the deck to limit the vertical deformation of the cantilever. Launched from the two abutments, the deck has been connected just above the Tarn River. Then, the 5 other pylons were assembled behind the abutments and have been carried on multi-axle transporters. They were moved just above the piers and lifted into their final position. The hangers could be set up and then, the temporary piers disassembled.

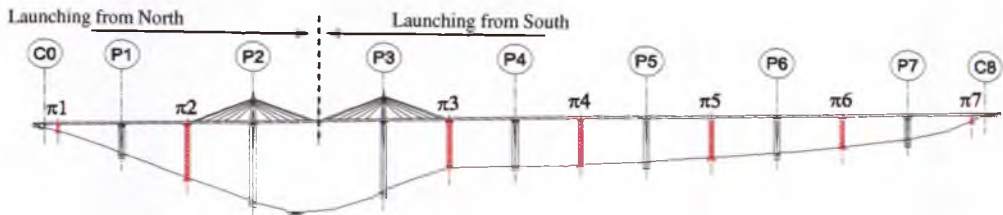


Figure 7 – Elevation view at the end of deck launching.

The top of each pier was equipped with translation systems, called translators and centrally controlled by computers.

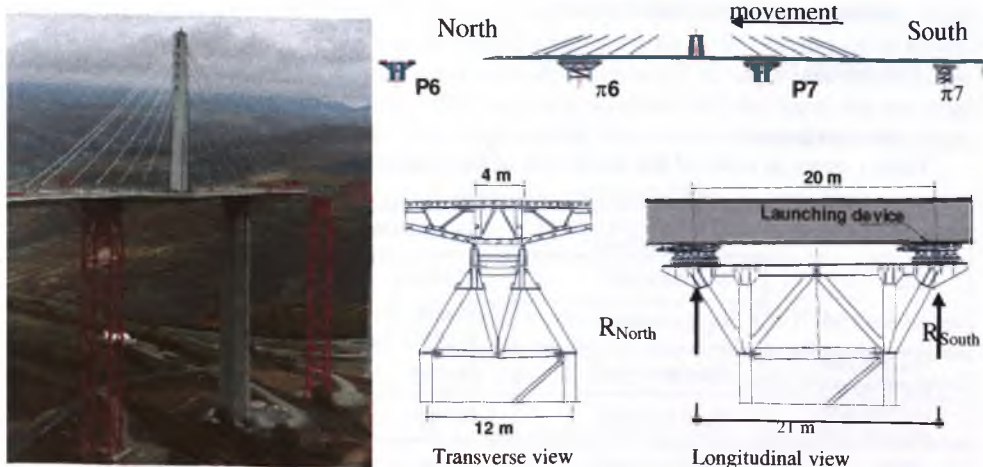


Figure 8. Launching pads

2 THE LAUNCHING TECHNICS

2.1 Introduction

The interest of the launching method for Millau was the building rate but also the security of the workers. 90 percent of the work was done on a platform and not at 200 m high.

On the other hand, the difficulty has been the computation to imagine any type of status with, each time, its own type of verification.

At this height, the main loading of the deck is the wind which induces vibrations. All verifications of the viaduct behaviour have been made with spectral analyses to take into account the spatial and time distributions of the wind and to evaluate the dynamic behaviour of the structure.

2.2 The safety during the building

The hypotheses for the wind speed were different for the service and the construction. Due to the duration of the exposure of the structure, for the service, a wind return period of 50 years has been adopted, i.e. 205 km/h for the gusts, whereas, for the building, the value was 10 years, i.e. 185 km/h for the gusts. The safety coefficient for this loading was equal to 1,50 and for the dead loading, to 1,35.

If these conditions are classical and have been used for most of the building time, it was decided to adopt specific hypotheses for specific operations and, mainly for the launching operations. The construction of the deck was made following several steps:

1. The assemblage of 171 m length of the deck, during about 3 weeks,
2. The launching of the assembled deck, during about 2 days.

And during the launching operations, several situations had to be considered:

- The movement of the deck

- Any incident stop due to any mechanical incident or due to an increasing wind speed announced by the weather report.

2.3 The design rules

2.3.1. The load factors

Table 1 gives an order of the magnitude of the loads applied on the structure.

deck	Dead load (current sections)	200 kN/m (building - 150 kN/m)
	Horizontal wind	12,5 kN/m
	Vertical wind	35 kN/m (building: wind effects= 25 % of total effects due to vertical loads)
Concrete piers last 90 meters	Transverse wind	38 kN/m
Concrete piers the lower shaft	Transverse wind	27 kN/m
pylons	Transverse wind	22 – 26 kN/m

Table 1. Loads on deck

For each situation, one wind speed and one set of safety coefficients were adopted. The choice of each one has been made on base of the safety rules by taking account of the occurrence probability of each event or configuration. Rules have been established to define the load factors for the dead load, the wind loading and the wind speed. The table 2 resumes the adopted values for the building operation of the Millau viaduct.

Building step of the deck	Maxim wind speed at the deck level [km/h]	Load factor		Events
		Dead load	Wind load	
1. Assemblage	185 km/h	1,35	1,50	Structure fixed on its supports
2.a. 2.b. 2.c. 2.d.	72 km/h	1,35	1,50	Movement
	72 km/h < speed < 85 km/h	1,25	1,50	Movement
	85 km/h < speed < 140 km/h	1,10	1,20	Stop of launching operations
	140 km/h < speed < 185 km/h	1,10	1,20	Stop of launching and safety procedure
3. Incident during launching	185 km/h	1,10	1,20	Safety procedure

Table 2.- Wind speed, load factors and procedure for the building

During the assemblage of the deck (Tab. 2 - step 1.), the structure already above the valley had to be fixed on the concrete piles and temporary piers and to be designed with the maximum wind speed, 185 km/h, and classical load factors.

Before giving the instructions to start the launching operations (Tab. 2 - step 2.a.), the staff had to receive, from Météo-France, a weather forecast which announced that the maximum wind speed at the deck level would be lower than 72 km/h during the number of days necessary for the launching operations, i.e. 3 days. With these conditions, the design load factors were the classical ones but with a design wind speed reduced to 72 km/h.

If during the movement of the deck, the wind speed increased and exceeded 72 km/h but stayed inferior to 140 km/h (Tab. 2 - Step 2.b. and 2.c.), the launching operations were stopped as from 85 km/h for safety reasons for the workers on the deck, but no special procedure had to be initiated. As far as the movement can continue till 85 km/h, the safety factor for the wind effects had to maintain at 1,50, but it was accepted that the factor for the dead load would be reduced at 1,25 because the weight of the each structural elements of the deck was measured before its final assemblage.

If Météo-France announced wind speed superior to 140 km/h (Tab. 2 - Step 2.d.), one procedure had to be initiate to safe the structure, i.e. to fix the deck on its supports or to block the cantilever of the deck on the following pier to limit its transverse displacements induced by the wind.

If, for any reason or incident, the movement of the deck was stopped and if the time necessary to finish the launching operations was superior to the overcast of the weather report (Tab. 2 - Step 3.), the same procedure as for the step 2.d. had to safe the structure for a wind speed equal to 185 km/h.

Table 2 shows that, during the assemblage and during the launching of the deck, the load factors are the classical ones, as well as for the dead load, as well as for the wind loads. All other configurations were defined as accidental situation. It is the reason why the load factors have been reduced to 1,10 for the dead load and 1,20 for the wind loading. In return, all imaginable incident situations had to be studied. Up to a wind speed of 140 km/h, each element of the structure had to resist without any intervention. For a wind speed superior to this value up to 185 km/h, some operations have to be initiated to safe the structure.

2.3.2. The admittance coefficients

Since the viaduct is very high above the valley, the stresses generated by the effect of the wind are critical for the dimensioning of the structure. Taking into account the latest knowledge on the subject, the very complete studies and trials conducted in the wind tunnel of the CSTB in Nantes were based on:

Determination of the wind model

Measurements of the aerodynamic coefficients of the different elements of the structure exposed to the wind: piers, deck, pylons and temporary piers

Determination of the aerodynamic admittances both in bending and in drag from a trial on a aeroelasctic model of the structure during its construction phase

Determination of the torsional admittance of the deck from a test on a cross-sectional model

If the admittance coefficients are the ratio between the measurements, σ_{measure} , and the global calculated responses, σ_{response} , with spectral analyses,

$$\sigma_{\text{response}} = \sqrt{\sigma_{\text{quasi-static}}^2 + \sigma_{\text{dynamic}}^2}$$

with

$\sigma_{\text{quasi-static}}$ = quasi-static standard deviation of the wind effect

σ_{dynamic} = dynamic standard deviation of the wind effect

The values are given in the table 3. The design values were obtained by the measured values with a safety of 25% on the profit brought by the effect of the admittance.

Admittance coefficients	Values from tests		Design values
Wind direction	45°	90°	45° and 90°
Transverse bending	0,68	0,56	0,75
Longitudinal bending	0,62	0,58	0,70
Torsion of the deck	-	0,48	0,60

Table 3 – Admittance coefficients

For the final structure, the admittance profit has been neglected. For the building steps, specific rules have been defined:

- The admittance for bending behaviour is neglected so that the safety versus the dynamic wind effects was increased: about 25 %.
- At SLS, the torsion admittance could be used with the following criterion: the absence of any traction on each support.
- At ULS, the torsion admittance could be used to check the local stability, neither for the global stability nor for the resistance of the structural elements.

The essential effect of the admittance coefficient was important for the computation of support reaction under the transverse wind and, particularly, to determine if traction on a support was possible or not. At each top of the pier, there were 4 supports. If a possible traction could appear on one support, the local stability was verified if three other ones could ensure the equilibrium. For the global stability or equilibrium, it was possible to use the notion of redistribution of reactions between the supports located on several piers thanks to the torsional rigidity of the deck.

2.4 Procedures during the building of the deck.

2.4.1. Introduction

For each launching step (the total number of the launching steps has been equal to 18), the design office of the authors had to verify the deck and all temporary structures for any location of the deck during the launching with the maximum wind speed. The aim was to verify as from which wind speed it was necessary to secure the deck on its supports and, if it was necessary, to define the procedure to obtain the security for the design wind speed, 185 km/h.

This has meant a lot of computations. The design was realised, essentially, in three steps :

1. for the assemblage of the deck (step 1-Tab.2)
2. for the movement (steps 2.a. and 2.b.-Tab.2)
3. for the incident during the launching (steps 2.c. and 2.d.-Tab.2)

2.4.2. The kinematics during the building of the deck

Besides the multiplicity of the elements to verify at each step, one aspect of the design complexity has been the several conditions to consider. At the top of the each pier, concrete ones and steel temporary ones, the deck cross-section was put on four devices, called "translators", disposed at the fours corners of a rectangle shape. In the direction of the movement, The rectangle was 21 m long, and transversely, 4 m width. These devices, used to push the deck, were located under the vertical webs of the box girder. Each one was supported by jacks.

During the movement, the jacks of two devices located under the same web were connected between them, so that the oil pressure inside was equal and, in consequence, so that the

vertical reactions were equal ($R_{North} = R_{South}$ - Fig.8.). In that case, the couple of two translators disposed under the same web was equivalent to a hinge. Of course, transversely, the jacks were not connected.

During the assemblage, the classical procedure was to disconnect all jacks so that the deck could be considered full restrained at the top of each pier ($R_{North} \neq R_{South}$ - Fig.8.). The advantage of this configuration was to avoid verifying at any time that the connection between each jack was efficient. The disadvantage was that, due to the transverse wind loading, the piers, at its top might be stressed by bending moments. For the concrete piers, these support conditions were not so different of the ones during the service life of the structure. The conditions were more critical for the steel temporary piers so that, for some configurations, it was necessary to investigate the possibility to connect some jack to suppress the bending moment induced by the deck at its top.

For a possible incident during the movement, it was necessary to investigate any type of support conditions at the top of the piers to insure the safety of the structure.

Obviously, the difficulty of the design was the fact that, on the one hand, several static schemes of the deck have to be considered and, on the other hand, the height of each pier was different, so that their rigidity was also different and that the behaviour of the deck was different at any step of the deck building.

2.4.3. Assemblage

During that assemblage, the structure would have to resist to the maximum wind speed with the classical load factors. At this moment, the deck extremity was supported by a pier and the launching pylon was located at the upright of the previous pier. Then, globally, there were two types of configurations depending on the location of the deck extremity:

1. on a steel temporary pier,
2. on a concrete pier.

The vertical support reaction due to the dead load was not sufficient to avoid traction on the deck support induced by transverse wind loading applied on the height of the pylon. To suppress this effect, two procedures have been imagined

1. to fix rigidly the deck on the pier with prestressing cables,
2. to enable the rotation of the deck extremity.



Fig. 9 - Two steps of the deck building:
pylon on the temporary pier P6 and after the following launching step: pylon on the P6 concrete pier

The first solution enables to equilibrate the transverse bending moment thanks to prestressing cables. These techniques have been adopted when the deck extremity was above a concrete pier. But, it was not possible on a steel temporary pier. The necessary prestressing force was to be about 6500 kN, too large value for reasons of local resistance. It is the reason why a special device has been developed, a device called bogie.

Its function was to guarantee the equality of the reactions of the two transverse supports, so that transverse bending moment was suppressed by enabling the rotation of the deck extremity. To obtain this result, the deck was supported by two sets of jacks whose internal pressure of oil was equal thanks to their interconnection with a feeder pipe. Some numerical simulations have been realized at the Liège University to check that the pressure losses in the pipe

remained weak in spite of the rotation speed of the deck under the wind effects. It was demonstrated that for a piston speed of 185 mm/sec and amplitude of 25 mm, the pressure losses would be about 2 %, value considered being acceptable.

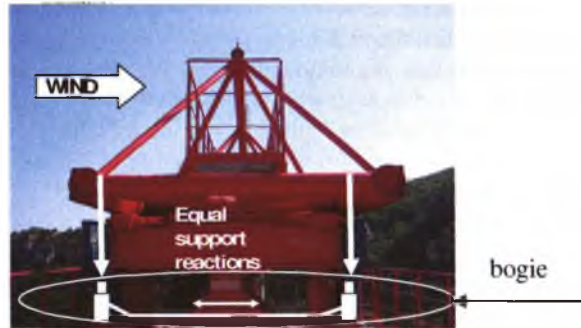


Fig. 10 - Schema of the bogie installed at the deck extremity.

2.4.4. The movement

The behaviour of the structure has been checked with nonlinear computations, each time the structure advanced of 5 m.

Initially, the internal forces have been computed under the vertical dead loads. Next, the wind effects were added. For all the configurations, about 600, all structural elements of the structure had to be checked, as example, the patch-loading effect in the cross-section located above each support, the behaviour of the steel temporary piers, of the cross-section bracings (Fig.11).

For the engineers, present on the site, it was very important to have under control the behaviour of the structure: to compare the actual behaviour with the theoretical or the computed one, to have some tools to estimate if measured values were dangerous or not for the stability of the structure. To this end, for each support, different curves have been drawn to follow the evolution of the vertical reaction versus to the movement of the deck:

1. Its nominal value
2. The threshold of vigilance: the maximum value, due to the dead loading, for which it was yet possible to add the reaction induced by a wind speed of 85 km/h without decreasing the global safety of the structure.
3. The limit of tolerance: the maximum value, due to the dead loading, for which it was not possible to add the reaction induced by wind without decreasing the global safety of the structure.

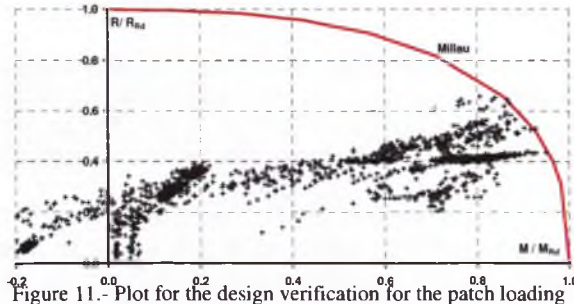


Figure 11.-Plot for the design verification for the patch loading

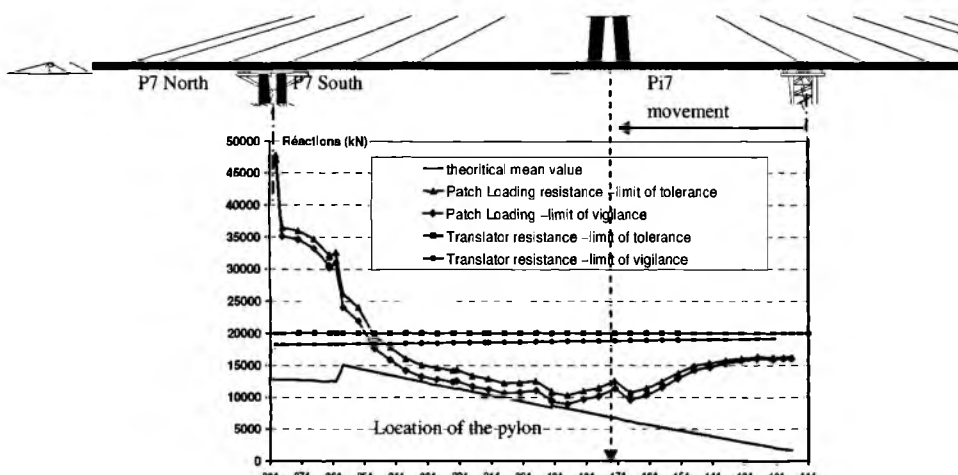


Figure 12 - Limits of vigilance and of tolerance for the P7 North pier supports for a launching step

Figure 12 gives an example of this type of curves. On the basis of these, the engineer located at the top of the concrete pier P7 during the movement of the structure could visualise the behaviour of the structure:

- At the beginning of the movement, the pylon was located on the temporary pier Pi7, so that the reaction on P7 was small and no problem of safety was to be feared,
- After 70 m, and during 60 m, it was very important to verify the value of the vertical reaction on the supports. It can be observed that nominal value was close to the limit of vigilance concerning the patch-loading phenomenon of the webs. Any abnormal increase was to be announced to the staff to make a possible decision.
- At the end of this launching step, the pylon arrived at the level of the P7 pier and the limits of the reactions were imposed by the resistance of the supports.

2.4.5. The incident stops

The evaluation of the safety and/or the definition of the safety procedures for any location of the deck during a launching operation was certainly the most delicate study. Once more, it was necessary for each structural element (supports, web resistance, fixations of the slip pads ...)

- To determine the maximum wind speed for which a safety operation was necessary
- To define the procedure to increase the resistance of the weak element.
- The figures 13 and 14 show an example of the design procedure for the launching when, initially, the pylon was located above the steel temporary pier Pi7 and, at the end, above the concrete pier P7. The figure 13 a. gives the maximum wind speed to have the security after the verification on each element. It can be observed that the 185 km/h speed was not reached. Moreover, on P7, traction could appear. This type of curves had to be drawn on each supports. It meant that special operations had to be imagined to obtain the security with 185 km/h wind speed. To suppress traction on supports, vertical settlements were possible to increase the reaction with the difficulty that, in this case, the safety under the patch loading phenomena decreased. The fig. 14 a. shows that settlements of the supports made it possible indeed to increase the maximum wind speed except during the last 80 meters (from pylon positions 204 and 254). Between pylon positions 204 and 254, the reactions decreased suddenly. It was due to the fact that, on P7 North supports, the reactions were

too large with respect to the phenomenon of patch-loading. To solve it, the South supports on P7 were lifted and the North ones, lowered same value to recover the safety on P7 North with respect to the patch loading without consequence on P7 South. But with this operation, new traction on P7 North supports appeared. To suppress it, the last solution was to fix the deck on these supports with prestressing cables: between positions 204 and 250, 30T15 and between positions 250 and 284, 25T15 were necessary.

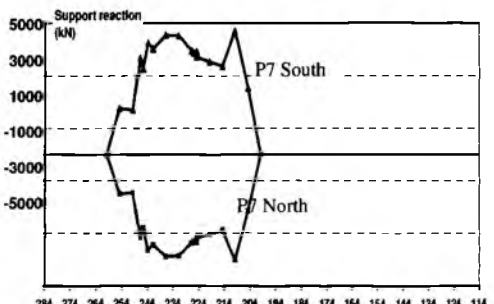
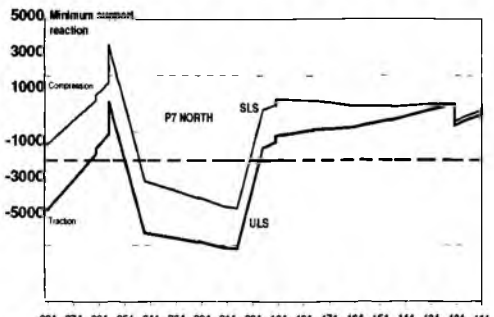
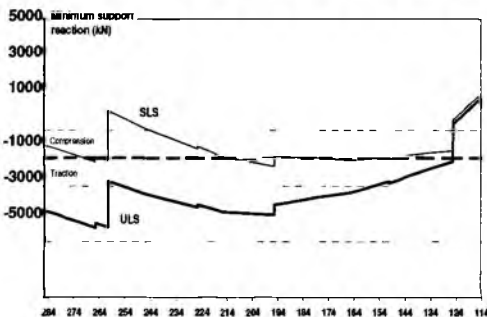
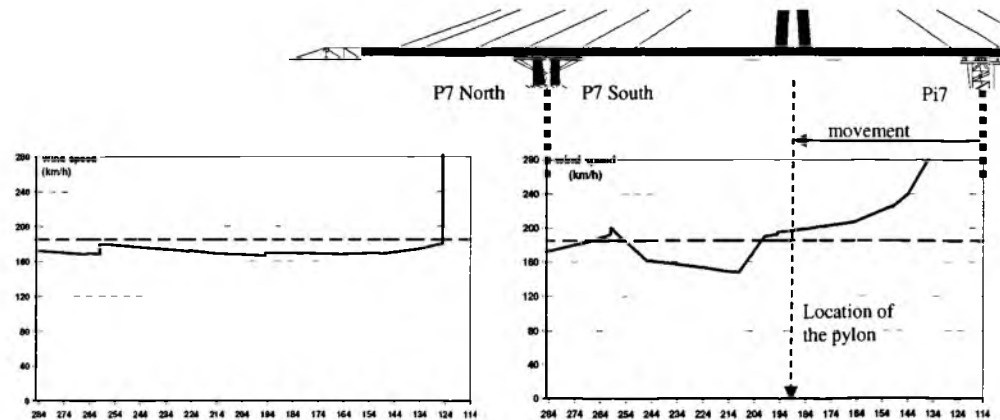


Fig.13. – structures parameters during the launching without special procedure (maximum wind speed – value of the minimum support reaction on the P7 pier).

Fig. 14. – Structure parameters after safety procedures (maximum wind speed, value of the minimum support reaction, effect on support reactions due to a longitudinal swing of P7 supports).

The figure 15 resumes the procedure to develop for any incident stop whatever the position of the pylon:

- The first line gives the wind speed from which an operation was necessary,
- On S1, support located at the back of the abutment, on the abutment and Pi7, settlements were envisaged,
- On the pylon P7, three types of operations were defined: the installation of the transverse bogie at the beginning of the launching, the swinging of the support reactions or prestressing cables
- On the temporary pier Pi6, the transverse bogie had to be placed at the end of the launching.

SETTLEMENTS (mm) OF SUPPORTS TO AVOID TRACTION ON S1, C8, PI7 (mm)													PI7
pylon position	205	206	207	208	209	210	211	212	213	214	215	216	217
Wind speed (km/h)	185		150		150	120	160	130	100	175	175	175	175
S1 (mm)			-250	0									
C8 (mm)				0	50	50	100	0	50	100	100	100	0
PI7 (mm)			240	0									

STRESSING CABLES, BALANCING OF SUPPORT REACTIONS AND TRANSVERSE BOGIE ON P7 TO AVOID PATCH-LOADING on P7													PI7
pylon position	205	206	207	208	209	210	211	212	213	214	215	216	217
Wind speed (km/h)	150	150				150					185		
P7 North and South			SWING OF SUPPORT REACTIONS										
P7 South	2 x 25T15 Stressing : 1000 kN/cable												
P7 North	2 x 25T15 Stressing : 1000 kN/cable		2 x 30T15 - Stressing : 2500 kN/cable										

OPERATIONS TO AVOID TRACTION ON PI6													PI7
pylon position	N	S	W	E	NE	SE	SW	NE	SE	SW	NE	SE	SW
Wind speed (km/h)	145												
PI6 South	TRANSVERSE BOGIE												

Figure 15 – Safety procedures during the launching between Pi7 and P7

3 CONCLUSIONS

If the final static schema of the Millau Viaduct seems very simple, its design for the building dimensioning appeared very complex with a constant concern of the safety concerning the structure and the workers. This difficulty was due to the multiple configurations to be considered and the quantity of results to investigate for each turbulent wind computations.

GARE TGV DE LIEGE-GUILLEMIN : COMPORTEMENT SOUS LES EFFETS DU VENT

V. de Ville de Goyet, Y. Duchêne, and Cl. Counasse

Bureau Greisch
Liège Science Park, allée des noisetiers, 25, Liège, Belgium
{vdeville, yduchene, ccounasse}@greisch.com

Keywords: Structural Design, large roof, wind loadind, wind tunnel tests.

Abstract. Drawn by the Spanish architect Calatrava, the roof of the new railway station for HSR trains at Liège, in Belgium, is spectacular for its shape and its dimensions. Its design has been tricky for several reasons: the proximity of a hill, the building conditions and the definition of the wind loading. Concerning this last point, the main difficulty was that the wind tunnel tests has been achieved at the same time as the final design based on the NBN codes. After a description of the new railway station, this paper presents the main hypotheses concerning the wind loading and the results obtained with tests. Some comparisons between tests results and values used for the design are given.

1 INTRODUCTION

La nouvelle gare de Liège Guillemins est un monumental dôme de verre et d'acier de 200 m de long qui couvre les voies et la nouvelle infrastructure essentiellement réalisée en béton blanc. Elle accueille notamment les TGV sur la ligne Paris-Köln.

La gare s'organise sur trois niveaux (Fig.1. et 2.):

1. le centre des voyageurs (salles d'attente, commerces, ...) est situé sous les voies, au même niveau que la place piétonne devant la gare. Des ponts-bacs supportent les voies. Des lamelles en béton supportent les quais en pavés de verre apportant de la lumière au centre,
2. les quais,
3. deux passerelles transversales et au-dessus des voies permettent l'accès direct aux différents quais depuis l'aire de dépose minute, située côté colline, à l'arrière de la gare.

Le dôme est prolongé de 5 longs abris de quais, de même composition. En l'absence de contreventement, ce sont les auvents latéraux qui assurent la stabilité transversale. Les sollicitations de vent ont été évaluées sur base d'essais en soufflerie. Les châssis en aluminium des panneaux de verre sont capables de suivre les déformations de la structure.



Fig. 1. Vue d'ensemble de la nouvelle gare - maquette

A l'arrière, la gare comporte un parking de 3 niveaux érigés dans le pied de la colline de Cointe. Ce parking est surmonté de l'aire de dépose minute et est directement raccordé sur la liaison autoroutière E40-E25.

En tant que Maître d'Ouvrage, EuroLiège TGV a fait appel à Calatrava, comme architecte, à l'issue d'un appel d'offre international. En mai 1999, Calatrava confie au Bureau Greisch l'ensemble de la mission de stabilité et d'assistance à la direction des travaux: mise en conformité de l'avant-projet vis-à-vis des normes belges en vigueur, prise en compte la poussée de la colline de Cointe, située à l'arrière du bâtiment, étude du comportement de la toiture sous le vent, étude des phases d'exécution et assistance sur le chantier .

2 L'INFRASTRUCTURE

2.1 Un parking en pied de colline

La construction du parking implique sur quelques 200 m l'enlèvement du pied de la colline de Cointe. Il s'agit en soi d'une entreprise d'envergure qui a nécessité un grand nombre

d'investigations, d'études et de mesures particulières afin de s'affranchir de tout risque de glissement de terrain. La stabilité de certaines couches de sol est précaire dans cette zone car un glissement de terrain de plusieurs milliers de m³ avait complètement recouvert et immobilisé plusieurs voies et quais en 1950.

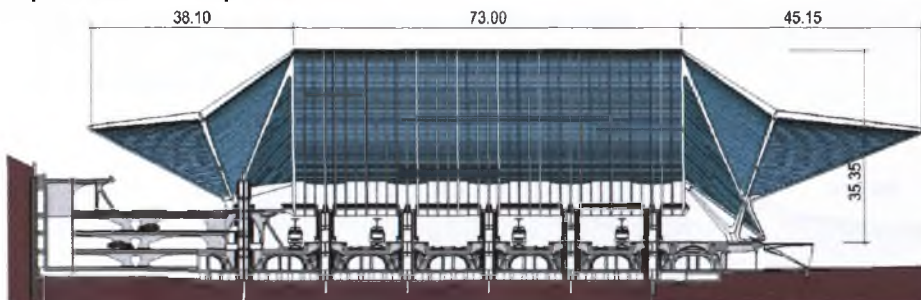


Fig.2. -coupe transversale de la gare

2.2 Une infrastructure très ouvragée en béton apparent

Si la partie la plus imposante de la nouvelle gare est sans conteste son dôme d'acier et de verre qui culmine à 40 m, il ne faut pas perdre de vue que le projet comprend la mise en œuvre de quelques 65.000 m³ de béton armé répartis entre :

- le parking (28.000 m³),
- le passage central et les couloirs techniques sous voies (17.000 m³),
- l'entrée de la gare avec ses 2 grands escaliers, le centre de voyage, les espaces commerciaux et de service ainsi que tous les aménagements en relation avec le premier quai (13.000 m³),
- les bassins d'orages, supports de auvents et ouvrages divers (7.000 m³).



Fig. 3 – Passage sous voies -Hall entre les parkings et la gare

Les formes à courbure variable dans l'une, voire deux directions, (Fig.3), nécessitent une étude très poussée des coffrages et de leur support. Une autre difficulté du projet réside dans la maîtrise de la qualité des parements à surfaces inclinées pour éviter le bullage. Cela a nécessité la mise sur pied d'une équipe de spécialistes pour maîtriser une quantité importante de paramètres tels que la composition du béton, sa teneur en eau, les adjuvants, la nature du coffrage et son traitement, les délais , la durée de vibrations, etc....

Les 39 arcs métalliques de la toiture principale ont des sections de type caisson reconstitué-soudé. La géométrie de leur section varie continûment sur toute leur longueur.

Les passerelles et les arcs sont entièrement solidarisés et forment véritablement l'ossature portante de la couverture (Fig.5.):

- Les arcs transmettent les charges dans le sens longitudinal
- Les passerelles, dans le sens transversal
- Le tout prend appui sur les quadripodes.

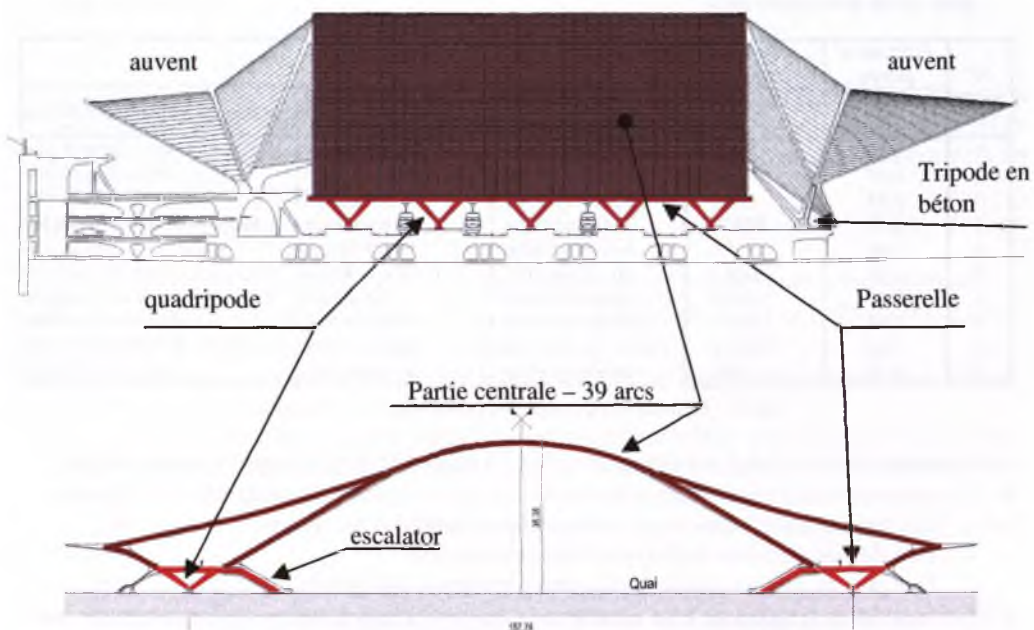


Fig. 5 – Eléments principaux de la toiture
Arcs de la toiture principale (brun), appuis des arcs: passerelles, quadripodes, escalators (rouge)

Les passerelles sont supportées, au niveau de chaque quai par un quadripode, constitué de 4 caissons métalliques disposés suivant les arêtes d'une pyramide à quatre faces et posée sur sa pointe.

La structure portante des auvents est constituée de 4 arcs, tous appuyés, à leur naissance sur des structures en béton, appelées, tripodes (Fig.6.). Les pannes, qui servent de support aux châssis de la verrière, relient respectivement les arcs A4 à A3 et A3 à A1; la couverture de ces deux surfaces courbes (Fig.6 – surfaces bleue et verte) servira d'abri aux voyageurs qui pénétreront dans la gare.

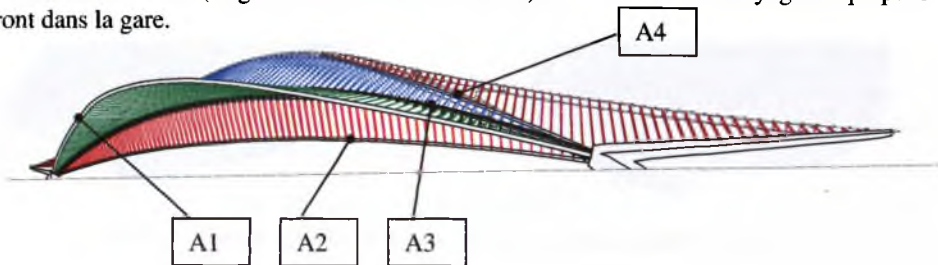


Fig. 6 – Structure des auvents

3.2 Fréquences et modes propres

3.2.1 Introduction

Pour des structures d'une telle portée, la valeur des fréquences propres de vibration et leur mode propre associé donnent des informations intéressantes sur le comportement d'ensemble:

- Avec la fréquence, sur sa raideur, sur sa sensibilité aux effets des rafales de vent,
- Avec ses modes, sur son schéma statique et sur sa sensibilité à des chargements symétriques et/ou dissymétriques,

N° mode	Fréquence propre	Masse généralisée	Mode		
	Hz	tonnes	type de comportement	géométrie du mode	partie de structure concernée
1	0.36	2419	flexion transversale	balancement	auvent colline et ville
2	0.42	2079	flexion verticale	dissymétrique	auvent colline et ville
3	0.44	343	flexion verticale	symétrique	auvent ville
4	0.45	85503	flexion verticale	symétrique	2 auvents et toiture principale
5	0.46	1333	flexion verticale	dissymétrique	auvent colline et ville
6	0.48	87041	flexion verticale	dissymétrique	toiture principale et 2 auvents
7	0.48	104868	flexion verticale	symétrique	toiture principale et 2 auvents
8	0.54	28611	flexion transversale	balancement	structure complète
9	0.54	234614	flexion transversale	balancement	structure complète
10	0.55	1998	flexion verticale	dissymétrique	toiture principale

Tab.1. – Premières fréquences et modes propres de vibration

L'examen du tableau (Tab.1.) et des modes (Fig.7.) permet de tirer plusieurs enseignements:

- Les modes mettent bien évidence les modes de déformations prépondérants de la toiture:
 - Un "balancement" transversal de la structure induit par les auvents
 - Une flexion verticale et dissymétrique des auvents
 - Une plus grande souplesse des auvents par rapport à la toiture principale.
- Les premières fréquences sont relativement basses; cela doit attirer l'attention sur le fait que la structure pourrait être sensible aux rafales de vent dont l'énergie est effectivement importante pour des fréquences faibles
- Certains modes ont des masses généralisées faibles vis à vis de la masse totale de la toiture qui est de l'ordre de 12.000 tonnes; cet indicateur montre que ces modes de vibration concernent seulement une partie de la toiture et/ou que l'ouvrage ou une partie sera d'autant plus facile à exciter par le vent que la masse à mettre en mouvement sera faible.
- Les fréquences des différents modes sont très proches les unes des autres. Ceci est dû aux deux plans de quasi-symétrie de la structure. Chaque mode dissymétrique est dédoublé.

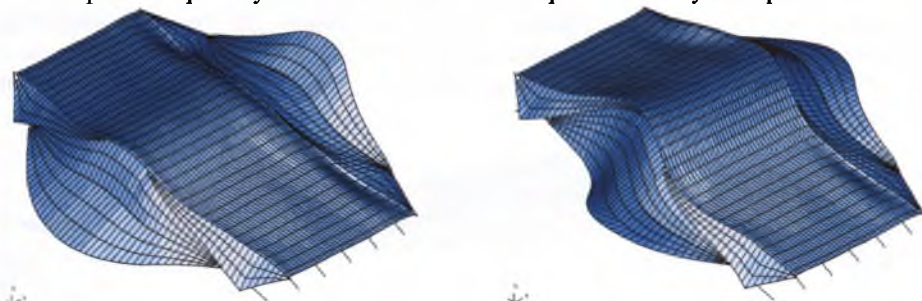


Fig. 7. – Modes propres de vibration – Mode 1: 0,46 Hz – Mode 2 : 0,42 Hz

3.3 Chargements

3.3.1. Charges permanentes

L'étanchéité de la toiture est assurée par une verrière de 30.000 m² qui couvre l'ensemble de la surface de la gare et des quais. Les charges permanentes se répartissent de la façon suivante: 4.300 tonnes pour la partie centrale, 3.050 tonnes pour les 2 auvents, 3.000 tonnes pour les 2 passerelles, 1.350 tonnes pour la verrière. Ces différentes charges sont pondérées par 1,35 à l'état limite ultime.

3.3.2. Charges variables statiques

Les différents types de charges variables prises en considération sont la température (variation uniforme de 30° et gradient de 10°), la neige (350 à 400 N/m²) et la foule sur les passerelles (5.000 N/m²). Ces charges sont pondérées, à l'ELU, par 1,50, combiné éventuellement à un coefficient d'accompagnement.

3.3.3. Charges variables de vent – vitesse de référence

Le comportement au vent a fait l'objet de deux approches différentes mais complémentaires:

- La première, à partir de la norme belge au vent (NBN B 03-002-1 et NBN 03-002-2) pour assurer le dimensionnement de la structure,
- La seconde, à partir d'essais en soufflerie, pour vérifier que le dimensionnement était sécuritaire sans excès.

La philosophie de la norme belge au vent est fort similaire aux Eurocodes avec néanmoins une nuance au niveau de la définition de la vitesse de référence et de sa période de retour:

- ENV 1991-2-4_1995_DAN: période de retour= 50 ans, soit 26,2 m/sec pour toute la Belgique
- NBN B 03-002-1: période de retour= 10 ans, soit ≈24 m/sec
- EN1991-1-4_2005_ANB: période de retour= 50 ans, soit 24 m/sec pour la moitié sud de la Belgique.

Si à l'époque du dimensionnement, en 1999, la norme belge pouvait être considérée comme insécuritaire vis à vis de l'Eurocode, version ENV, elle peut être considérée aujourd'hui comme étant compatible avec la version EN en tout cas pour le sud de la Belgique !

Parallèlement, des essais en soufflerie ont été entrepris pour la vérification finale. Ils ont permis de:

- déterminer le profil du vent au droit de la gare en prenant en compte tout son environnement: le milieu urbain et la proximité immédiate d'une colline,
- mesurer la distribution des pressions au cours du temps sur toute la surface de la toiture,
- Vérifier le comportement structurel, statique et dynamique, de la toiture sous l'effet du vent,
- vérifier les critères de confort des voyageurs à l'intérieur de la gare.

3.4 Dimensionnement sous le vent - approche normative

Le chargement du vent est, classiquement, remplacé par des distributions de pressions statiquement équivalentes suivant la formule (avec le formalisme de l'ENV 1991-2-4)

$$\text{Pressions}_\text{équivalent} = C_D \cdot C_p \cdot 1/2 \cdot \rho \cdot V^2$$

- avec - V , la vitesse du vent intégrant les caractéristiques du site (rugosité, relief,...) et de la région (vitesse de référence, hauteur de la structure,...)
 - ρ , la densité de l'air
 - C_p , le coefficient de pression pour prendre en compte la géométrie de la structure
 - C_D , le coefficient dynamique.

La pression dynamique, $\frac{1}{2}\rho V^2$, adoptée, est de 1000 N/mm². C_D intègre deux effets au travers des coefficients B et R :

1. B , la distribution spatiale du vent sur la surface du bâtiment:
2. R , les effets dynamiques induits par les rafales.

Pour la toiture, tous calculs faits, ces deux coefficients ont pour valeur, $B = 0,43$ et $R = 1,48$. Cela donne, finalement, un coefficient dynamique C_D égal à 1,25. Cette valeur supérieure à l'unité tend également à montrer que le comportement au vent méritait d'être étudié en détail.

Il restait alors à définir la distribution des pressions au travers du coefficient C_p . Deux types de vent ont été considérés:

1. Un vent longitudinal, parallèle à l'axe des quais
2. Un vent transversal, perpendiculaire aux quais.

Pour le vent longitudinal, la structure (Fig. 8.) a été assimilée à un auvent à double pente avec une inclinaison de l'ordre de 21°. Ceci a conduit à considérer quatre combinaisons de distributions de pressions comme décrit dans la figure 8.

Pour un vent transversal, la figure 9 schématisse les surfaces opaques: Les surfaces en trait gras, plein sont considérées comme faisant partie d'un auvent avec leur pente associée; on en déduit les coefficients de pressions, C_p . Les surfaces en traits dédoublés sont assimilées à des parois verticales d'un bâtiment présentant un certain degré de porosité. Après avoir dressé le bilan des parois "pleines" et des parois "ouvertes", les coefficients C_p sont calculés. Finalement, trois combinaisons de distributions ont été envisagées.

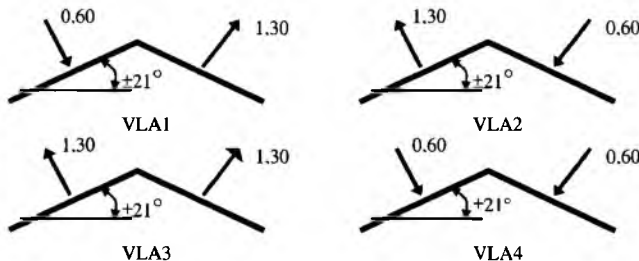


Fig.8. – distributions des coefficients de pressions, envisagées pour le vent longitudinal

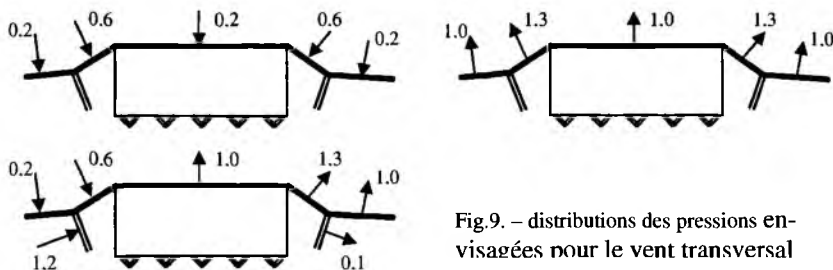


Fig.9. – distributions des pressions envisagées pour le vent transversal

3.5 Dimensionnement sous le vent – essais en soufflerie

Sur base d'un cahier des charges établi par le bureau Greisch, PSP-Technologies a réalisé des essais en soufflerie en quatre temps:

1. détermination du profil de vent au droit de la gare
2. mesure de la distribution des pressions sur toute la surface de la toiture
3. calcul du comportement dynamique de la structure
4. vérification des critères de confort.

3.5.1. Détermination du profil de vent au droit de la gare

Le profil du vent a été déterminé au moyen d'une maquette qui reproduisait le futur bâtiment des voyageurs et ses environs à une échelle de 1/750^{ème} (Fig. 10). L'ensemble du relief ainsi que le milieu urbain dans lequel la structure est implantée étaient modélisés; une zone d'un rayon de 1 km autour de la gare était ainsi couverte.

La Colline de Cointe, située à l'arrière du bâtiment constitue une donnée essentielle de cet environnement ; en effet, tout en faisant écran au vent d'ouest, elle forme une barrière pour le vent d'est (soufflant de la ville). En butant contre la colline, il subit des changements de direction qui peuvent avoir des effets divers sur la toiture.



Fig. 10. – maquette à l'échelle 1/750



Fig. 11. – maquette à l'échelle 1/200

3.5.2. Mesure de la distribution des pressions .

Une deuxième maquette du bâtiment, cette fois, au 1/200 (Fig. 11), a permis de mesurer la distribution dans le temps et dans l'espace des pressions sur la surface extérieure et intérieure de la toiture. Elle reproduisait la géométrie de la structure avec tous ses détails. Chaque arc, chaque pente, les deux passerelles étaient représentés avec leur géométrie afin de recréer la rugosité réelle des surfaces rencontrées par les flux d'air.

Le modèle local de vent, déterminé grâce aux essais précédents, a été artificiellement recréé dans le tunnel de la soufflerie. Soumise à cet environnement, cela a permis de déterminer de façon plus fine, la distribution de la pression exercée par le vent sur la toiture.

Les mesures ont été multiples:

- 12 directions de vent, soit tous les 30°
- pour chaque direction de vent, l'essai était répété 30 fois afin d'obtenir une distribution statistique
- la durée d'un essai était équivalente à plus de 10 minutes dans la réalité.

Les schémas de la figure 12 reprennent les pressions et dépressions caractéristiques, d'une part, adoptées pour le dimensionnement de la toiture et, d'autre part, obtenues lors des essais. Il faut noter qu'il s'agit bien de valeurs enveloppes sans aucune notion de concomitance.

Les directions de vent prépondérant pour le dimensionnement sont également indiquées.

Globalement, on peut en conclure :

- Les valeurs de dimensionnement sont bien enveloppées des mesures
- Seule la pression sur l'avant côté ville a été sous-estimée
- Les dépressions sur la structure ont été surestimées
- Et surtout, bien que cela ne puisse pas transparaître sur ces figures, les cas dissymétriques fort défavorables pour le dimensionnement, ne se retrouvent que partiellement dans les mesures.

Ces constatations doivent être nuancées par le fait que cette comparaison se limite aux pressions :

- de dimensionnement, hors de tout effet dynamique pris en compte par le coefficient dynamique C_d , pris égal à 1.25
- mesurées sur les maquettes rigides, donc également sans effet dynamique

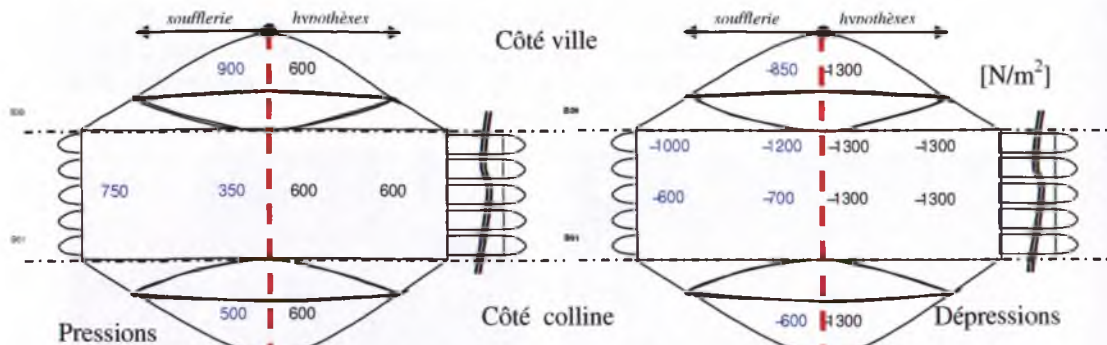


Fig. 12. – Pressions et dépressions enveloppes - Comparaison hypothèses et essais

3.5.3 Calcul du comportement dynamique de la structure

Il était indispensable de vérifier son comportement dynamique sous l'effet du vent qui est un chargement variable dans le temps dans la mesure où la structure a plusieurs modes propres de vibrations compris entre 0.35 Hz et 1.00 Hz. Il a été simulé numériquement en utilisant les résultats des essais en soufflerie comme données de base. Les pressions mesurées ont été transformées en forces concentrées appliquées aux noeuds de la structure modélisée avec des éléments finis de type poutre. Le modèle utilisé a été mis au point par le bureau Greisch.

Deux méthodes ont été utilisées pour le calcul des efforts et des déplacements :

- l'une est basée sur la Transformée de Fourier du signal mesuré et complétée par la technique de la superposition modale,
- l'autre est une analyse transitoire pas à pas avec résolution du système d'équations complet.

La technique de superposition modale combinée à la notion de transformée de Fourier permet de limiter les opérations mathématiques. Vingt modes ont été pris en compte dans le calcul, la fréquence de ceux-ci étant du même ordre de grandeur que les fréquences dominantes du vent. Cette procédure, proposée par Greisch et le bureau de contrôle SECO, a été inspirée de celle utilisée pour l'interprétation des résultats de soufflerie réalisés pour le stade de France (voir article de Biétry paru dans la « Revue française du génie civil » Vol 1 - n°1/1997 p 50 - 66).

La seconde méthode s'est avérée beaucoup trop coûteuse en temps de calcul: de l'ordre de 3 à 4 jours. Elle n'a donc été utilisée que pour vérifier la validité de la 1^{re} méthode.

Afin de limiter encore le volume des calculs et des résultats à traiter, il a été décidé d'opérer de la façon suivante :

- Pour chaque direction de vent (tous les 30°), 2 événements ont été simulés numériquement pour finalement trouver les 3 directions de vent qui donnaient les déformations les plus grandes de la toiture.
- Pour les 3 directions choisies, des simulations numériques ont été réalisées pour les 30 événements créés en laboratoire.

Les efforts et déplacements pour les 30 événements de ces trois directions ont ensuite été calculés et les résultats traités de manière statistique afin d'en retirer des valeurs caractéristiques avec la formulation suivante:

$$P_{\text{caract}} = P_{\text{moy,max}} + \sigma$$

avec $P_{\text{moy,max}}$, la moyenne des efforts internes (ou déplacements) maximum sur les 30 événement et σ , l'écart type des efforts internes (ou déplacements) maximum. Les valeurs caractéristiques ont été ainsi calculées pour :

- Les déplacements de points représentatifs de la toiture
- Les déformations locales au niveau de la couverture afin de déterminer le jeu à prévoir pour les châssis,
- Les efforts internes des éléments de structure pour lesquels le dimensionnement de Greisch avait fait apparaître un taux de travail plus important.

Le calcul des contraintes a été réalisé à partir des efforts fournis par PSP pour les huit combinaisons suivantes :

$N_{\max} + M_y \max + M_z \max$	$N_{\min} + M_y \max + M_z \max$
$N_{\max} + M_y \max + M_z \min$	$N_{\min} + M_y \max + M_z \min$
$N_{\max} + M_y \min + M_z \max$	$N_{\min} + M_y \min + M_z \max$
$N_{\max} + M_y \min + M_z \min$	$N_{\min} + M_y \min + M_z \min$

Le graphique de la figure 13 est une comparaison de l'enveloppe du taux de travail obtenue

- d'une part pour les sept combinaisons de vent retenues par Bureau d'Etudes Greisch pour le dimensionnement,
- d'autre part pour les huit combinaisons définies ci-dessus à partir des mesures en soufflerie.

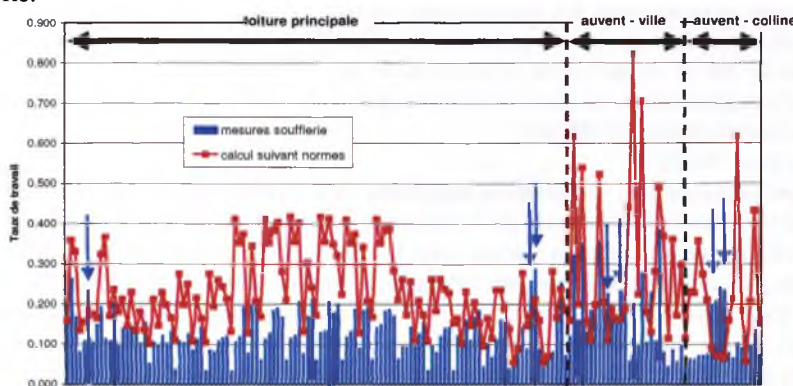


Fig.13. – comparaison du taux de travail dans la structure sous le seul effet du vent

L'ordonnée représente le taux de travail, soit le rapport entre la contrainte obtenue et la limite élastique de l'acier, sous le seul effet du vent. L'abscisse du graphique correspond à la liste des sections de la structure dans lesquelles le taux de travail est évalué. La numérotation permet de localiser la zone où la section est vérifiée.

L'examen des résultats a permis de tirer les conclusions suivantes:

- Les contraintes calculées sont nettement enveloppées de celles mesurées.
- Les distributions symétriques de surpressions, proposées par les normes, ne sont pas significatives ou dimensionnées.
- les contraintes mesurées au niveau des auvents ne peuvent être approchées qu'avec des distributions de dépressions sur les même auvents.
- La distribution des contraintes sur la toiture principale semble être le mieux approchée avec un vent longitudinal et une distribution dissymétrique de pression, notée VLA1 à la figure 8 (pression au vent et dépression sous le vent). Cette distribution est cependant surestimée d'un facteur de l'ordre de 1,30. Il est probable qu'adopter des tels coefficients de dépressions des surfaces aussi importantes est trop défavorable.
- Les mesures ont mis en évidence quelques zones indiquées par des flèches (fig.13) pour lesquelles les contraintes étaient nettement plus élevées que celles fournies par le calcul. Il s'agit d'éléments situés sur les auvents et dans les arcs auxquels sont accrochés ces mêmes auvents. Il a dès lors été nécessaire de vérifier à nouveau ces sections pour les combinaisons ELU, charges permanentes combinées au vent et à la neige. Il s'est avéré que la sécurité était toujours garantie.

Les essais ont donc permis de valider le dimensionnement sans avoir à le modifier. Les hypothèses adoptées sur base de la norme belge au vent se sont donc avérées correctes. Ceci ne veut évidemment pas dire que les essais étaient inutiles.

Il faut rappeler que les essais en soufflerie ont été demandés par le Bureau d'Etudes Greisch dans le cadre des études d'exécution et que, faute d'un délai d'études suffisant, ils ont été réalisés en parallèle au dimensionnement avec pour but de vérifier que le caractère sécuritaire du dimensionnement.

Il est clair que de tels essais sont, logiquement, réalisés au niveau de l'avant projet afin de pouvoir utiliser ces résultats pour la définition des hypothèses de dimensionnement.

4 CONCLUSIONS

La nouvelle gare TGV de Liège est une gare hors norme:

- Couverture des quais sur une longueur de plus de 400 m, longeur en façade de la toiture principale de 200 m, et hauteur de la toiture de 35 m
- Poids de la superstructure en acier de 10 000 tonnes
- Infrastructure en béton: 65 000 m³
- Surface vitrée: 30.000 m²

Les études ont nécessité une mobilisation importante afin d'être certain de maîtriser parfaitement le dimensionnement, d'une part de l'infrastructure, et d'autre part, de la superstructure, sous son poids propre important et surtout sous les effets du vent susceptibles d'induire des effets dynamiques qui ne pouvaient être négligés. Même si, chronologiquement, le dimensionnement sous le vent a été entrepris sur base des normes belges au vent, pour une telle structure, des essais en soufflerie devraient être systématiquement entrepris au stade de l'avant-projet afin d'être certain de maîtriser des paramètres tels que la configuration du terrain avoisinant (la colline) ou celle de la géométrie de la structure. L'absence de contreventement a également obligé les ingénieurs à étudier la structure comme un tout et non comme un ensemble d'éléments qui auraient pu être dimensionnés séparément.

INTRODUCTION TO RISK ASSESSMENT STRATEGIES FOR ACCIDENTAL DESIGN SITUATIONS IN CIVIL ENGINEERING

Y. Rammer

Université Libre de Bruxelles
50, av. F.D. Roosevelt – CP 194/2– B-1150 Brussels - Belgium
vrammer@batir.ulb.ac.be

Keywords: Risk analysis, Strategy assessment, Structural design principles, Reliability of structures, Safety appraisal, Accidental design situations.

Abstract. *Eurocode EN 1991-1-7 provides a description of principles and application rules for the design of load bearing structures subjected to accidental actions. Two types of strategies are proposed in informative annex B of this standard in order to assess accidental design situations: those based on identified accidental actions and those based on limiting the extent of localized failures. However, discrepancies regarding vocabulary and flow charts appear towards earlier ISO/IEC guides related to risk management system. This situation can add confusion to an already difficult subject to professional consulting engineers.*

The aim of this paper is to illustrate the basic concepts behind risk analysis, and to try and propose a unified framework for the assessment of accidental project situations.

1 INTRODUCTION

Eurocode EN 1991-1-7 [1] provides a description of principles and application rules for the design of load bearing structures (buildings and bridges) subjected to accidental actions, including impact forces (from vehicles, trains, ships), actions due to internal explosions and actions due to local failures.

Two groups of strategies are proposed in order to assess accidental design situations: those based on identified accidental actions and those based on limiting the extent of localized failures.

In the first group, it is proposed to design the structure to have sufficient minimum robustness, to prevent or reduce the effect of the accidental action or to directly design the structure to sustain the action.

The second group of strategies is based on limiting the extent of localized failure, either by increasing redundancy of the structure or designing “key elements” to sustain notional accidental actions and applying some prescriptive rules like integrity or ductility.

Informative annex B of this standard gives some guidance for the planning and execution of risk assessment.

Other engineering fields are more accustomed to risk management, and some relevant standards exist in order to define the basic concepts [2-3].

This brief is intended to introduce and link those different standards.

2 THE PHILOSOPHY OF RISK

Lev ZETLIN, a prominent structural design engineer, is quoted by Henry PETROSKI [4] as a good example of design paradigms:

“Engineers should be slightly paranoid during design stage. They should consider and imagine that impossible could happen. They should not be complacent and secure in the mere realization that if all the requirements of the design handbooks and manuals have been satisfied, the structure will be save and sound.”

If this quotation is quiet understandable, the underlining concept of risk is more difficult to assess, because a precise definition or rules of application to evaluate risk acceptability does not exist [5]. However, for the purpose of study risk it is often proposed to formulate risk as a combination of “hazard” (i.e. harm created by a situation) and “exposure” (intended to incorporate the concepts of frequency and probability).

James REASON [6] and Charles PERRROW [7] have investigated concepts like “human error” or what can be called “normal accidents” in living with high-risk technologies.

It can be seen that the most difficult part of any risk assessment is defining a level of acceptable or tolerable risk. In the case of accidental actions due to human activities a draft of a dedicated standards was elaborated [8], but withdrawn in 2006. However, some definitions are interesting for our purpose: characteristics of accidental actions are that they are not a consequence of normal use, that they are undesired and that extensive efforts must be made to avoid them. This means also that the probability of occurrence is small; whereas the consequences (damage) may be catastrophic.

In this standard, it is proposed that the representative value for an accidental action should be chosen in such a way that the probability is less than $p=10^{-4}$ per year that this value could be higher.

As for the consequences, there is more discussion in available literature and research papers, as the level of individual or societal risks are evaluated with variable cultural, ethical or political biases. A mean value could be that the fatality rate should not exceed 10^{-4} per year.

3 CONSTRUCTION FAILURES

Jacob FELD [9] published a fine classic text on construction failures, exposing, classifying and illustrating construction failure types and common causes.

In the process of identifying possible accidental risks, it is important to use some forms of check-lists. The following is proposed:

1. Fundamental errors in concept
 - a. Scale of project outside envelope of past experience
 - b. Unreliable prediction of unusual environmental effects
2. Site selection and site development errors
 - a. Unwise land-use or site selection
 - b. Problems related to specific soil conditions
3. Programming deficiencies
 - a. Unacceptable difference between expected and observed performance
 - b. Unclear or unrealistic expectations
 - c. Lack of communication during the programming phase
4. Design errors
 - a. Errors in design concept
 - b. Lack of structural redundancy
 - c. Failure to consider a load or a combination of loads
 - d. Deficient connection details
 - e. Calculation errors
 - f. Misuse of computer software
 - g. Detailing problems, including selection of incompatible materials or assemblies that are not constructible
 - h. Failure to consider maintenance requirements or durability
 - i. Inadequate or inconsistent specifications for materials or expected quality of work
 - j. Unclear communication of design intent
5. Construction errors
 - a. Excavation accidents
 - b. Construction equipment failure
 - c. Improper construction sequencing
 - d. Inadequate temporary supports
 - e. Excessive construction loads
 - f. Premature removal of shoring or framework
 - g. Nonconformance to design intent
6. Material deficiencies
 - a. Lack of understanding about material mechanics
 - b. Ignorant juxtaposition of incompatible materials
 - c. Manufacturing or fabrication defects
7. Operational errors
 - a. Alterations made to the structure
 - b. Change in use
 - c. Operational judgment errors
 - d. Inadequate maintenance

4 ACCIDENTAL, EXTREME AND ABNORMAL LOADS

4.1 Frequency of accidental situations.

SECURITAS [10] made a thorough statistical analysis of 10.000 cases of failures reported to insurance companies between 1968 and 1978. Among other results, following items are interesting for assessing the frequency of accidental actions:

- 12% of analyzed cases causes collapse or near collapse, resulting to 15% of total repair and indemnity costs compensated by insurances;
- 23% of cases are caused by climatic loads.

Another analysis performed by Pr SCHNEIDER of the Polytechnic of Zürich on 800 cases of severe failures (reported by MATHIVAT J. in [11]):

- 13 % of cases analyzed are caused by underestimation of influences and 4% by *prior* unknown hazards, and causing 27% of indemnified costs and 11% of injuries or fatalities;
- 3% of cases are resulting of risks not taken into account, causing 13% of costs.

John LANCASTER [12] assembled historical data with the objective to study and compare various major failures in industrial situations or normal human activities.

4.2 Typology of loads.

Again, in order to identify sources of hazards, following check-list is proposed.

1. Normal Actions
 - a. Permanent (mass of structure, superstructure, finishes, fittings, equipment)
 - b. Variable (loads, moving loads)
 - c. Particular (horizontal forces, prestressing, ground pressures, differential settlements, vibrations)
 - d. Construction (temporary, erection)
 - e. Natural (temperature, snow, ice, wind, rain, current, tide, earthquake)
 - f. Material properties modifications (creep, shrinkage)
2. Abnormal Loads
 - a. Avalanche, boulder falls, soil erosion, landslides
 - b. Floods
 - c. Vibrations
 - d. Material properties alterations (corrosion, fatigue)
3. Accidental Actions
 - a. Internal or external blasts and explosions (gas, vapor, dust, volatile liquids)
 - b. Collisions (cars, trains, ships, aircrafts, dropped objects, flying fragments)
 - c. Subsidence of subsoil, erosion
4. Extreme events
 - a. Earthquakes
 - b. Tornadoes (wind, snow)
 - c. Fire
5. Combined hazards
6. Effects caused by intentional, warfare or terrorist acts.

5 RELIABILITY METHODS IN ENGINEERING DESIGN

The basic requirements of the probabilistic model code [13] are that design, construction and maintenance of structures and structural elements shall be that, with appropriate levels of reliability:

- they remain fit for their required use (SLS);
- they shall withstand repeated actions occurring during their lifetime (ULS) ;
- they shall not be damaged by accidental events to an extent that could be disproportionate to the initial triggering event.

Those methods are well described in [14], [15] and [16]. Eurocodes give the appropriate minorating and majorating factors on actions and resistances for accidental situations. The corresponding probabilities for failure can be computed by using usual probabilistic analysis. An illustrative summary is given in Fig.1.

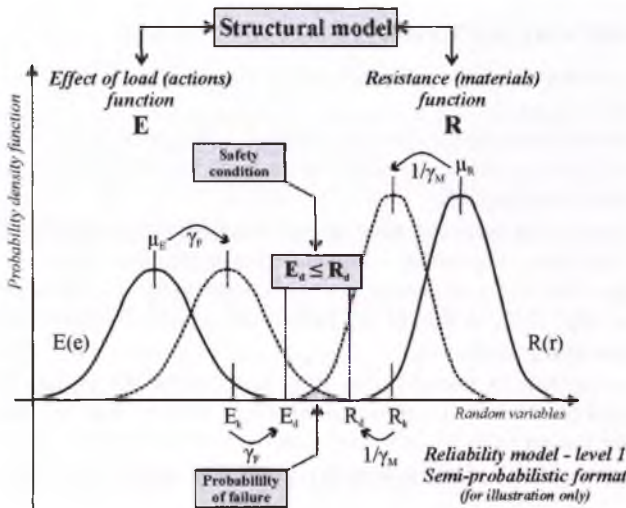


Figure 1: Semi-probabilistic format illustration.

6 RISK MANAGEMENT

Risk management is the overall concept and framework that coordinates all activities to direct and control an organization with regard to risk: risk assessment, risk treatment, risk acceptance and at last risk communication.

The process of risk assessment combines risk analysis (source identification and risk estimation) and risk evaluation.

Risk treatment expresses how the organization (the designer) will deal with the results of the risk assessment (avoidance, optimization, transfer or retention).

It was already stated that risk acceptance is the most difficult part of the risk management concept. At last, results of the analysis should be documented and communicated to who it may concern.

Translations in English, French and Dutch of the risk management vocabulary are proposed in appendix 2.

The qualitative approach is illustrated in Fig.2.

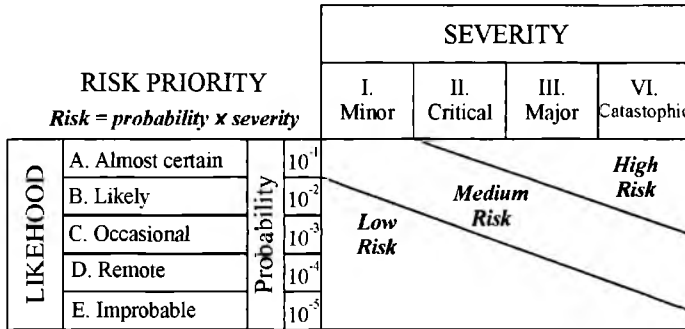


Figure 2: Risk matrix

7 PROPOSED RISK ASSESSMENT FRAMEWORK

The corresponding flow-chart is produced in Appendix 1. It was obtained combining proposed charts in [1] and [2].

As can be understood, the process goes through a first initial step of “basic design”, then to a second step of defining the scope of the assessment, hazard scenarios and corresponding accidental situation consequences.

Following step is the more sensitive step of risk estimation, usually started with a qualitative approach and then – if possible – a quantitative approach.

The last step of the risk assessment process is performing an evaluation of the results of the risk estimation step. This can lead to risk optimization either by modifying initial design or by adopting mitigating measures.

At last, if acceptable or tolerable risk level is achieved, the project feasibility in terms of costs or technical possibilities must be reassessed in order to abandon (risk avoidance) or start the construction project.

A few examples of risk identification in construction projects can be found in [18] and [19].

8 CONCLUSIONS

If the concept of risk is at the present well understood in the engineering community, it must be emphasized that extensive additional research is needed for both probability of occurrence of accidental actions and related damage and consequences.

The acceptable or tolerable level of remaining risk is another important field for further investigation.

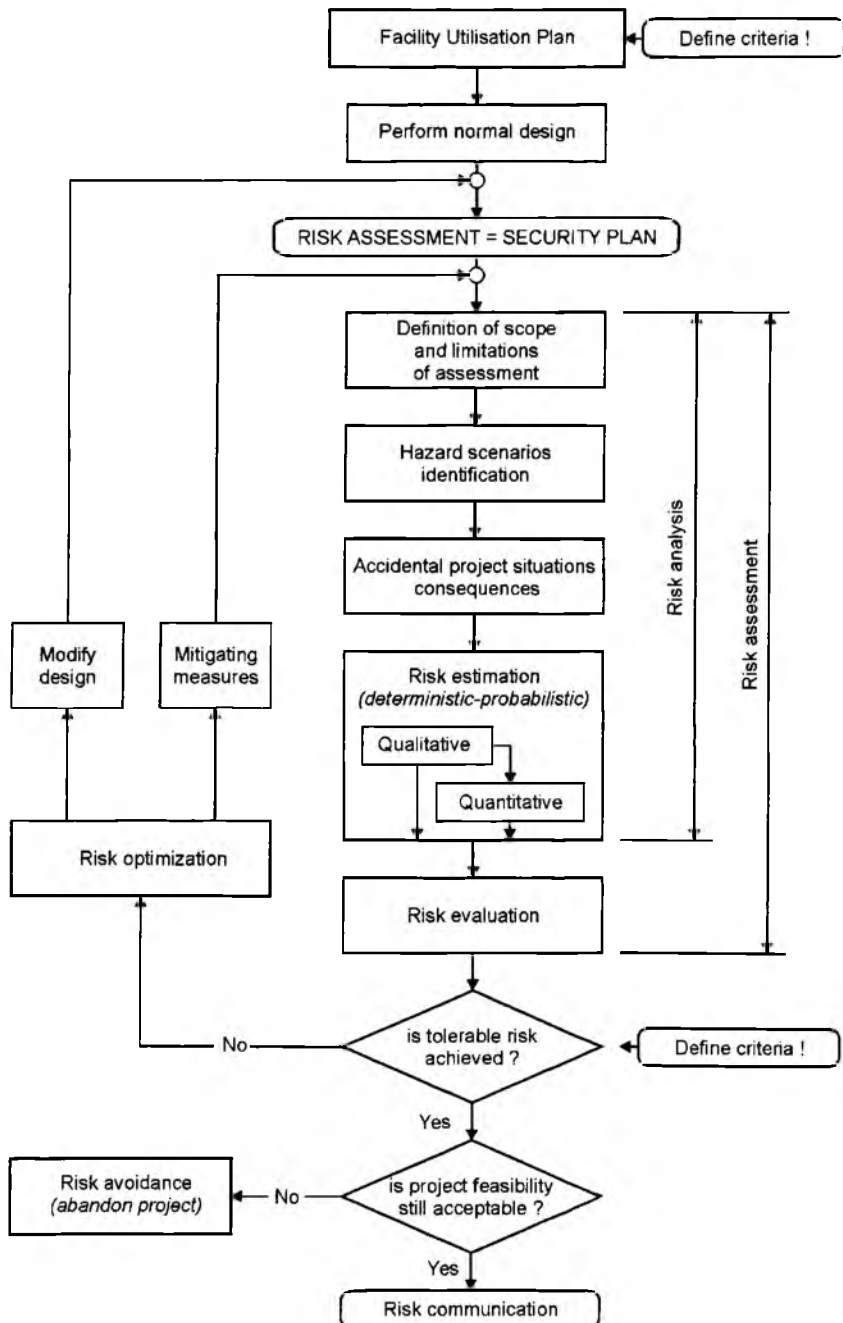
9 ACKNOWLEDGEMENTS

The author wishes to thank particularly Pr.Dr.ir Marc VAN OVERMEIREN from the Vrije Universiteit Brussel for providing useful information and advice on risk management philosophy.

REFERENCES

- [1] EUROPEAN COMMITTEE FOR STANDARDIZATION, 2005, *Eurocode 1 - Actions on structures (Part 1-7): General actions – Accidental actions*, prEN 1991-1-7:2005(E).
- [2] INTERNATIONAL STANDARD ORGANIZATION (ISO), 2002, *Risk management Vocabulary – Guideline for use in standards, 1st Edition*, ISO/IEC Guide 73.
- [3] ISO, 1999, *Safety aspects – Guidelines for their inclusion in standards, 2nd Edition*, ISO/IEC Guide 51.
- [4] PETROSKI H., *Design Paradigms*, Cambridge University Press, 1994.
- [5] CHICKEN J.C., POSNER T., *The Philosophy of Risk*, Thomas Telford, London, 1998.
- [6] REASON J., *Human Error*, Cambridge University Press, Reprint, 2002.
- [7] PERROW Ch., *Normal Accidents*, Princeton University Press, Reprint, 1999.
- [8] ISO, 1995 (withdrawn feb.2006), *Bases for design of structures – Accidental actions due to human activities*, ISO/DIS 10252.
- [9] FELD J., CARPER K.L., *Construction Failures*, 2nd Ed, J. Wiley & sons, 1997.
- [10] DUFOUR J., *Etude statistique de 10.000 dossiers de sinistres – Bureau SECURITAS*, in Annales de l'ITBTP, n°378, 12/1979,
- [11] MATHIVAT J., BOITEAU C., *Procédés généraux de construction – T1*, Eyrolles, 1992.
- [12] LANCASTER J., *Engineering Catastrophes*, Abington Pubs, Cambridge, UK, 1997.
- [13] ISO, *General Principles on reliability for structures, 2nd Edition*, ISO 2394.
- [14] CALGARO J.-A., *Introduction aux Eurocodes*, Presses des Ponts et Chaussées, 1996.
- [15] DESROCHES A., *Concepts & Méthodes probabilistes de base de la sécurité*, Lavoisier, Paris, 1995.
- [16] SMITH D.J., *Reliability Maintainability and Risk*, Butterworth, 6th ed., 2001.
- [17] FAVRE R. et al, *Dimensionnement des structures en béton*, Presses Polytechniques et Universitaires Romandes, new Ed, Lausanne, 1997,
- [18] BLOCKLEY D., *The Nature of Structural Design and Safety*, J.WILEY & Sons, 1980.
- [19] SUNDARAJAN C., TRUONG V., *Probabilistic structural mechanics in system and plant risk assessment*, SUNDARAJAN C. ed, *Probabilistic structural mechanics handbook*, Chapman & Hall, 1995.
- [20] BOUILLARD Ph., RAMMER Y., *Evaluation globale des risques structurels : application aux immeubles de grande hauteur*, Rapport de synthèse, Université Libre de Bruxelles, 2001.

APPENDIX 1: General flowchart for risk assessment of accidental project situations for load bearing structures, proposed by the author, with elements from [20]:



APPENDIX 2: Risk Management Vocabulary Multilingual Dictionary:

Adapted from following Lecture Notes published by the Vrije Universiteit Brussel :
VAN OVERMEIREN M, OLIVIER P., Betrouwbaarheids- en Risico-analyse van Industriële Systemen – deel 2 : Risico-analyse, 2000.

English	French	Dutch
Risk	<i>Le risque</i>	<i>Het risico</i>
Accident	<i>L'accident</i>	<i>Het ongeval</i>
Event	<i>L'événement</i>	<i>De gebeurtenis</i>
Safety	<i>La sécurité</i>	<i>De veiligheid</i>
Damage	<i>Le dommage</i>	<i>De schade</i>
Hazard	<i>Le danger</i>	<i>Het gevaar</i>
Hazardous situation	<i>La situation dangereuse</i>	<i>De gevaarlijke situatie</i>
Harm	<i>La nuisance</i>	<i>De hinder</i>
Harmful event	<i>L'événement nuisible</i>	<i>De schadelijke gebeurtnis</i>
Thread	<i>La menace</i>	<i>De bedreiging</i>
Severity	<i>La gravité</i>	<i>De ernst</i>
Frequency	<i>La fréquence</i>	<i>De frequentie</i>
Probability	<i>La probabilité</i>	<i>De waarschijnlijkheid</i>
Source	<i>La source</i>	<i>De bron</i>
Cause	<i>La cause</i>	<i>De oorzaak</i>
Effect	<i>L'effet</i>	<i>Het effect</i>
Consequence	<i>La conséquence</i>	<i>Het gevolg</i>
Management	<i>Le management</i>	<i>Het management</i>
Control	<i>La maîtrise</i>	<i>Het beheersing</i>
Assessment	<i>L'appréciation</i>	<i>De beoordeling</i>
Analysis	<i>L'analyse</i>	<i>De analyse</i>
Identification	<i>L'identification</i>	<i>De identificering</i>
Inventory	<i>L'inventaire</i>	<i>De inventaris</i>
Estimation	<i>L'estimation</i>	<i>De waardering</i>
Evaluation	<i>L'évaluation</i>	<i>De schatting</i>
Treatment	<i>Le traitement</i>	<i>De behandeling</i>
Acceptance	<i>L'acceptation</i>	<i>De aanvaardbaarheid</i>
Reliability	<i>La fiabilité</i>	<i>De betrouwbaarheid</i>
Protection	<i>La protection</i>	<i>De beveiliging</i>
Prevention	<i>La prévention</i>	<i>De preventie</i>
Reasonable risk	<i>Le risque raisonnable</i>	<i>Het redelijk risico</i>
Acceptable risk	<i>Le risque acceptable</i>	<i>Het aanvaard risico</i>
Tolerable risk	<i>Le risque tolérable</i>	<i>Het draaglijk risico</i>



This book contains the contributions presented at the workshop "Structural Design of Constructions subjected to Exceptional or Accidental Actions" held in Brussels on April 9th, 2008.

The design codes for constructions under exceptional or accidental actions are in constant evolution. Recent advances have been made to better understand and model these actions and the structural response.

All the persons involved in the design process, i.e. engineers, architects, researchers, public or private clients, will find here a state of the art of the recent codes or regulations together with an overview of some research results or industrial applications.